PHD BY PUBLICATION

The influence of minimum stress on the fatigue life of non strain-crystallising elastomers

Abraham, Frank

Award date:
2002

Awarding institution:
Coventry University
Deutsches Institut fur Kautschuktechnologie

THE INFLUENCE OF MINIMUM STRESS ON THE FATIGUE LIFE OF NON STRAIN-CRYSTALLISING ELASTOMERS

Volume I - Thesis

by

Frank Abraham

A thesis submitted in partial fulfilment of the University's requirements for the degree of Doctor of Philosophy

December 2002

Coventry University

in collaboration with

the Deutsches Institut für Kautschuktechnologie e. V.

Summary

This PhD-Thesis describes the fatigue life and dynamic crack propagation behaviour of elastomers, especially their dependency on test parameters. It, furthermore, presents concepts of data evaluation in order to develop criteria for more precise predictions of service life of elastomeric parts. Fatigue life was investigated using EPDM and SBR dumbbell specimens tested under load control at 1Hz until failure. Tests were made in order to create a common Wöhler-(S-N)-curve while increasing stress amplitude. Additionally, the influence on fatigue properties of increasing minimum stress at constant stress amplitude was investigated. All testing were carried out in the Deutsches Institut für Kautschuktechnologie e.V. (DIK). The results of these tests confirmed the well-known amplitude dependence of fatigue life in filled rubbers. An additional significant influence on fatigue life was found to be the level of minimum stress and consequently mean stress applied to these materials, which in turn to most other materials increase the fatigue life of rubbers. This additional influence on fatigue life is not dependent on strain crystallisation in Ethylene-Propylene-Diene Polymer (EPDM) or Styrene-Butadiene Polymer (SBR) as it is for Natural Rubber (NR).. It could be proved that this effect rather specific to filled systems. The investigation shows that the fatigue behaviour of carbon black filled non strain crystallising rubbers can not be described with a maximum stress or a maximum strain criterion. It shows that an energy criterion should be considered.

Another important effect is highlighted in this research. Following the dependence on load cycles it can be seen that most mechanical properties,

but particularly the stiffness of specimens change throughout the whole test, and never reach equilibrium. This behaviour is particularly observed in elastomers containing reinforcing fillers. It was found that all carbon black filled EPDM test specimen failed when they reached approximately 76% of their initial stiffness or complex modulus, despite the high variation of test conditions. The carbon black filled SBR test specimen failed when they reached 71% of their initial stiffness. These results indicate that there is a characteristic material parameter of loss in complex modulus that is reached at failure.

The results of the dynamic crack propagation tests on these unfilled and carbon black filled non strain crystallising elastomers show a similar behaviour like the fatigue to failure tests with respect to their minimum load dependence. Increasing minimum loads at a constant strain (displacement) amplitude under pulsed as well as sinusoidal excitation decrease the crack growth rate of the carbon black filled rubber material and, thus can lead to a higher service life of parts produced from these materials. The unfilled materials showed the expected opposite effect on an increase of the minimum load at constant strain amplitude which confirms the findings of the fatigue to failure experiments. It should be noted that maximum stress and maximum strain criteria are no tools to uniquely describe the crack propagation properties of filled rubbers.

As the normal failure observed during the fatigue to failure experiments was a sudden catastrophic crack after reaching a certain level of remaining stiffness or modulus it is assumed that these tests characterise the initiation process. It

is, thus, an important finding of this research that crack initiation and crack growth of rubber material show a similar dependence on test parameters. Furthermore, initiation and growth seem to be energy controlled processes in rubber materials.

Acknowledgements

I would like to thank the Deutsches Institut für Kautschuktechnologie e.V. (DIK) and the Deutsche Kautschuk-Gesellschaft e.V. (DKG) for supporting this work.

I would especially like to thank Dr. Steve Jerrams and Dr. Thomas Alshuth for their support and help throughout the duration of this work.

Also many thanks are due to my colleagues at DIK and my mother for her special support.

Contents

Abbreviations

NR	Natural Rubber
EPDM	Ethylene-Propylene-Diene Polymer
SBR	Styrene-Butadiene Polymer
E-SBR	Emulsion-Styrene-Butadiene Polymer
E*	complex modulus
E'	storage modulus
E''	loss modulus
tan δ	loss factor
Δx	dynamic displacement range
T	tearing energy
ε	strain
λ	engineering strain
σ	stress
F	force
W	strain energy (density)
c	crack length
f	frequency
n	fatigue life, service life
FEA	Finite Elements Analysis
Q	ozone concentration
GR-S	Butadiene-Styrene Rubber
OR-15	Butadiene-Acrylonitrile Rubber
BR	Butyl Rubber

1 Introduction/Literature Search

1.1 Aims

The fatigue behaviour of linear materials such as the majority of metals and ceramics is well researched and described in the literature. In particular emphasis has been placed on testing of fatigue properties with varying stress amplitudes at particular values of minimum stress or mean stress and these data have largely been represented as Wöhler curves and Haigh diagrams. Few fatigue analyses of non-linear elastomeric materials have been carried out and these used Natural Rubber (NR). The influence of minimum stress and stress amplitude on the fatigue resistance of NR has been studied by André *et al* [1] and the data was displayed on Haigh diagrams. Fatigue life was shown to increase as minimum stresses, both compressive and tensile, increased from zero for a single stress amplitude. The improved fatigue and crack growth resistance with increased minimum (and hence maximum) stresses was previously explained by Cadwell et al [2] and Lake & Thomas [3] and attributed to the strain crystallisation of NR inhibiting crack growth. A subsequent analysis carried out by the DIK also showed a reduction of crack propagation with increases in minimum stress for non strain crystallising rubber.

Consequently, the principal objective of this work is the characterisation of the dependence of fatigue on stress amplitude and minimum stress in non strain crystallising elastomers. Additionally, materials with and without filler are considered in the investigation. This permits simultaneous studies of the effects

of reinforcement, stress softening and Payne-effects [**4**, **5**, **6**, **7**] in filled systems.

A second objective is to clarify the question of which criteria (stress, strain, energy etc.) characterises the fatigue properties of elastomeric materials. Reliable predictions of the service life of dynamically loaded components, using fracture mechanics concepts as well as FEA, depend entirely on the use of the correct criteria and their characterisation.

The third objective is to develop a fatigue criterion which can be used in FEA-software and the characterisation of a material parameter to describe the fatigue properties under different test conditions of pre-stressing and pre-straining.

A fourth possible objective could be to find an in-service criterion which will allow for the replacement of a rubber component just before failure. This criterion should be capable of integration into an online measurement system.

An understanding of elastomeric fatigue behaviour is very important for the development of new elastomeric materials. Additionally it gives the industry the opportunity to develop/design components made from elastomers with increased fatigue lives and to design smaller, lighter and cheaper parts with less material consumption whilst retaining service life levels.

If for example the automotive industry could use the results of this research in the development of elastomeric parts, it will reduce costs, sizes and weights during production and consequently will be able to save energy during manufacture and service and thereafter only small amounts of elastomeric material will have to be recycled, burned or dumped.

The development of an online measurement system to evaluate the fatigue status of an in service elastomeric part will increase the safety of vehicles and machines and also it will reduce the number of parts to be replaced and dumped.

One other aim is the comparison of results of different testing procedures. A comparison of fatigue and cut growth of rubbers under nonrelaxing conditions was previously made by Gent et al [8] and Lake & Lindley [9]. The fatigue to failure properties of the elastomeric materials should be compared with the crack propagation properties of the same material. Both should be tested under a variation of minimum loads. The conclusions of this research will increase the knowledge of materials and their dependency on different testing procedures. This is very important for the research and development of new components and the predictive testing of their in service performance.

The output of this research has the potential to have a large positive influence on the environment and will simultaneously reduce costs. The results will help designers and compounders to improve the service lives and/or reduce the mass of individual products.

1.2 Introduction

Elastomers have the ability to withstand very large strains without permanent deformation or fracture which makes them an ideal material for many engineering applications. For elastomers it is possible to work at high static strains and even dynamic strains for long time periods. Elastomeric materials are used dynamically in many different engineering components. The first reason for this is certainly their unrivalled flexibility, combined with the potential to dissipate energy. But elastomers also offer high friction coefficients even under wet conditions and additionally there are tailor-made elastomers which function over a broad range of temperatures. Additionally various types of elastomers are resistant to fluids including very aggressive fluids, which combined with high flexibility makes them ideal as sealing materials. Modern fast transportation and advanced machine development have become possible because of the use of rubber products like tyres, belts, seals, springs and mounts.

Under most service conditions dynamic loads are applied to elastomeric parts and only a few are used under displacement control. Typical examples for dynamically loaded components are timing belts, V-belts, conveyor belts, rubber springs, engine mounts and tyres. Dependent on the applied load, elastomeric components are deformed according to their stiffness.

A very important property in nearly all applications is fatigue. The designer is often required to create an elastomeric component for imprecisely described service conditions. A component should attain a certain service life but should be correctly sized and certainly not too heavy and expensive for its functions.

At the moment, no acceptable method exists to calculate the fatigue lives of elastomeric components. The designer produces prototypes and tests them under service conditions and this is very expensive and time consuming. There is a high probability that the part has to be optimised by an interactive design process. Alternatively the component is over designed so that the expected service life is easily obtained, but this results in the problem of producing parts that are too heavy, large or expensive for mass production.

Hence, there is a great need for calculation/simulation of the fatigue behaviour of technical rubber components. At the moment it is not clear how service life can be determined. One possibility is the maximum strain criterion [**10**], another the maximum stress criterion [**11**, **12**] and also different energy criteria [**13**, **14**] have been suggested for use.

The characteristic of the equilibrium state is a certain distance between the molecular ends. Under external loading the molecule chains are oriented to a more linear form as shown on the right in Figure 1. The distance between the molecular ends can be increased by strain up to a few hundred percent. This explains the ability of elastomers to achieve very high strains. With unloading the stretched molecules return to the coil like state, with the initial end to end distances and this behaviour can be explained with reference to the law of thermodynamics. An ordered system changes on its own to a disordered form. This is why the rubber elasticity is called entropy elasticity.

Unlike metals, elastomers are markedly non-linear. Figure 2 shows the typical stress-strain curve of a vulcanised elastomer when tested under standard quasi-static uniaxial tensile loading.

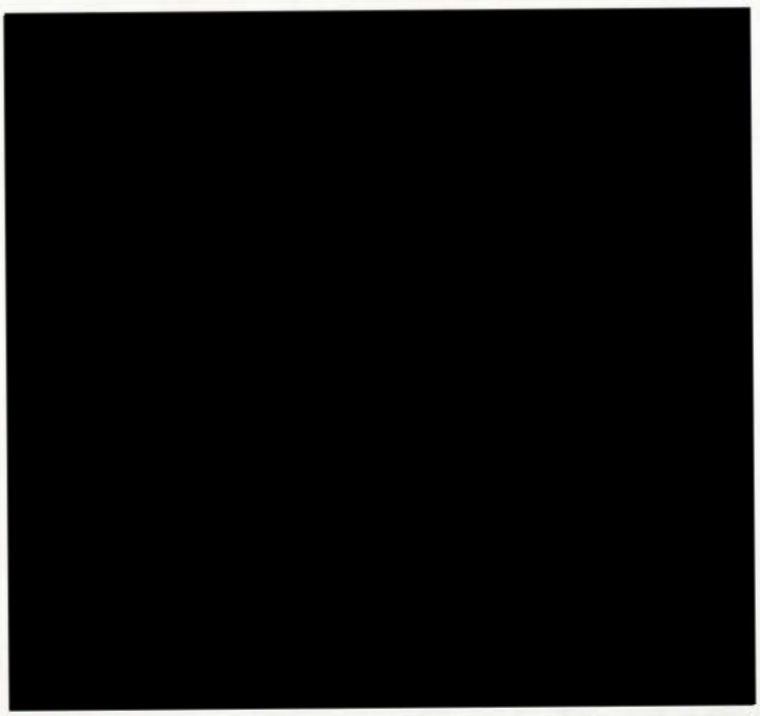

Figure 2 **Typical force-extension curve for vulcanised rubber (L. Treloar [16])**

It can be seen that in rubber high strains at very low stresses are possible when compared with metals. The stiffness changes during the extension and is not linear as for metals in the elastic region. A precise description of the stiffness variation with strain is a prerequisite for Finite Elements Analysis (FEA) simulation of elastomers which has led to a number of material models being developed in the past forty years. The form and plausibility of the values from the stress-strain curve are strongly dependent on the elastomer, crosslinking system, filler material, curing temperature and time, operating temperature, age, loading history, loading rate and the environment. Figure 3 shows the effect of an inactive and active filler in comparison with the unfilled elastomer.

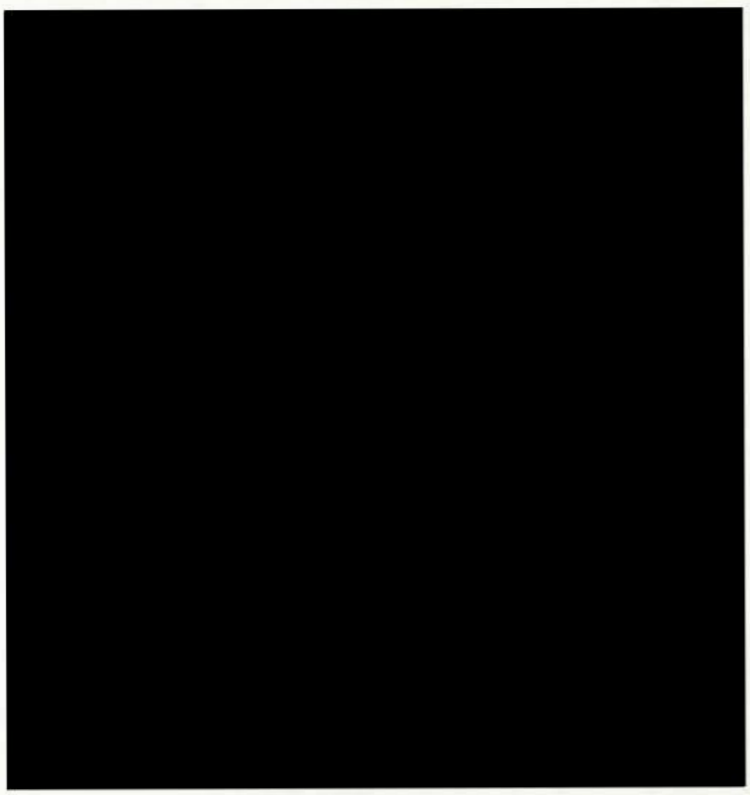

Figure 3 **Stress-strain curve of an amorphous elastomer (G. Kraus [17])**

A **elastomer without filler,**
B **elastomer with an inactive filler,**
C **elastomer with an active filler.**

1.3.2 Temperature Dependence of Properties

Rubber materials show a strong temperature dependency in their physical properties. Mullins [18] has shown the rebound resilience of five different elastomers over a range of temperatures (Figure 4). Different elastomers show a minimum value of rebound at different temperatures. These minima are known to correspond to a maximum of the loss factor. This point is called the glass transition temperature and is a specific value for each polymer and the applied frequency or velocity of the test (see also Frequency Effect and Figure 12).

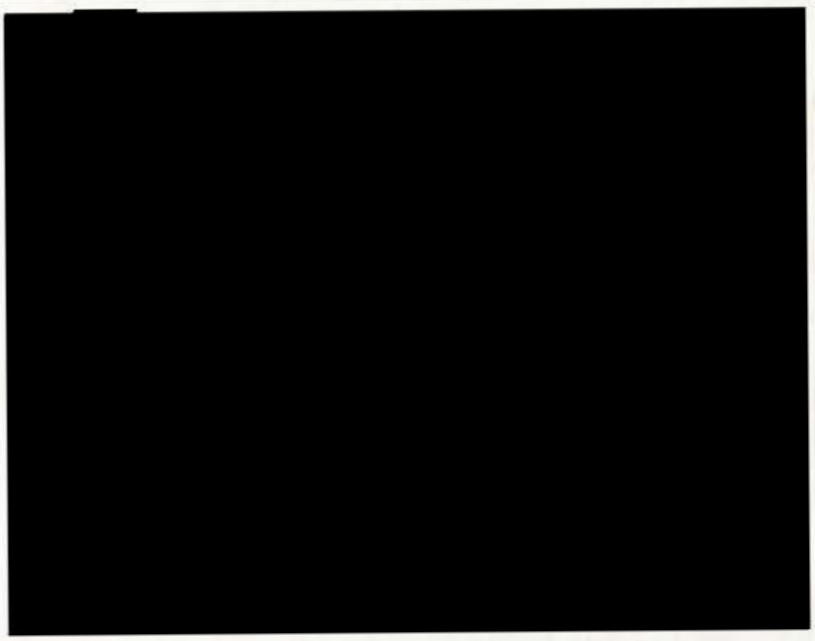

Figure 4 **Rebound resilience as a function of temperature. (L. Mullins [18])**
(1) Natural rubber. (2) GR-S (butadiene-styrene).
(3) Neoprene (polychloroprene). (4) Hycar OR-15 (butadiene-acrylonitrile).
(5) Butyl rubber.

Figure 5 depicts the different temperature regions for a single elastomer. This temperature behaviour is similar for a lot of elastomers with the exception of inhomogeneous blends. Elastomers are commonly used in the rubbery region and occasionally in the transition region if higher damping is needed, indicated

by the maximum of the loss factor tan δ. In the glassy region the elastomer is frozen and hard as well as brittle, not unlike glass and the complex modulus is about 1000 times higher compared with the rubbery region.

Figure 5 **Effect of temperature on dynamic properties. (L.P. Smith [19])**

1.3.3 Amplitude Dependence of Dynamic Properties - Payne Effect

The amplitude dependence of dynamic properties of elastomers with active fillers was described by A. R. Payne [**4, 5**]. His experiments have shown that active fillers increase the modulus of elastomers tremendously at very low dynamic strain amplitude. When increasing the dynamic strain amplitude the modulus of these elastomers decreased significantly (Figure 6).

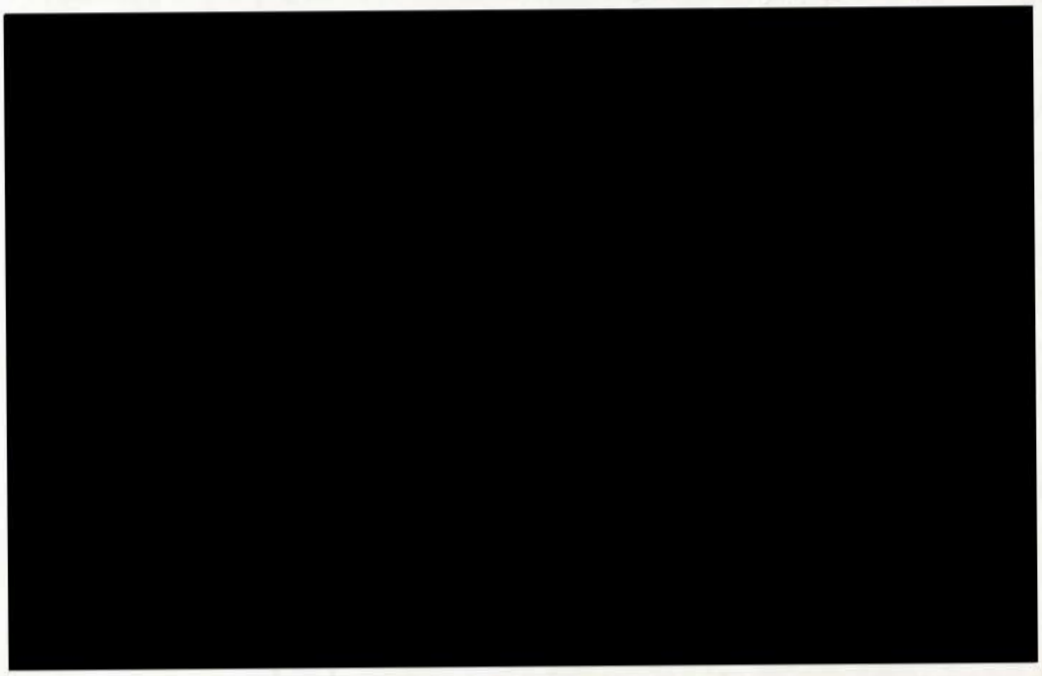

Figure 6 **Dependency of Young's modulus E* on the dynamic double strain amplitude for a natural rubber vulcanisate containing various proportions of carbon black. (A.R. Payne [4])**

At very high strain amplitudes the modulus gets closer to the modulus of the unfilled rubber. This so called Payne-Effect is directly dependent on the amount of filler in the elastomer. While the modulus decreases with increasing strain amplitude the loss factor tan δ increases till a filler and filler concentration specific maximum is reached, as shown in Figure 7.

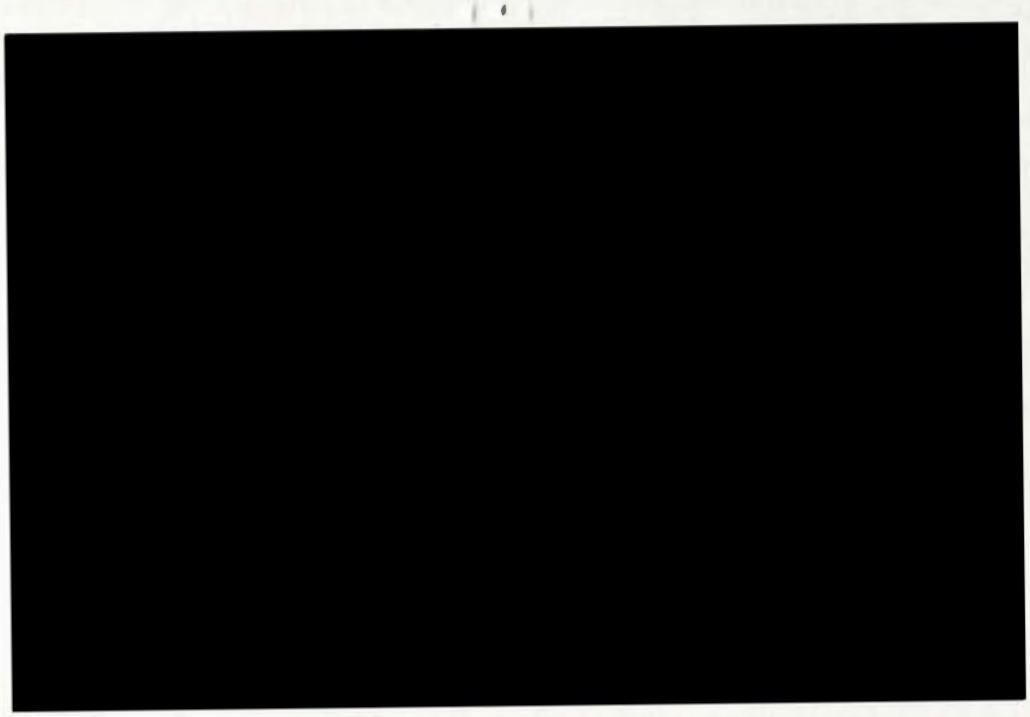

Figure 7 **Dependency of the loss factor tan δ on the dynamic double strain amplitude for a natural rubber vulcanisates containing various proportions of carbon black. (A.R. Payne [4])**

Active fillers are carbon blacks and silica with a special microstructure and crystalline form. Other fillers show no or minimal dynamic amplitude effects.

A. R. Payne gave an explanation for the behaviour at different dynamic amplitudes. The rapidly changing part of the modulus curve is related to the structure effects or otherwise the filler-filler interactions (Figure 8).

The strain independent contributions to the modulus are firstly referred to the modulus of the unfilled rubber. A second contribution is connected to the hydrodynamic effect of the hard, solid filler in the rubber matrix. The third strain independent contribution is brought about by a few strong links between the filler surface and the polymer matrix, called polymer-filler-interactions.

Figure 8 **A qualitative interpretation of the shear modulus, strain amplitude curves. (A.R. Payne [5])**

1.3.4 Stress Softening - Mullins Effect

The stress softening phenomena in filled or unfilled rubber materials are called Mullins Effect. Mullins examined this effect very closely in the 1940's and 1950's and in one publication **[20]** described many different stress softening effects. Figure 9 shows the typical Mullins effect. One unfilled NR test specimen is stretched several times to a fixed elongation and with every cycle the resultant load is reduced. After the first cycles the loss in stiffness is greatest and with successive cycles the reduction in stiffness loss is reduced.

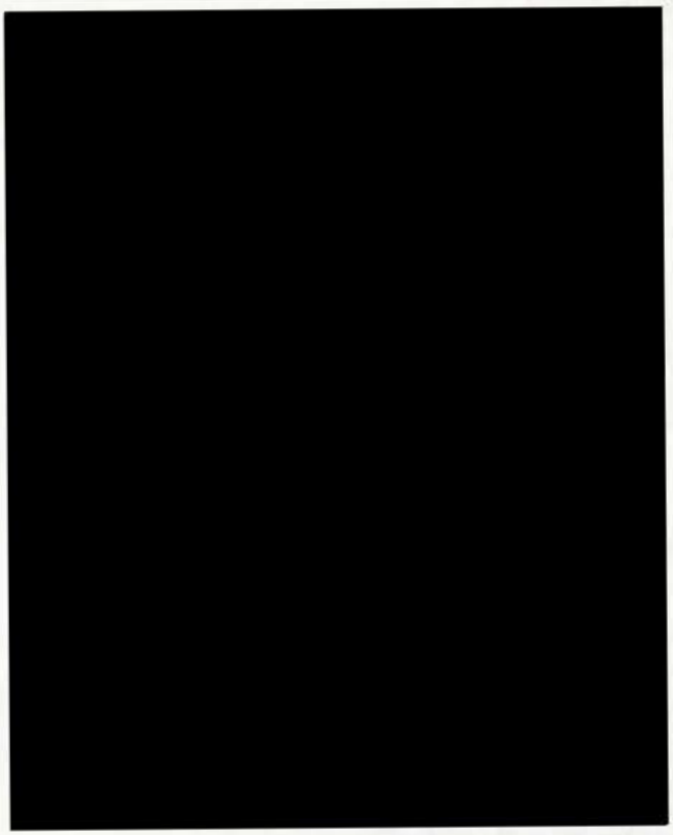

Figure 9 **Effect of repeated stretching on load-extension curves of NR vulcanizate gum. (W.L. Holt [21])**

The Mullins Effect is much greater in highly filled rubber with active carbon black.

Results of tests on a tyre tread vulcanisate have also shown that most of the softening occurs in the first extension and after three or four successive extensions, further softening was very small. The softening effects are explained by the breakdown of the filler structure which includes interactions between the surfaces of the filler particles and the rubber as well as the breakdown of filler aggregates.

A visualisation of the stress softening in filled elastomers in shown in Figure 10. The result of the molecular slippage is an alignment of the chains with an increase in length which prevents their rupture and so increases the strength. This uniformly distributes the applied stress and brings about a reinforcement of the compound. Secondly this process leads to a softening of the whole network at small strains.

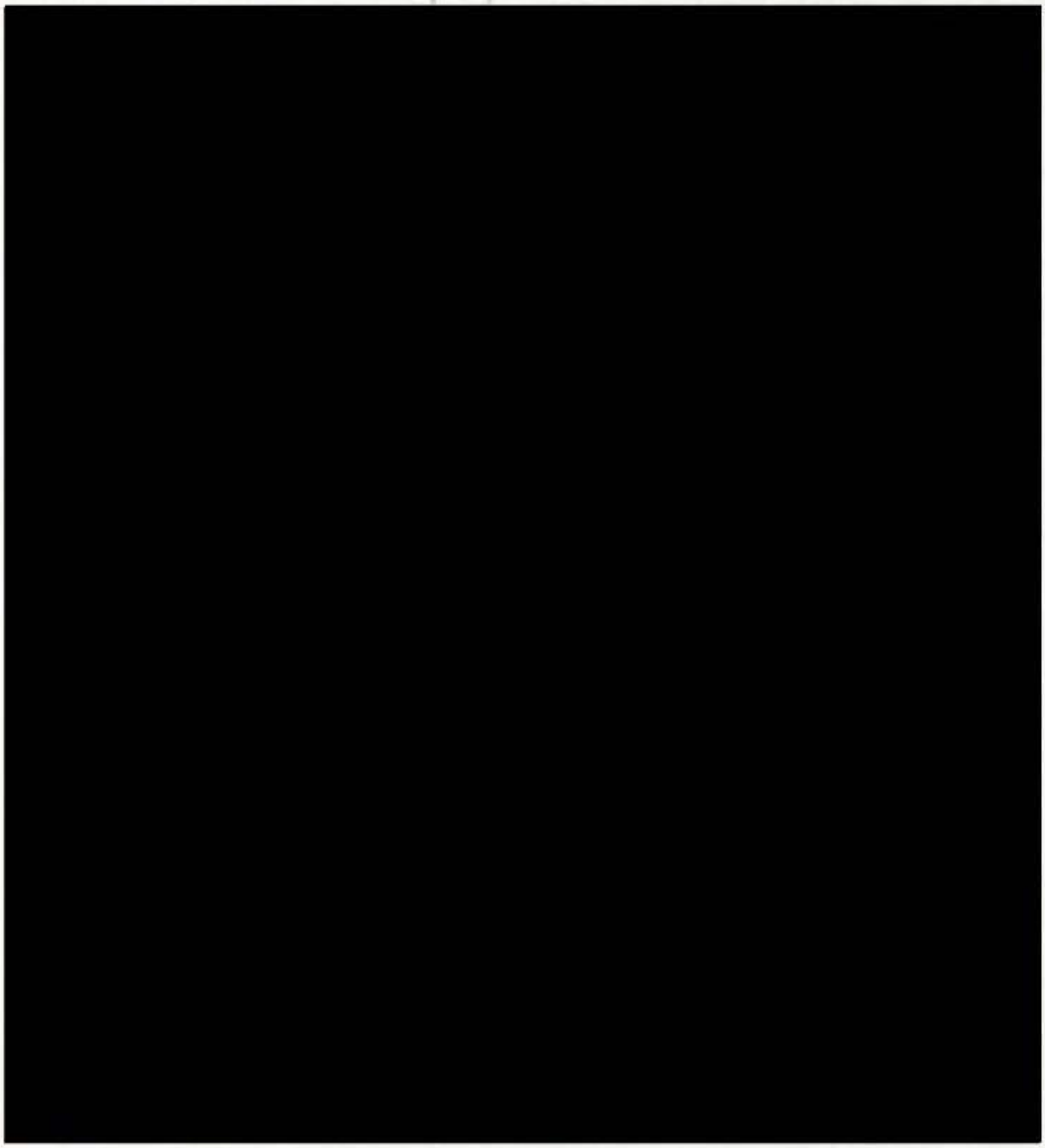

Figure 10 **Schematic diagram showing slippage of chains attached to two filler Particles. (E.M. Dannenberg [22])**

A rubber which has been softened by previous stretching shows recovery towards its initial stress-strain properties on standing. Recovery is small at normal (room) temperatures and more rapid and more complete at higher temperatures.

Figure 11 shows that in tensile stress-strain tests, considerable softening was only present at elongations less than the previous stretch and that at higher

elongations the stress-strain curve was relatively unaffected by previous stretching.

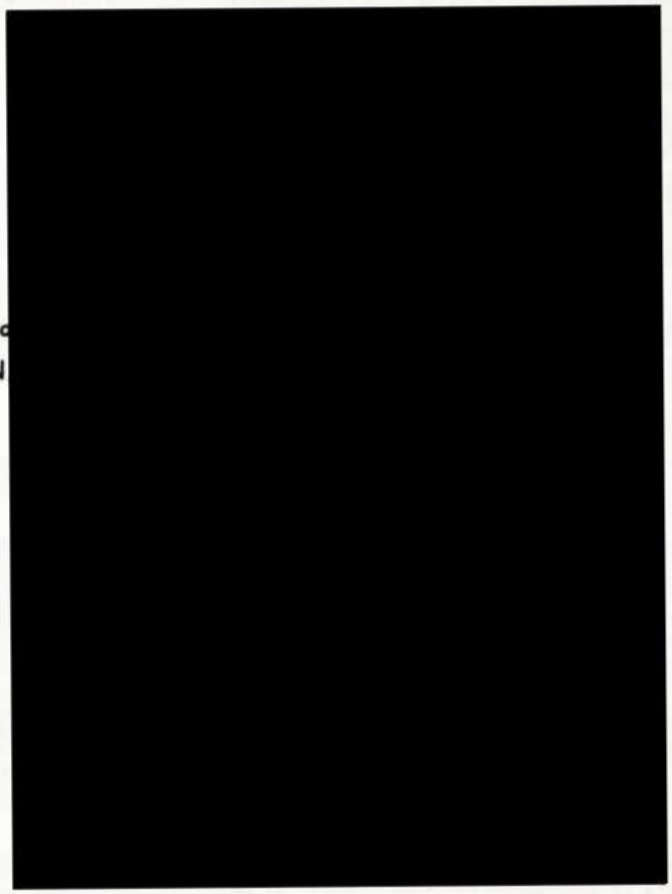

Figure 11 **Stress induced softening of a carbon black-filled vulcanised copolymer of styrene and butadiene (25:75);**
- - - stress-strain curve of a corresponding unfilled vulcanisate.
(A.V. Tobolsky [23])

1.3.5 Frequency Effect

The stiffness or modulus of elastomers depend strongly on the applied excitation velocity or frequency. Figure 12 shows the relative deformation for different frequencies plotted against the test temperature. These tests by Aleksandrov and Lazurkin 1939 [**24**] have been carried out under load (stress) control.

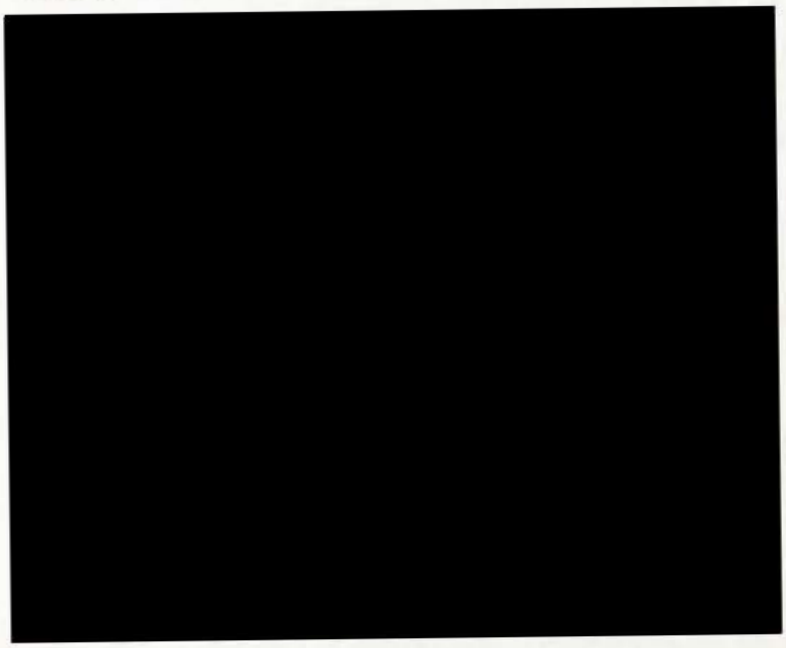

Figure 12 **Relationship between frequency of vibration and temperature at various Frequencies for natural rubber. (Aleksandrov [24])**

It can be seen that with increasing frequency the relative deformation decreases for a particular temperature. This means the stiffness of the material increases with increasing frequency. The diagram also shows the temperature related behaviour of the material at a particular frequency (see also, 1.3.2 Temperature Dependence of Properties, page 9).

1.3.6 Strain Induced Crystallisation

A few elastomers show an increased tensile strength at high strains with an upturn in the stress strain curve (Figure 13).

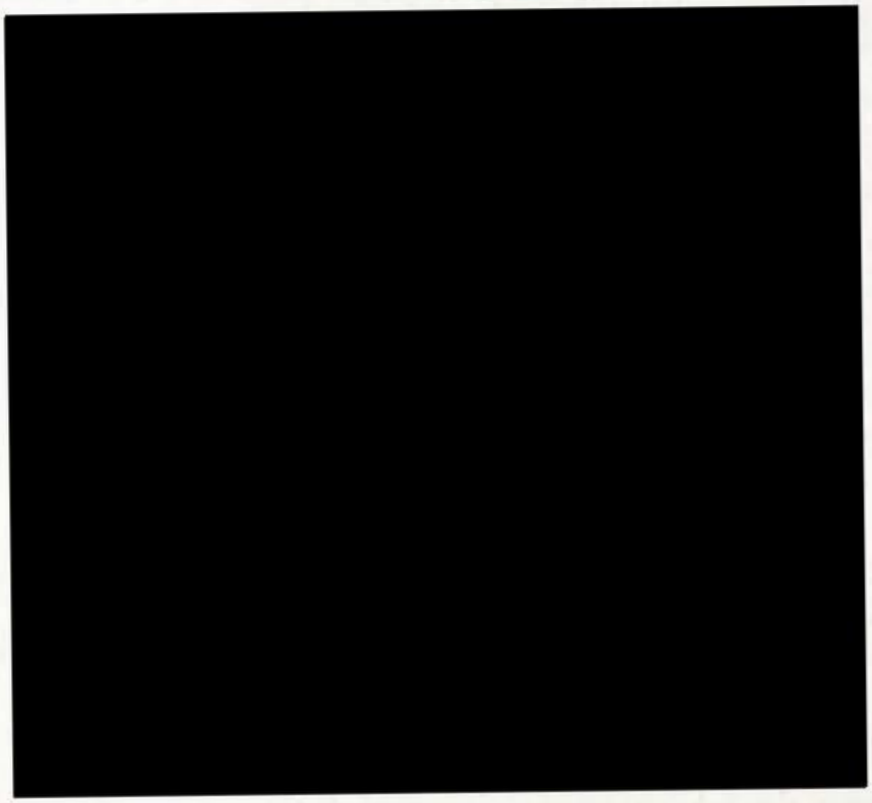

Figure 13 **Stress-strain-curve of different polymers (U. Eisele [25]).**

This effect is called "strain induced crystallisation" and can be seen for example in NR, IR and BR. The increase in tensile strength is caused by the high orientation of the cross linked macro molecules of the network.

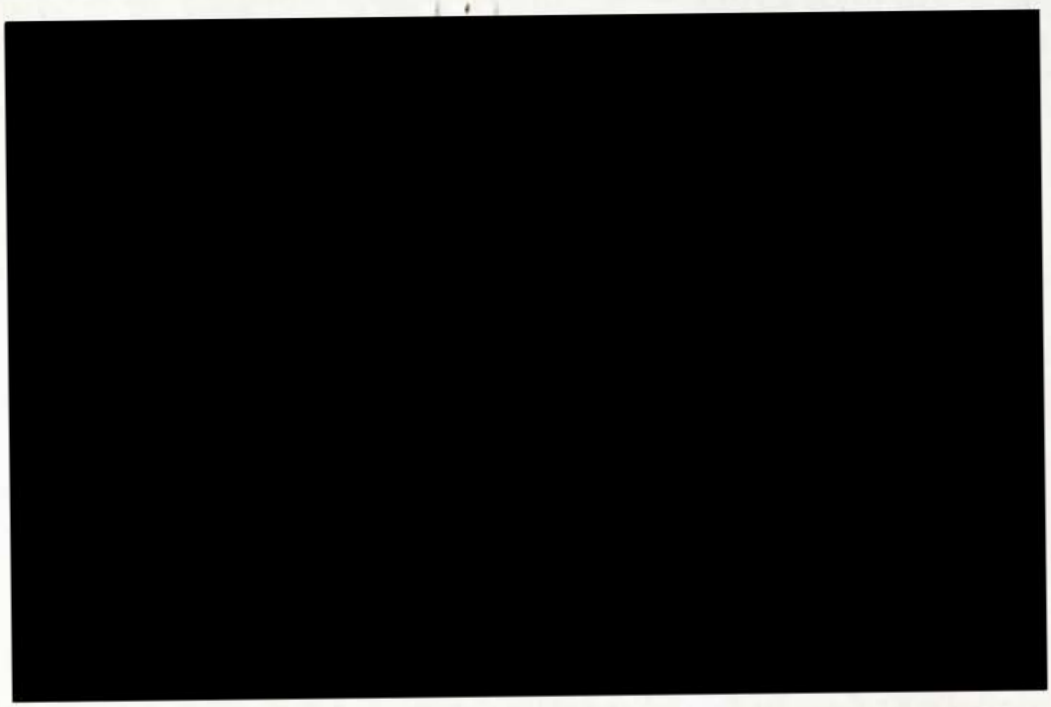

Figure 14 **Stress-strain-curve of a cured rubber – a: experimental; theoretical (U. Eisele [25]).**

Figure 14 shows a theoretical stress strain curve contrasted with an experimental curve of a vulcanised elastomer. Also sketches of the unstretched network (with a statistical distribution), the stretched network and the highly stretched and orientated system are also shown in the diagram. The high orientation of the macromolecules causes the increase in tensile strength and in X-ray measurements, the crystallites (Figure 15) in the highly stretched regions of the elastomer can be seen.

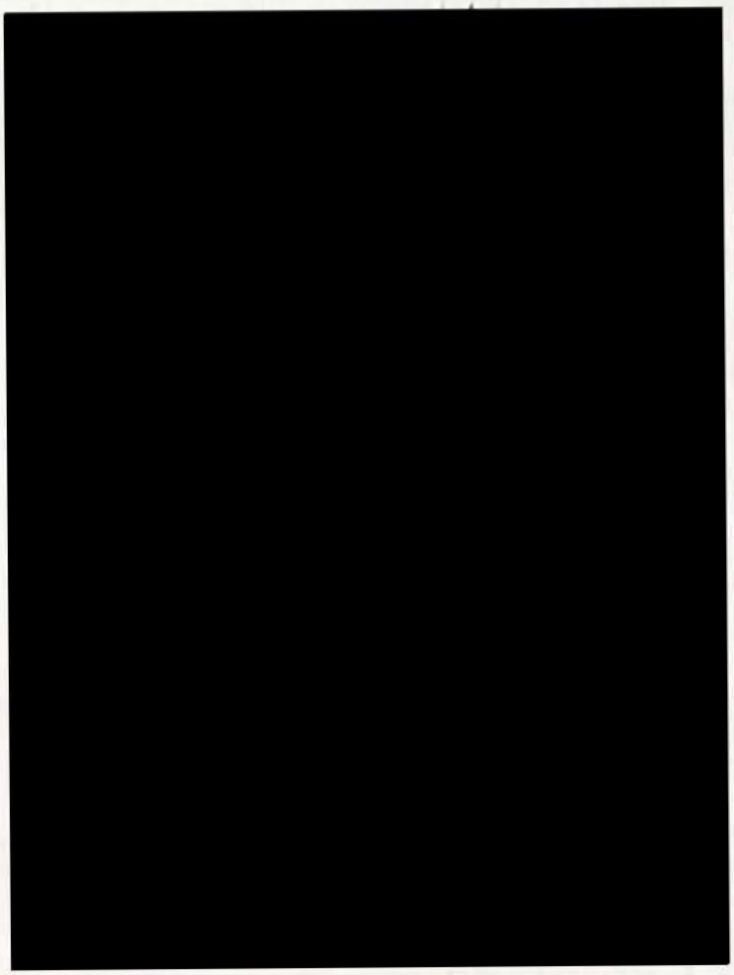

Figure 15 **X-ray diagram showing different distances to the crack tip of a five times stretched NR-test specimen (U. Eisele [25]).**

A comprehensive account about the crystallisation and morphology of rubber was published by Magill **[26]**.

1.4 Literature Search – Fatigue and Fracture Mechanics

In the literature, only a limited number of papers have been published dealing with fatigue properties of elastomeric materials.

Although elastomeric materials exhibit very high strains for relatively small stresses, making them appropriate for many commercial, industrial and automotive applications, they still have behaviour in common with other materials. In particular they have a limiting strength and tend to fatigue. Mechanical fatigue of elastomers is manifested in a progressive reduction of the physical properties as a result of crack propagation during continuous dynamic excitation. Well founded research into metals [**27, 28**] has shown that fatigue results from atomic and molecular processes. Similar research for elastomers is at a very early stage, because of the complex interaction between polymers, fillers, softeners and other additives. Predictions of the fatigue properties of elastomeric materials and components are currently partially empirical in nature. Though there are levels of stress or strain below which elastomers will not suffer fatigue damage, such limits are not well established. There are few Wöhler curves [**29**] in the literature for rubbers due to the inordinate amount of time required to collect the data. Producing durable rubber automotive components, despite the increasing use of FEA, remains a challenge. The question of determining a sole criterion for predicting elastomeric fatigue is unresolved. Arguments have been made that fatigue resistance is dependent on stress [**11, 12**], strain [**10**] and also dynamic strain energy per unit volume [**13, 14**]. All energy concepts are based on the strain energy release rate first postulated by Griffith [**30**]. Griffith assumed that, the

elastic energy of a cracked plate would be entirely converted into crack surface energy. The Griffith criterion can be applied to metals but the work is based on tests on glass.

When characterising crack propagation and fatigue properties, there are two problems unique to elastomers that must be surmounted for a computer simulation to model fatigue:

i) Fatigue properties of rubber are not only dependent on the basic chemical composition of the polymer, but also on individual considerations like the particular cross-linking system and the ageing protection applied to it.

ii) As a result of their hyperelastic and viscoelastic properties, elastomers behave with sensitivity to the application of different modes of loading, frequencies, strain rates and temperatures.

Each of these problems proves the importance of optimising a material definition so that it can represent the physical behaviour that a component experiences in service. Additionally, component testing must realistically represent in-service behaviour to allow accurate determination of fatigue characteristics.

1.4.1 Tearing Energy

Early theoretical approaches to the crack growth rate in rubbers were published by Rivlin and Thomas [**13, 31**]. They defined the tearing energy 'T' as the decrease of elastic strain energy caused by the growth of the crack per unit area, with 'W' as the total elastic energy and 'A' as the crack area of the crack surface. In equation (1.1) the index '/' indicates that the specimen is held under constant deformation so that applied external forces do no work.

$$T = \left(\frac{\delta W}{\delta A}\right)_l \tag{1.1}$$

The tearing energy 'T' has the same definition as 'G' the "strain energy release rate" or the "fracture energy" which is used for plastics and metals. In Figure 16 the most commonly used test specimens are shown. For the "tensile strip" or "single edge notched" SEN-specimen (Figure 16a) the tearing energy can be calculated using the following relations [**32**, **33**, **34**].

$$T = 2 \cdot k \cdot W_0 \cdot c \tag{1.2}$$

$$k = \frac{\pi}{\sqrt{\lambda}} \tag{1.3}$$

'W_0' is the strain energy density at distance from the crack (i.e. strain energy divided by the specimen volume), 'c' is the crack length and 'k' a constant.

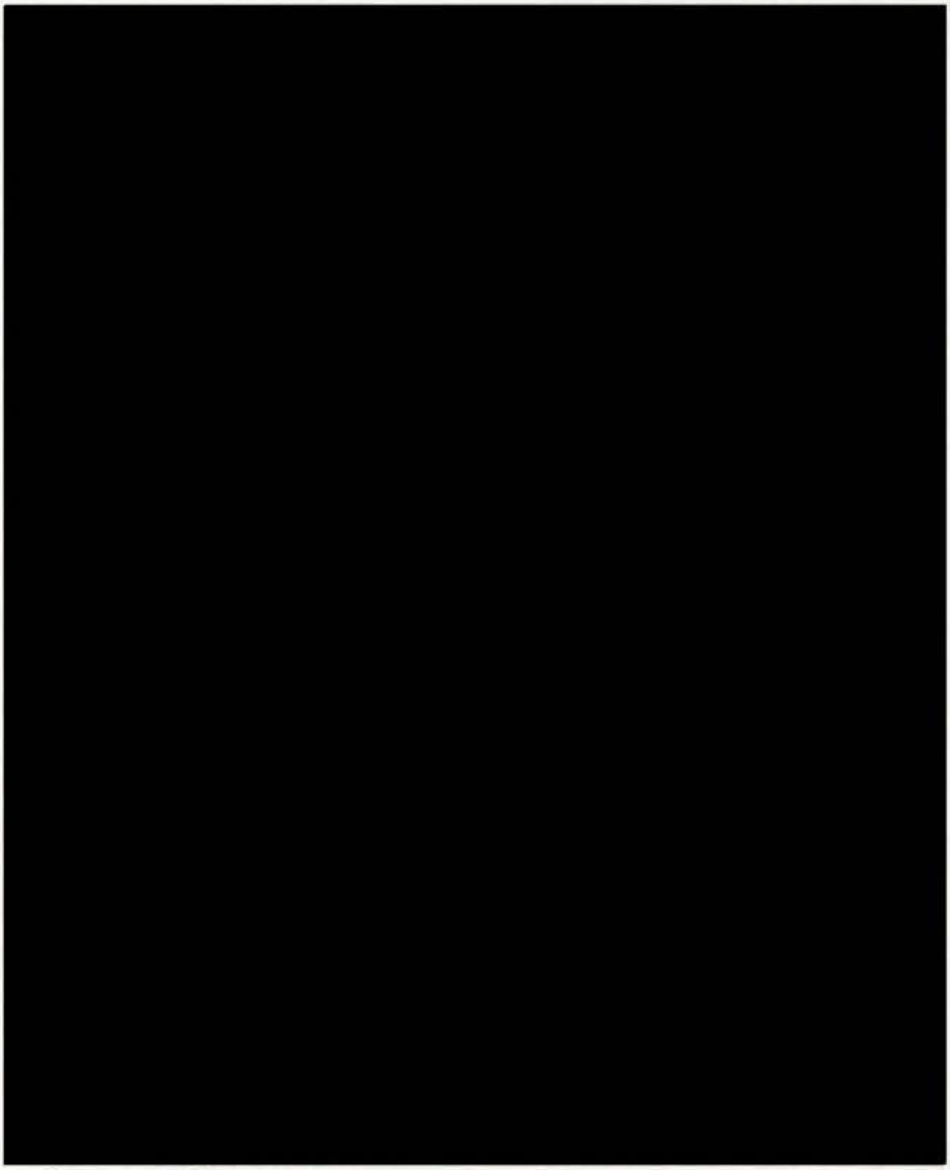

Figure 16 **Crack growth test specimens, (R. Seldén [35])**

a) single edge notched, SEN or tensile strip,

b) "trouser" specimen,

c) centre notched,

d) pure shear specimen

For the trouser test specimen in Figure 16b the tearing energy can be calculated with equation (1.4):

$$T = \frac{2 \cdot F}{t} \qquad (1.4)$$

with 'F' as the applied force and 't' the specimen thickness. The legs should not extend significantly.

Figure 16c gives the tearing energy in the case of the centre notched specimen:

$$T = \frac{\pi \cdot W_0 \cdot c}{\lambda^{1/2}} \tag{1.5}$$

The tearing energy of the pure shear specimen as shown in Figure 16d is calculated with equation 6 where 'h' is the height of the undeformed specimen.

$$T = W_0 \cdot h \tag{1.6}$$

1.4.2 Fatigue Crack Growth

The tearing energy for a notched specimen under cyclic loading (as shown in Figure 16a) can be calculated using equation (1.2) **[35]** by using the maximum strain energy density 'W_{max}' at $\lambda = \lambda_{max}$ instead of 'W'. The calculated tearing energy is correlated with the measured crack length as a function of the number of cycles in Figure 17. The tests have been carried out at several tearing energies and a typical diagram is shown in Figure 18 for an unfilled NR.

Figure 17 **Relationship between rate of crack growth, dc/dn, and tearing energy, 'T' for natural rubber. (A.N. Gent [8])**

- ● **SEN-specimens**
- △ **trouser specimens**
- ▲ **pure shear specimens**

Typical crack growth curves can be divided into four regions as depicted in Figure 18 [**36, 37, 38, 39**].

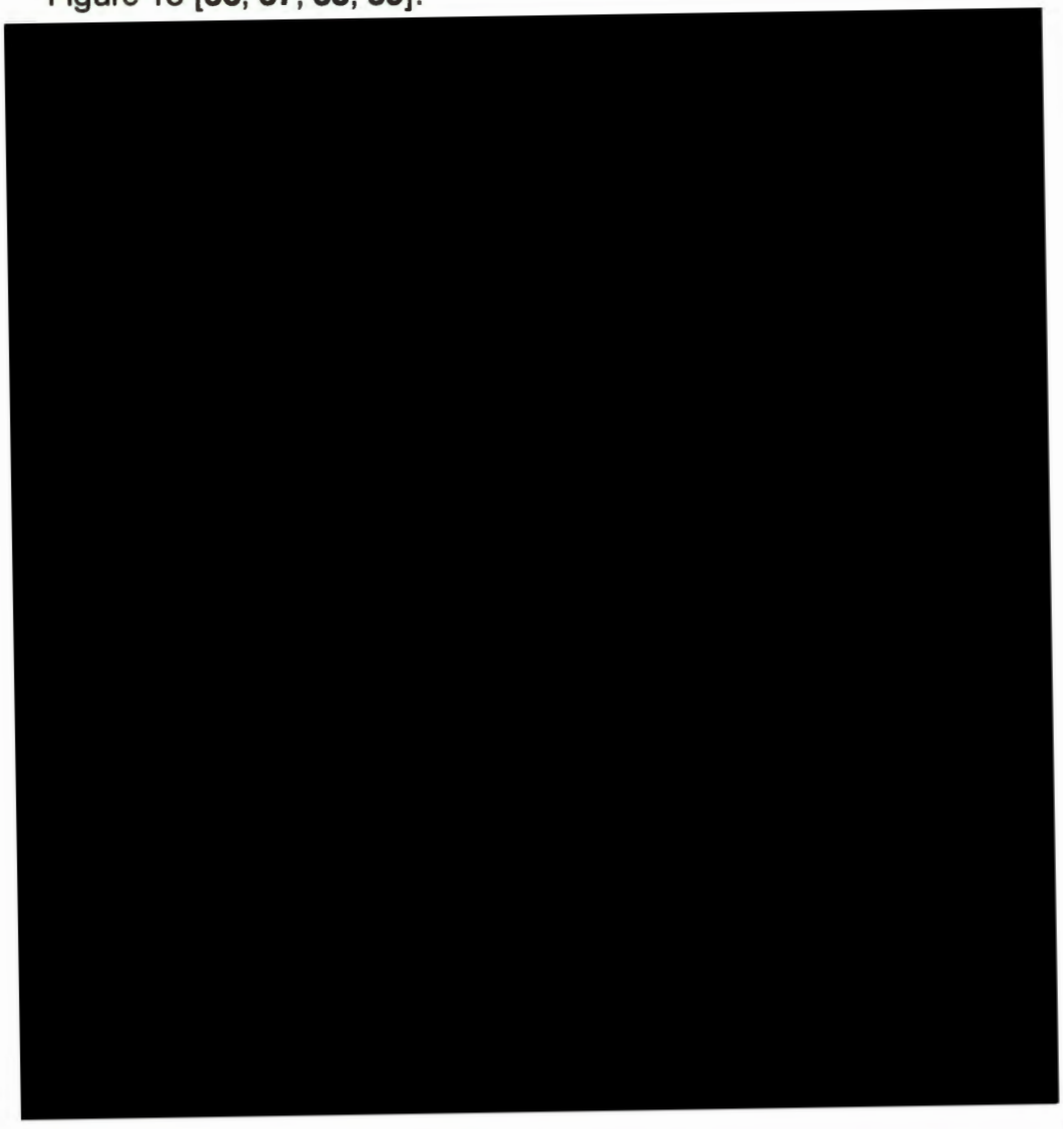

Figure 18 **Crack growth rate, dc/dN, vs. tearing energy, T for unfilled NR in laboratory atmosphere at 1.67 Hz (R. Seldén [35]).**

At sufficiently low tearing energies ($T<T_0$) the crack propagation rate is very low and independent of the tearing energy and given by:

$$\frac{dc}{dN} = \frac{F}{f} \cdot \alpha \cdot q = \text{constant} = r \qquad T<T_0 \qquad (1.7)$$

'r' is a constant independent of 'T', while 'F' is part of the load cycle during which the material is loaded at 'f' the testing frequency. 'q' is the ozone concentration in the surrounding medium (usually air) and 'α' a material constant equal to the static crack growth rate per unit ozone concentration in air. 'T_0' denotes the fatigue threshold and is the limit below which no mechano-oxidative crack growth will occur.

If the tearing energies are immediately above the threshold, the following relation applies for most rubbers, were 'A' is a constant:

$$\frac{dc}{dN} = A \cdot (T - T_0) + r \qquad T_0 < T < T_t \qquad (1.8)$$

A linear relation between crack growth rate and tearing energy exists in this region.

At intermediate and high tearing energies a power law relation often applies. Similar relations hold for many polymers and metals.

$$\frac{dc}{dN} = B \cdot T^{\beta} \qquad T_t < T < T_c \qquad (1.9)$$

'B' and 'β' are material constants.

The highest tearing energies follow from this equation:

$$\frac{dc}{dN} = \infty \qquad T > T_c \qquad (1.10)$$

An unstable crack growth occurs in this region. The magnitude of T_c can be determined by a tensile test having the geometry described earlier.

1.4.3 Calculation of the Fatigue Life

Two different approaches are used for the simulation of the fatigue life of a component. The fatigue method compares the calculated maximum stresses in a component with the maximum stresses obtained by fatigue to failure tests [11]. The disadvantages of this method are that it is necessary to calculate the maximum stresses existing in the loaded component with great accuracy using complicated methods like Finite Elements Analysis. In addition many long-term fatigue tests under conditions that replicate service conditions are needed for a precise prediction of the service life.

The second method uses the crack growth approach. This approach requires the calculation of the cycles to failure using material properties obtained from crack propagation tests [8]. For this method it is necessary to know the initial effective size of the natural occurring flaws in the component and the size of surface defects from which a crack will grow. Furthermore, it is essential to know which strains and elastic energies exist in the component to perform the calculation. To determine these values it is again necessary to carry out Finite Element analyses. In addition to this, the equation published by Gent [8 relies solely on the geometry of a tensile strip test specimen. Components having a more complex design need an individually defined equation for the calculation of the service life.

2 Materials and methods

2.1 Materials

For the first tests an ethylene propylene rubber (EPDM) was used because of its non strain crystallising behaviour. The EPDM used in the fatigue tests, was Buna EP G 5450. The chemical composition is described in Table 1. The carbon blacks used for the filled material were chosen to represent a material with a low to medium level of reinforcement.

The unfilled EPDM test specimens, tested to establish the influence of the active filler, contained all the chemicals except carbon black and oil.

All compounds were mixed in a GK 1,5 E (1.5 litres) laboratory internal mixer and the curing agents were added on a laboratory roller mill. The vulcanisates for all materials were made using a compression mould at a curing temperature of 160°C. Two batches were prepared for each material, one for the dumbbell test specimens and one for the tensile strip specimens.

EPDM	**100.0 phr**
Carbon black N550	**70.0 phr**
Carbon black N772	**40.0 phr**
Stearic acid	**1.0 phr**
Zinc-oxide	**5.0 phr**
Oil Sunpar 2280	**70.0 phr**
Sulphur	**1.5 phr**
Accelerator CZ (CBS)	**1.0 phr**
Accelerator Thiuram (TMTD)	**0.8 phr**

Table 1: Chemical composition of the filled EPDM material.

This material is not typical for dynamic applications, but it is used in DIK to show the influence of different mixing procedures on the physical properties of

the cured rubber. For the fatigue test specimens, an optimised mixing procedure assures a good carbon black dispersion. Previous investigations have shown that well mixed and softer material show an increase in service life under displacement control, compared with less thoroughly mixed EPDM [40]. The latter harder material almost reaches the fatigue properties of the well-mixed compound under load controlled tests.

A non strain-crystallising elastomer, was also used for the second test series. Styrene-Butadiene Polymer, SBR 1712 is a standard E-SBR containing 37.5 phr softener oil. The chemical composition of the carbon black filled SBR is described in Table 2. The N234 used represents an active carbon black with high reinforcing properties.

The unfilled SBR test specimens, used to establish the influence of the active filler, contained all the chemicals except carbon black.

SBR 1712	**137.5 phr**
Carbon black N234	**70.0 phr**
Stearic acid	**2.0 phr**
Zinc-oxide	**3.0 phr**
Antioxidant 6PPD	**2.0 phr**
Antioxidant TMQ	**1.0 phr**
Light protection Antilux 500L	**2.0 phr**
Sulphur	**1.75 phr**
Accelerator CZ (CBS)	**1.0 phr**
Accelerator DPG	**0.4 phr**

Table 2: Chemical composition of the carbon black filled SBR material

The results of the quasi static tensile tests are shown in the following diagrams. The testing facility for the tensile tests utilised a Zwick tensile tester with an

optical device for real strain measurement. The same dumbbell test specimens were used for the tensile tests as those for the fatigue tests in preference to a flat S2-test specimen. A description of the dumbbell test specimen can be found in Section 2.2 Methods of Fatigue Tests (page 38). Two reflecting dots were glued on the cylindrical surface of the small diameter of the dumbbell test specimen and a laser devise incorporated into the Zwick tensile test machine measures the displacement between the dots. With this procedure the real strain can be measured and clamping effects do not influence the results.

The plots of the tensile test results for the unfilled EPDM material are shown in Figure 19. It can be seen that both curves are similar with a very small difference in elongation at rupture.

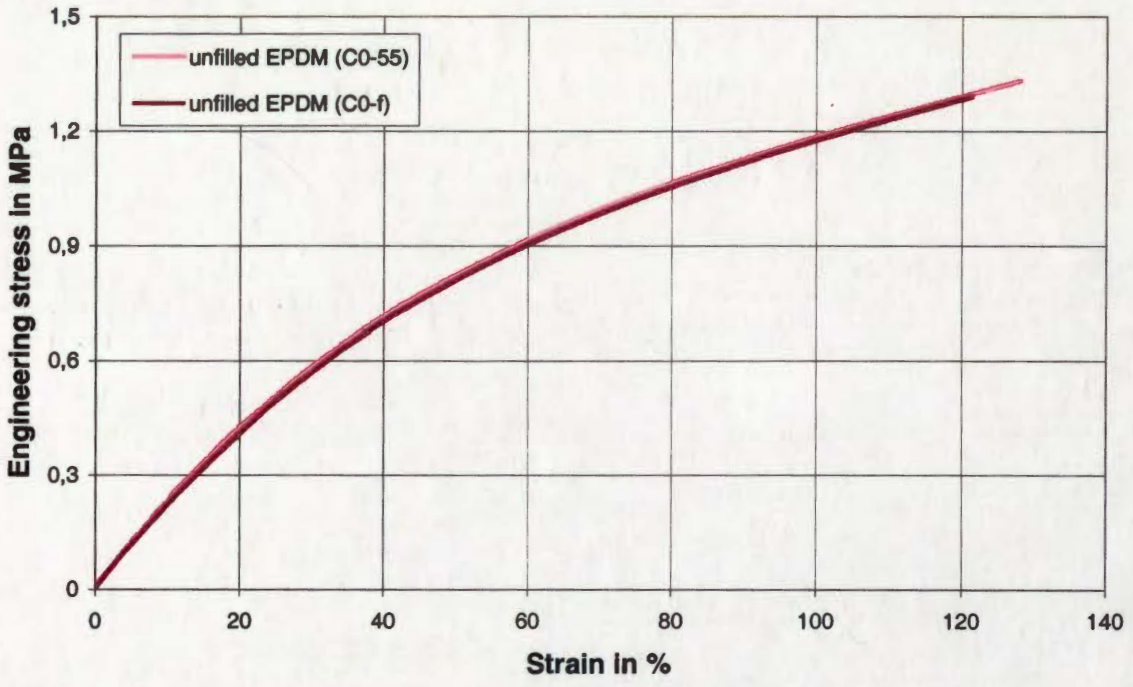

Figure 19 **Plot of the quasi static tensile test for the unfilled EPDM material.**

The results of the quasi static tensile test for the carbon black filled EPDM are shown in Figure 20. Additionally the results for the unfilled material are plotted

in this diagram. It can be seen that the stresses at the same strain state for the carbon black filled material are much higher when compared with the unfilled material. Furthermore, the elongation in length at rupture is increased by a factor of 2.

Another difference is the change of slope of the curve of the carbon black filled material. At approximately 100% strain the tensile curve starts to turn up. It can be seen that the two curves of the filled material do not match as well as the ones for the unfilled material. The reason for this behaviour can mainly be found in the slippage of the test specimen in the clamps at high loads.

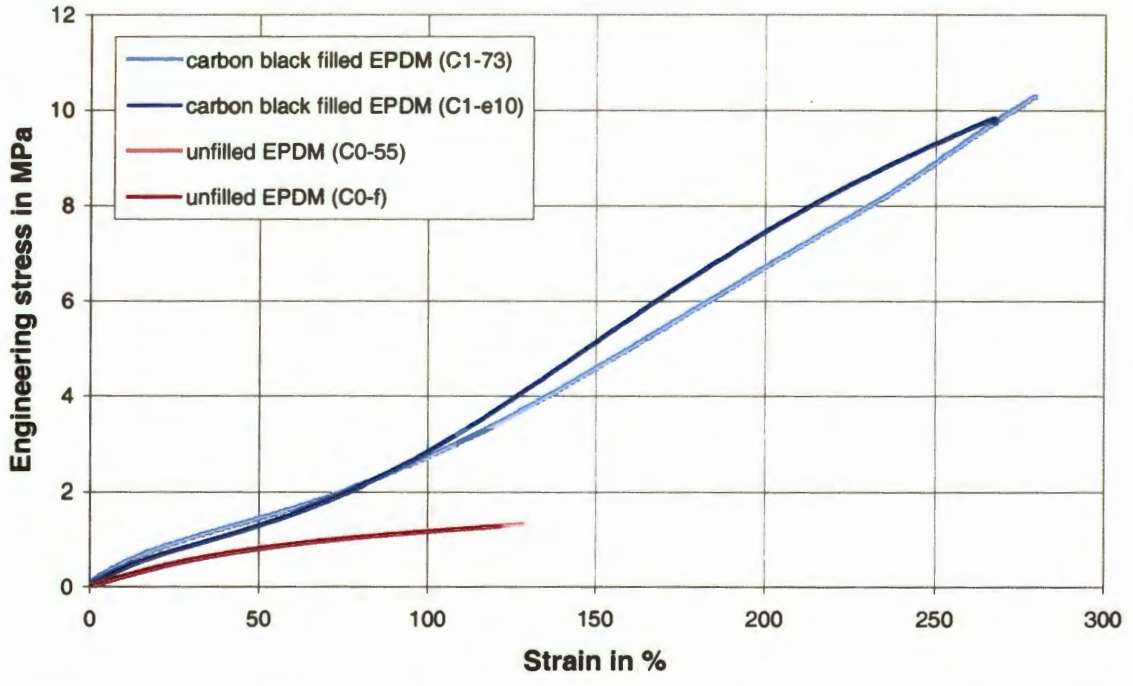

Figure 20 **Plot of the quasi static tensile test for the carbon black filled and the unfilled EPDM material.**

The results of the quasi static tensile tests for the unfilled SBR are shown in Figure 21. The curves in this plot are similar even for elongation at rupture. As

for the unfilled EPDM material differences are less pronounced in the unfilled SBR material.

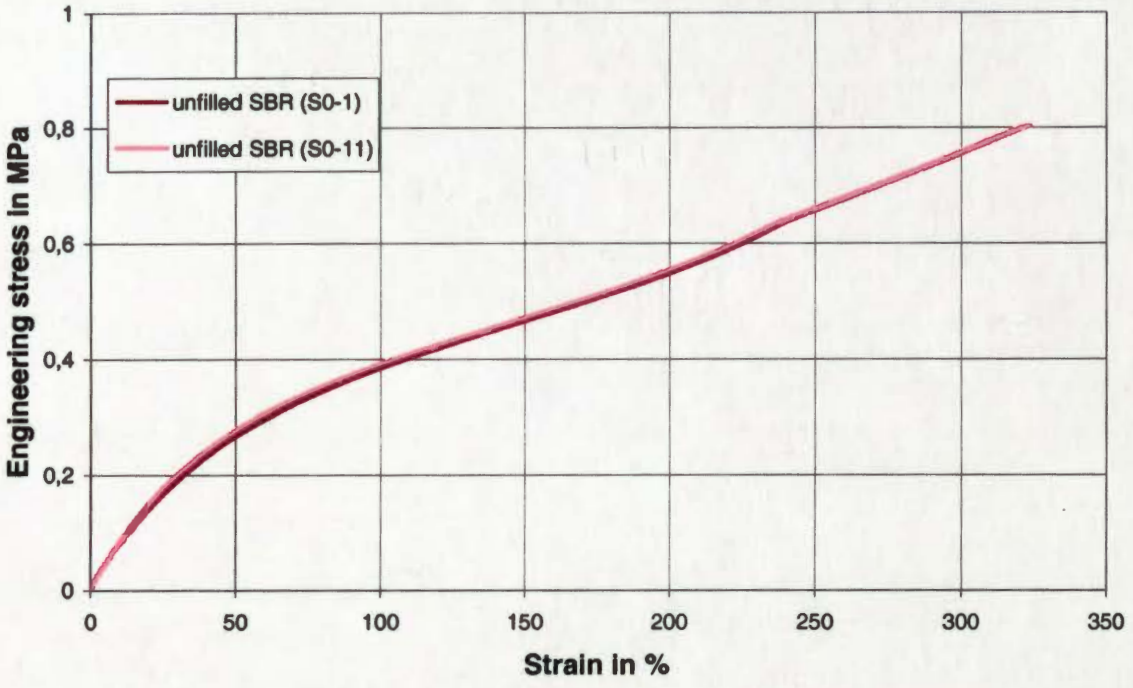

Figure 21 **Plot of the quasi static tensile test for the unfilled SBR material.**

By contrast with the EPDM material it was not possible to measure the elongation at rupture for the carbon black filled SBR, as the test specimen slipped out of the clamps before failure. Figure 22 shows that the tests reached approximately 220% strain, but it can be seen that for the filled SBR the stresses are significantly increased compared with the unfilled material, as is the case for the EPDM material. Similar to that for the filled EPDM, the slope of the carbon black filled SBR shows an upturn at approximately 100%.

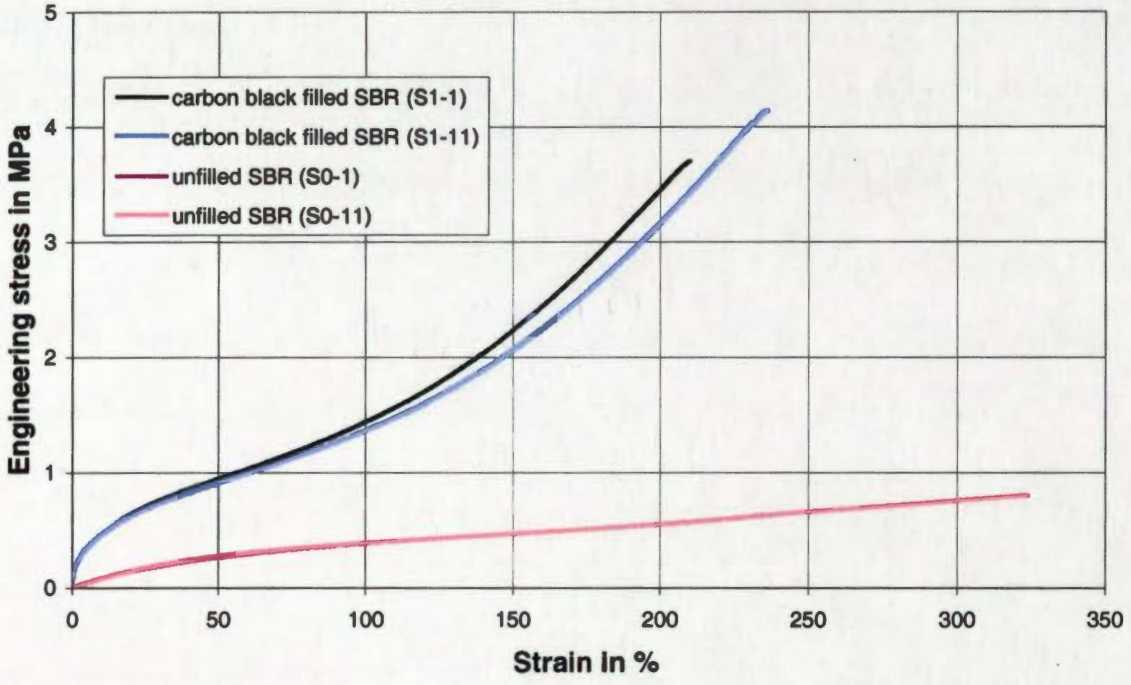

Figure 22 **Plot of the quasi static tensile test for the carbon black filled and the unfilled SBR material.**

2.2 Methods of Fatigue Tests

For the fatigue to failure tests, dumbbell test specimens were used as shown in Figure 23 and Figure 24 shows a test specimen in the clamps. The major and minor diameters of the test-piece were nominally 25 and 15 mm respectively and the fillet radius, essential for allowing the test-piece to be cycled between tension and compression, was 5 mm. The gauge length was 25 mm.

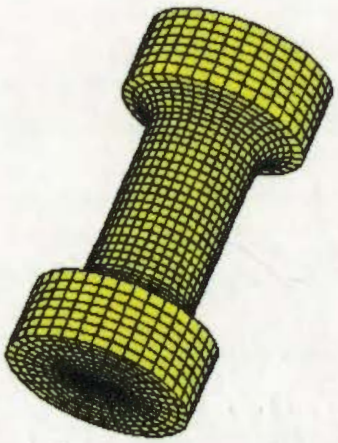

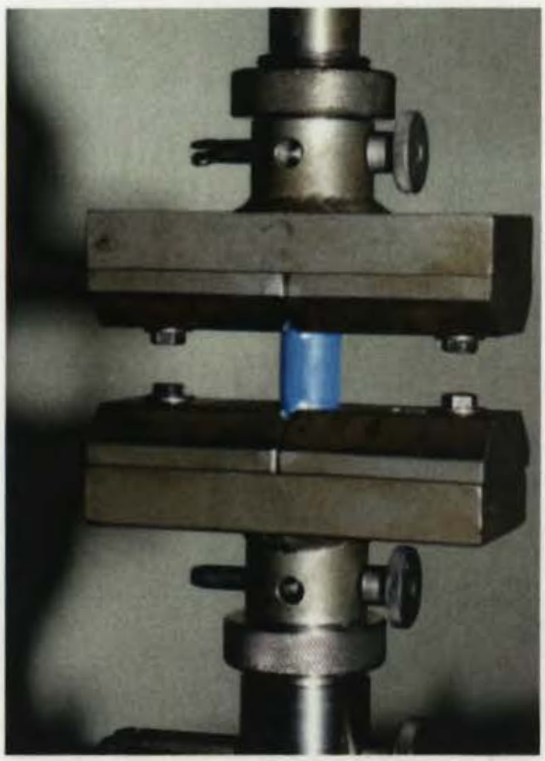

Figure 23 Model of a dumbbell test specimen **Figure 24 Test specimen in clamps**

The geometry of this dumbbell test specimen allows compression up to 30% without the significant barrelling which happens to simple cylindrical test-pieces in compression at much lower strains.

The specimens were tested using an MTS servo-hydraulic elastomer test facility (MTS 831.50) with temperature chamber, possessing the capability of applying frequencies up to 1000 Hz under load or displacement control. For tests under

load control it is necessary to optimise the control parameter (PID and the MTS added F-Parameter) for each material or test specimen design. Otherwise the system can not generate an exact sinusoidal excitation for the extremely non-linear and soft test pieces.

A special elastomer software, TestWare SX, part of the TestStar control software allows the online analysis of the dynamic visco-elastic properties of the tested specimen.

The materials were tested under load control with zero minimum load and different maximum loads to create a Wöhler-curve (σ-n-curve). Both filled materials were also tested over two load ranges by varying the minimum load from compression to tension. For the unfilled materials the minimum load dependency was evaluated for just one load range. All tests were to failure at a frequency of 1Hz. The frequency was chosen to induce failure due to the initiation and growth of cracks as opposed to internal friction causing large increases in temperature and consequent thermal break-down [**35**]. The frequency was the same as that used by Andre' *et al* [**1**] in their tests on NR. All fatigue tests were carried out at room temperature.

Three standard test procedures (Figure 25) were used which are described below.

Procedure 1: Each specimen was subjected to tensile cycles with zero minimum load. The peak load in a test was kept constant, but increased in subsequent tests. The magnitude of the peak load was material specific.

Procedure 2: Each test-piece was subjected to one or two load ranges. The minimum load for each set of tests was initially strongly in compression, rising to a minimum of zero.

Procedure 3: Each test-piece was subjected to one or two load ranges. The minimum load for each set of tests was initially zero, rising to a material dependent minimum load in tension.

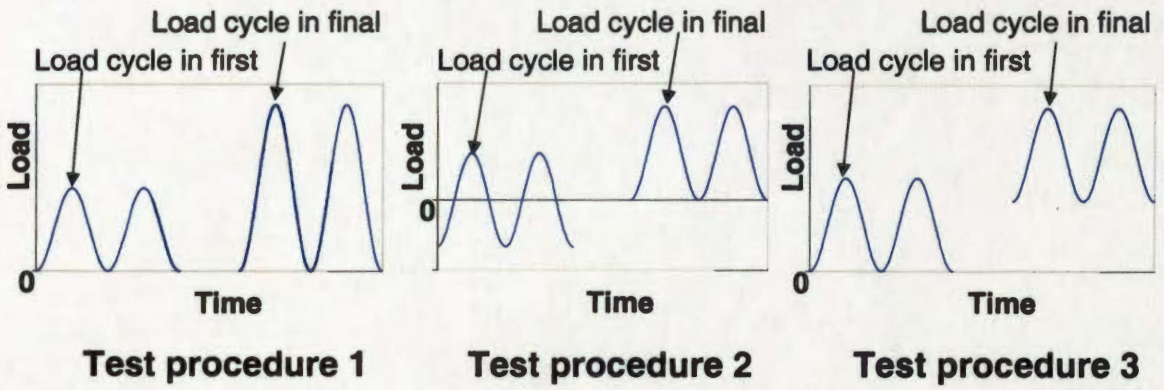

Figure 25 **Three fatigue test procedures**

To determine the influence of fillers on fatigue life, each test procedure was also carried out on specimens that did not contain carbon black and oil. These tests used smaller load ranges for test procedure 1 and only one load range of 180N for test procedures 2 and 3. The smaller load ranges were necessary because of the lower stiffness of the unfilled elastomers.

During all tests the dynamic visco-elastic properties of the test specimens were recorded to evaluate the influence of the different amplitudes and test procedures as well as the changes during the time of cycling.

The visco-elastic properties like E*, E', E'', tan delta [**41**] are defined as for linear elastic materials. These are:

The complex dynamic modulus $$E^* = \frac{\sigma_a}{\varepsilon_a} \quad (2.1)$$

where σ_a is the stress amplitude

ε_a is the strain amplitude

The phase angle between stress and strain δ (2.2)

as shown in Figure 28

The storage modulus $$E' = E^* \cdot \cos(\delta) \quad (2.3)$$

The loss modulus $$E'' = E^* \cdot \sin(\delta) \quad (2.4)$$

To enable the MTS-software to calculate the visco-elastic properties of the rubber materials a sinusoidal regression was chosen. This method uses the major sinusoidal oscillation for the calculation of the dynamic properties and neglects nonlinearities. The alternative DIN-method [**42**] merely uses the end points of the hysteresis loop and its area. The only problem in the sinusoidal regression method is that the higher harmonic contributions to the signal are neglected in the calculation, causing a small deviation or error in the case of non-linear material properties. The main limitation in the calculation of dynamic properties of elastomers is thus the high non-linearity for which principally no

E-modulus is defined. The sinusoidal regression method is however the best compromise in commercially available software solutions.

It is known that internal heat build up during the different test procedures and load amplitudes can lead to problems with the results. All filled specimens tested at high amplitudes reached an internal temperature of less than 55°C while the internal temperature of the specimens tested at lower amplitudes was approximately 30°C. For all unfilled test specimens the internal temperature was not higher than 30°C for all testing conditions. The same is true for differing minimum loads. The chosen frequency of 1Hz is a good compromise between a small heat build up and time consumption for a fatigue test.

To achieve a representative mean value of the fatigue properties, the arithmetic average of between three and seven tests under one condition was used. This was necessary because of the high scatter in fatigue life, although the specimens were produced under exactly similar laboratory conditions.

The fatigue properties of the materials used were plotted against the usual criteria maximum stress, dynamic strain range, stored energy and total energy.

The mean values of all the physical properties were calculated for each test specimen. All data points in the service life diagrams represent the mean values for all test specimens tested under identical condition. The calculation of energies is diagrammatically shown in Figure 26. The dissipated energy is the area within the hysteresis loop in a load vs. displacement diagram. The total energy is the energy which was needed for the deformation. It is represented by the whole area below the hysteresis loop including the dissipated energy (the area marked with vertical lines), while the stored energy is the elastic

stored energy in the rubber. This is the area below the hysteresis loop (the area marked with horizontal lines).

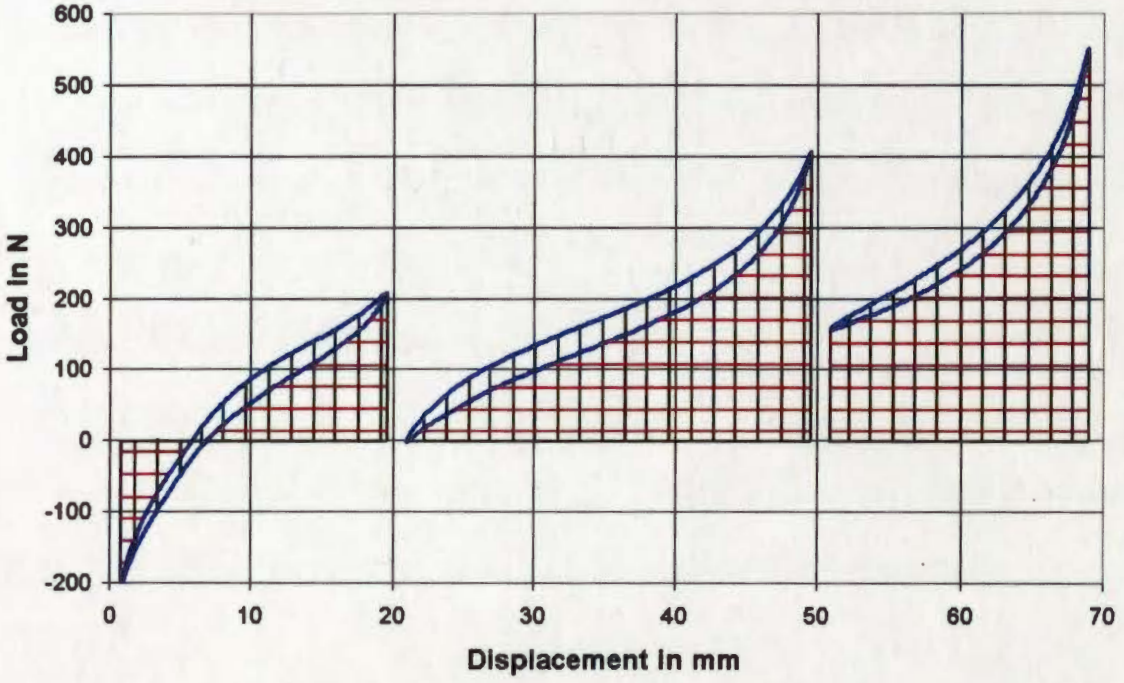

Figure 26 **Diagrammatic representation of the stored energy (area of horizontal lines) and total energy (area of vertical lines) for the different test procedures.**

The calculation of all energies was done using a representative hysteresis loop at a number of cycles equal to 50% of the service life for each specimen.

2.3 Methods of Dynamic Crack Propagation Tests

Single edge notched tensile strip specimens as described in Figure 16a were used for the dynamic crack propagation tests. The dimensions of the test specimens were 55mm length, 15mm width and 2mm thickness. The notches were cut with a razor blade in a holder to ensure an exact perpendicular cut in the middle with length of 1mm.

Dynamic crack propagation properties were investigated with a Coesfeld "Tear Analyzer" System Bayer **[43]** (see Principle Sketch, Figure 27). This servo hydraulic testing facility allows temperature and atmosphere controlled tests under pulsed, sinusoidal, rectangular or free programmable deformation.

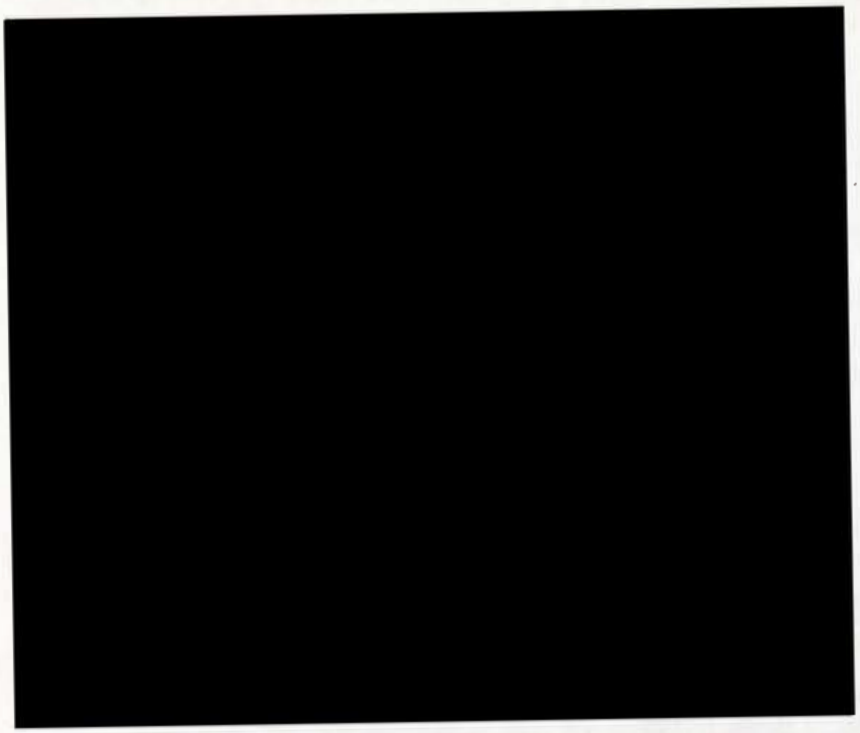

Figure 27 **Principle Sketch of the Tear Analyser (S. Kelbch [44])**

Up to 10 test specimens can be cycled simultaneously, but allowing individual measurement of Load and Displacement vs. Time (Figure 28). From these

data, loss angle, total energy, stored energy and dissipated energy were calculated.

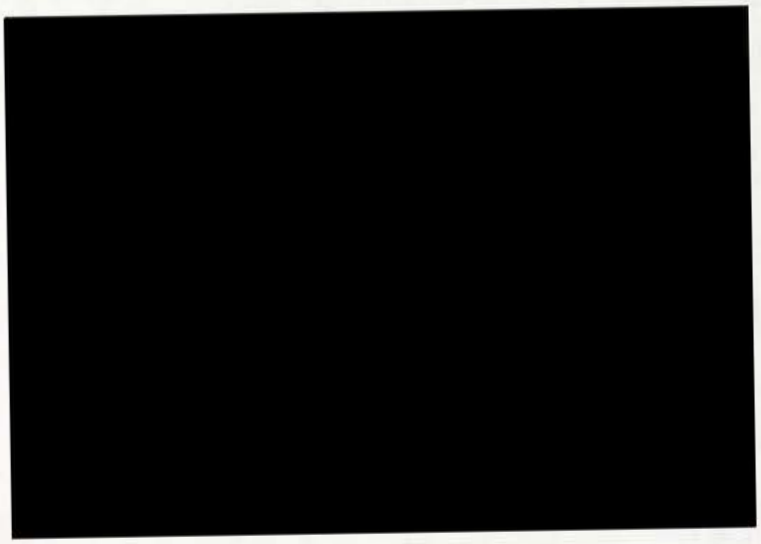

Figure 28 **Individual recording of stresses and strains (S. Kelbch 44)**

The position of each clamp is adjusted by an individual stepper motor (Figure 29) to ensure a constant minimum load applied to each specimen. This feature is important because of the differing permanent sets of carbon black filled and unfilled materials. Without this feature the tensile strips would buckle after a few cycles and the dynamic displacement would be uncontrolled and result in undefined crack propagation.

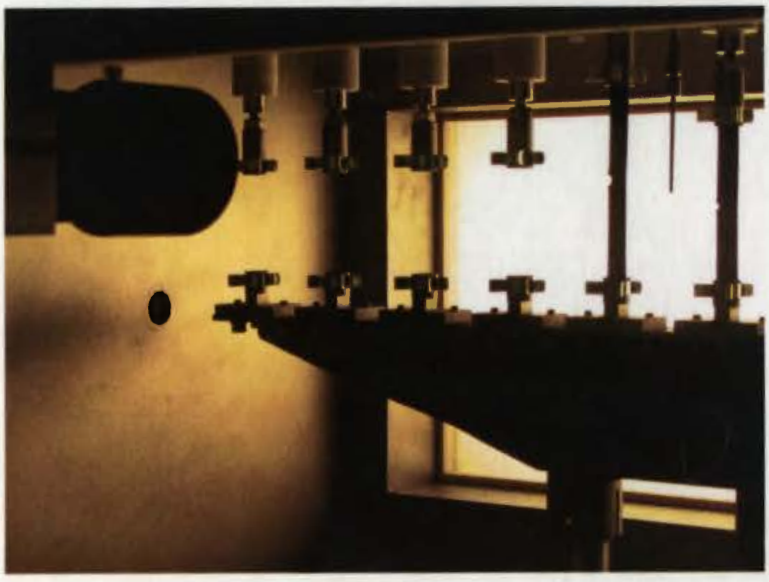

Figure 29 **Clamping with 2 test specimen at different minimum loads**

A further highly important characteristic of the Tear Analyzer is the optical measurement of the crack contour length of all test specimens during testing. A high speed CCD-camera takes a pictures of the cracks which are analysed online to calculate the crack contour length dependence on the number of cycles. Figure 30 shows the analysis of crack contour length by the Tear Analyzer software. To account for the crack contour length, the software looks for holes in the direction of the straight lines in front of the crack tip.

Figure 30 **Analysis of the crack contour by the Tear Analyzer**

Test procedures 1 and 3 in the fatigue tests were applied for the dynamic crack propagation tests (Figure 25 in Chapter 22.2, Methods of Fatigue Tests). For test procedure 1 small minimum loads of 1N for the unfilled materials and 2N for the carbon black filled materials are necessary to enable the machine to compensate precisely for the permanent set and to measure the crack exactly before the next dynamic loading. In contrast to the fatigue to failure tests the dynamic crack propagation properties were investigated with 50ms pulse lengths under displacement control and a repetition frequency of 10 Hz. A second dynamic crack propagation test series was carried out under sinusoidal excitation of 1 Hz. This additional test series allows a direct comparison with the fatigue to failure tests. All dynamic crack propagation tests were carried out under temperature control of 23°C.

To achieve a representative mean value of the dynamic crack propagation properties, the arithmetic average value of the results of five to ten test specimens tested under one condition were used. This was necessary because of

the high scatter in the dynamic crack propagation, although the specimens were produced under the same laboratory conditions.

For an evaluation of the dynamic crack growth rate, crack contour lengths were plotted against the number of cycles for each specimen as shown in Figure 31. The crack propagation typically starts with a stable propagation rate for the first 2 to 3 mm. This initial stable crack propagation is followed by an unstable crack propagation region and a subsequent catastrophic crack growth to rupture of the specimens.

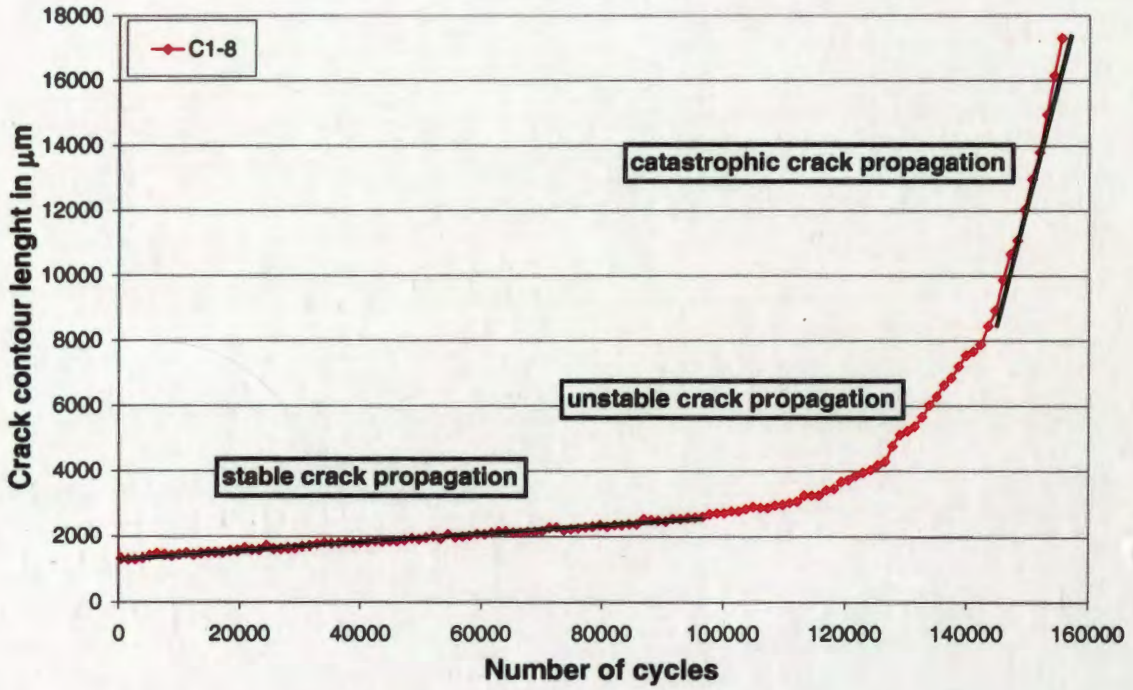

Figure 31 **Typical crack contour length dependence on number of cycles for a carbon black filled EPDM, tested with pulses of 50ms, at 10Hz, 20% and 2N minimum load.**

Only the initial stable crack propagation region was used for the evaluation of the dynamic crack growth properties. Figure 32 shows a linear fit to the stable crack growth region. The resultant slopes were used for the calculation of the arithmetic mean values of propagation rate for a set of specimens tested under

the same conditions. The same procedure was applied to calculate the mean values of stresses, energies etc.

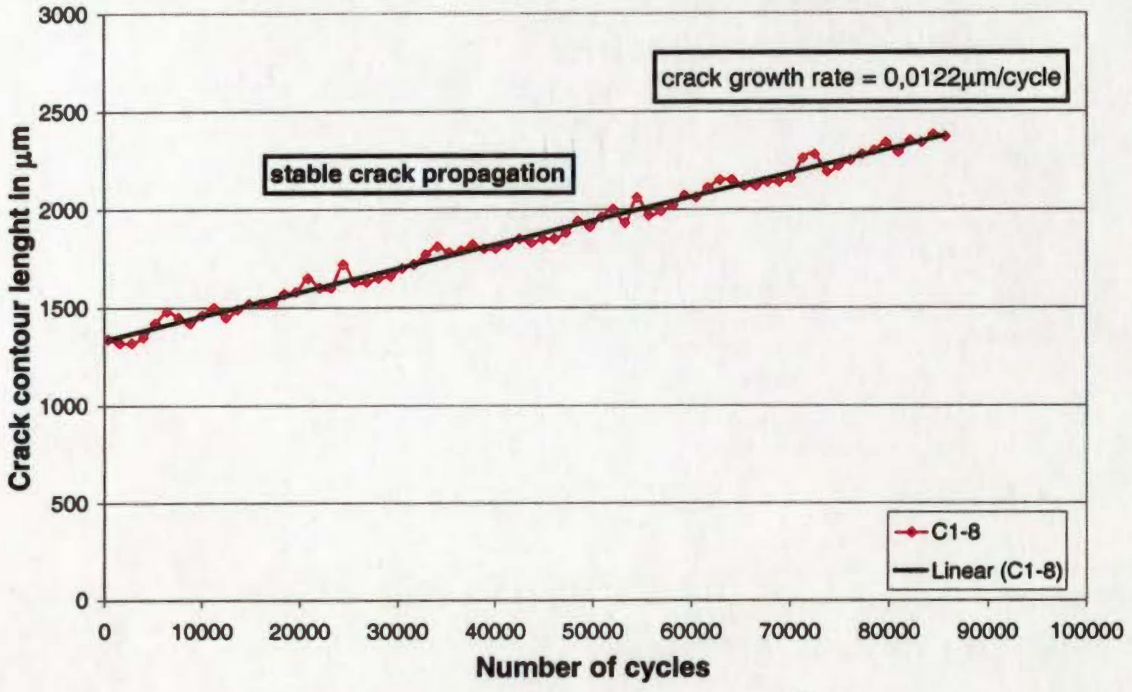

Figure 32 **Estimation of the stable crack propagation rate.**

Equations 2 and 3 in chapter 1.4.1 were used for the calculation of the tearing energy 'T'. The tearing energy 'T' depends on the actual crack length for the single edge notch tensile strip.

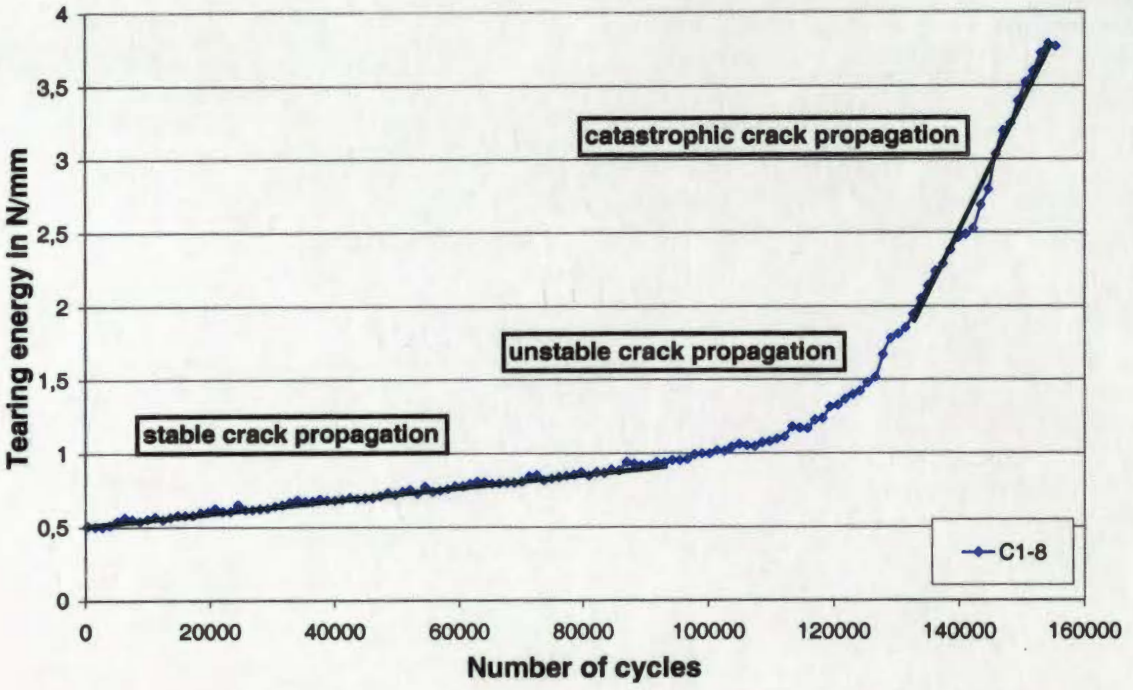

Figure 33 **Typical plot of the tearing energy dependence on numbers of cycles for a carbon black filled EPDM, tested with pulses of 50ms, at 10Hz, 20% and 2N minimum load.**

When the tearing energy 'T' is calculated for the specimen shown in Figure 31, the result is a curve dependent on the number of cycles, as shown in Figure 33, even if the region of the stable crack propagation only is observed. Correspondingly, for each test specimen a mean value of the tearing energy was calculated for the stable crack propagation region (Figure 34) and the average of all mean values of the specimens tested under one condition were plotted in the diagrams in Chapter 4, Results of Dynamic Crack Propagation Tests.

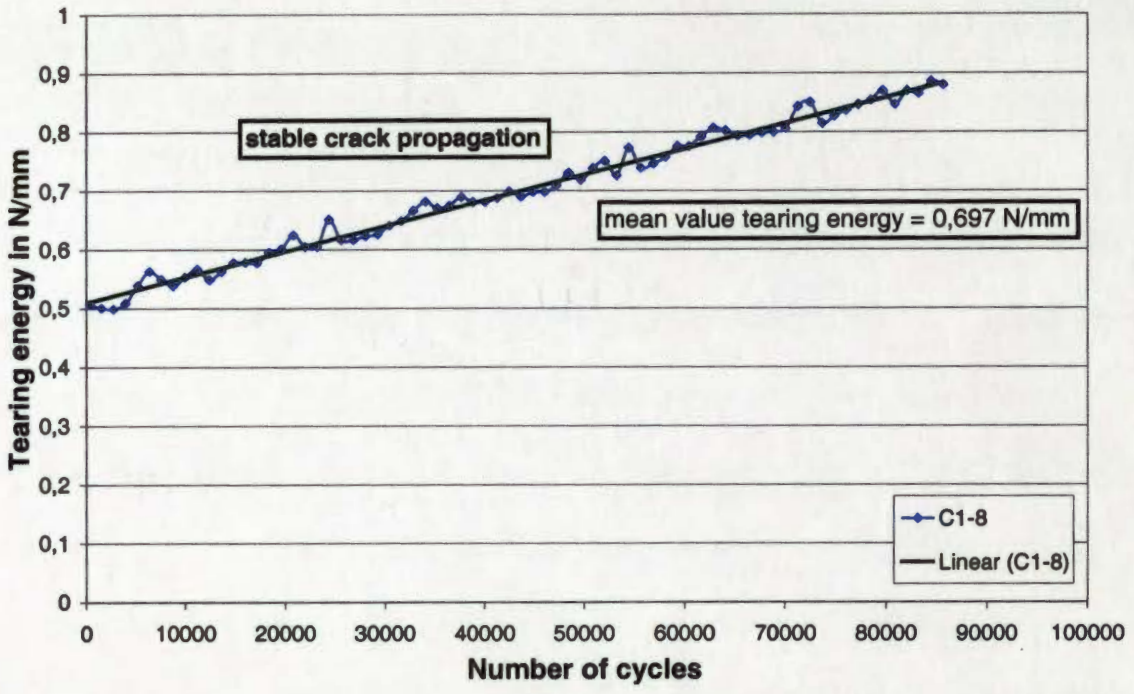

Figure 34 **Estimation of the mean value of tearing energy in the stable crack propagation region.**

3 Results of Fatigue Tests

3.1 Fatigue in Carbon Black Filled EPDM

Figure 35 shows hysteresis loops for a test on filled EPDM in which the mean load was successively increased. Each loop represents the 50th cycle, at a given mean load, to remove effects of conditioning. The non-linear load-displacement relation is evident in this diagram. The areas of hysteresis loops diminish and the material stiffness increases when non-zero minimum loads are used under both, tensile and compressive conditions. The results from the fatigue tests on the filled rubber are shown in Figure 36 and Figure 37. Most significantly the fatigue life for each load range is lowest when the minimum stress in the cycle is zero. Any increase in tensile minimum stress, or decrease to give a compressive minimum stress, causes an increase in fatigue life (▲, △, ■, □). Higher load ranges result in lower fatigue lives, but the increases in fatigue life with non-zero minimum stress is common to each load range (400N and 500N) for test procedures 2 and 3. The results obtained from test procedure 1 (●) indicate that fatigue life reduces as mean stress increases where each test has σ_{min} equal to zero.

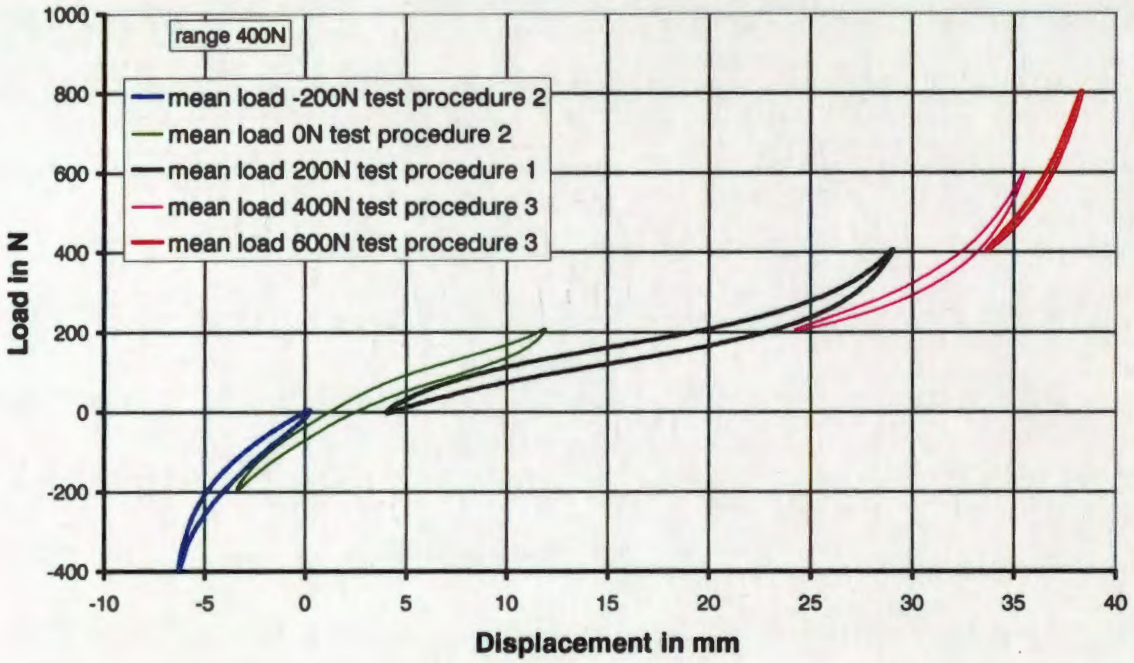

Figure 35 **Examples of the three fatigue test procedures with a 400N load range.**

Figure 36 shows mean load plotted against cycles to failure whilst Figure 37 presents the data as conventional Wöhler curves where maximum engineering stress (σ_{max}) is plotted against cycles to failure. The points of convergence for the two sets of curves (▲, Δ and ■, □) are equivalent to σ_{min} = zero. Uniquely, load cycles that have a value of σ_{min} equal to zero result in the lowest fatigue life for each load range. Variations in σ_{min} in both, tension and compression, produce increases in fatigue life. The 'R^2' values depicted on these and subsequent graphs represent the root mean square error values between each curve and the associated points. Individual fatigue tests were repeated several times as mentioned previously. In fatigue testing of elastomers, repeatability is less easy to achieve in tests on un-notched specimens [**38**]. Crack propagation is far more reproducible than crack initiation and consequently it is assumed

that the fatigue failures in the tests described emanated from defects of similar size, thought to be of an effective size of 25 μm [**8**], inherent in the manufacturing process.

Figure 38 indicates, that in common with maximum stress, maximum strain can not be used as a criterion for determining fatigue life in filled EPDM for all test conditions. Previous research has suggested that maximum strain [**10**] and maximum stress [**11, 12**] are each suitable criteria for predicting fatigue life of elastomers. Figure 38 and Figure 37 substantiate that this statement is supported for cycles when $\sigma_{min} = 0$, but not for load applications where $\sigma_{min} \neq$ zero.

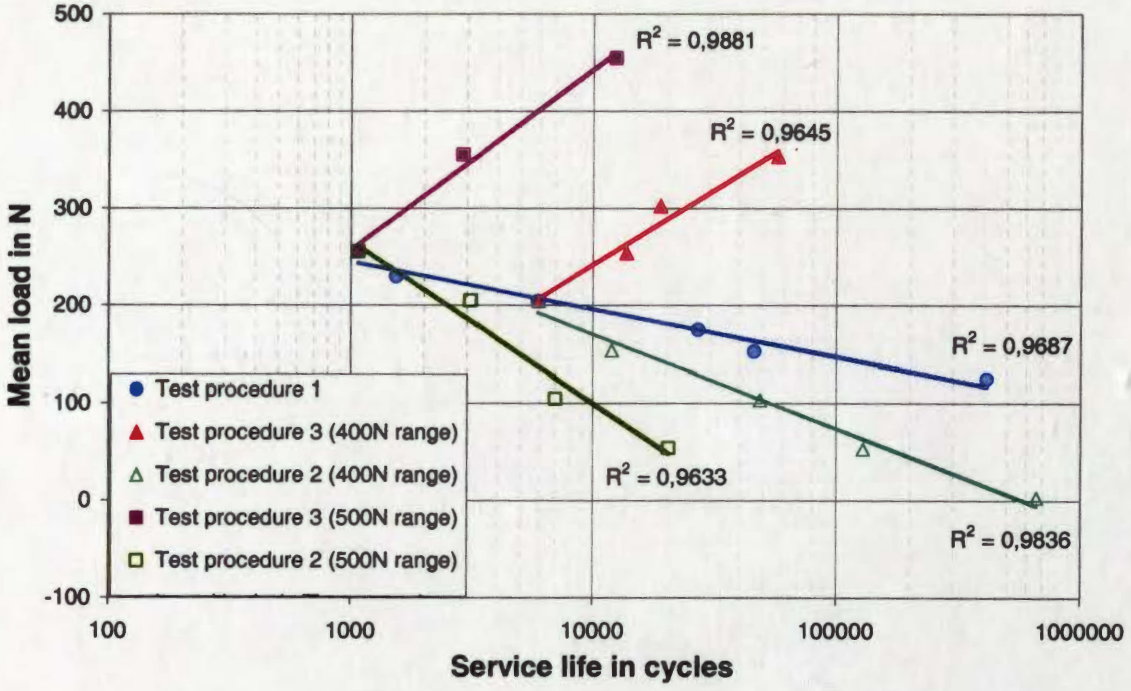

Figure 36 **Fatigue test results for filled EPDM, showing mean load dependence.**

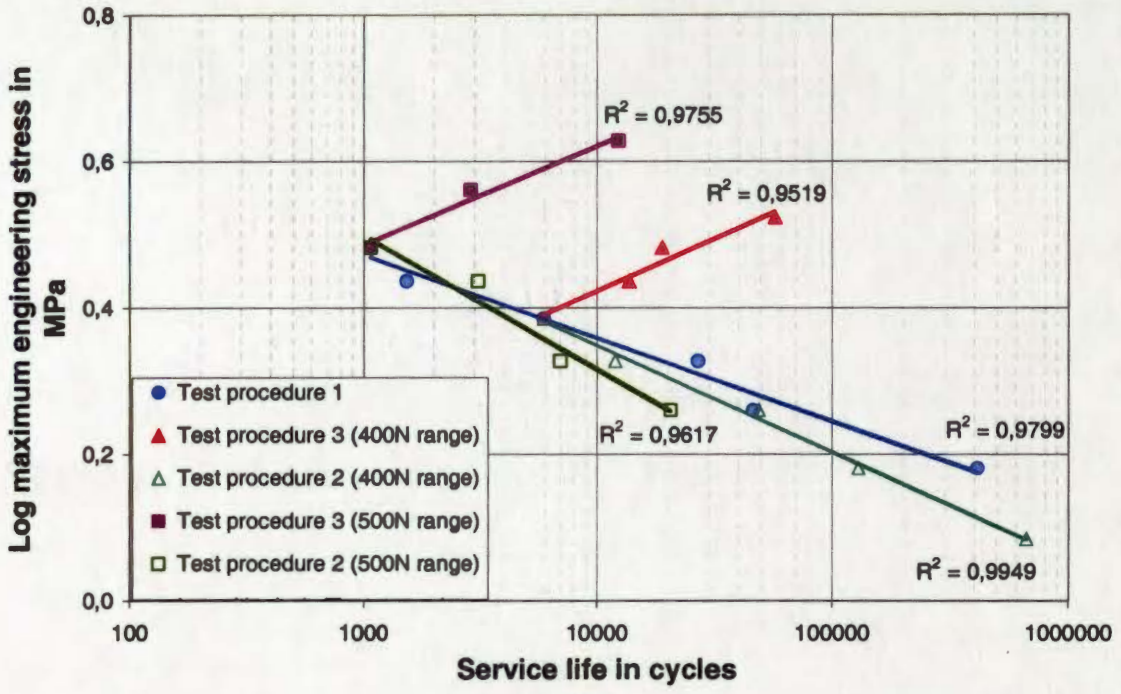

Figure 37 **Fatigue test results for filled EPDM, showing maximum stress dependence (Wöhler curve).**

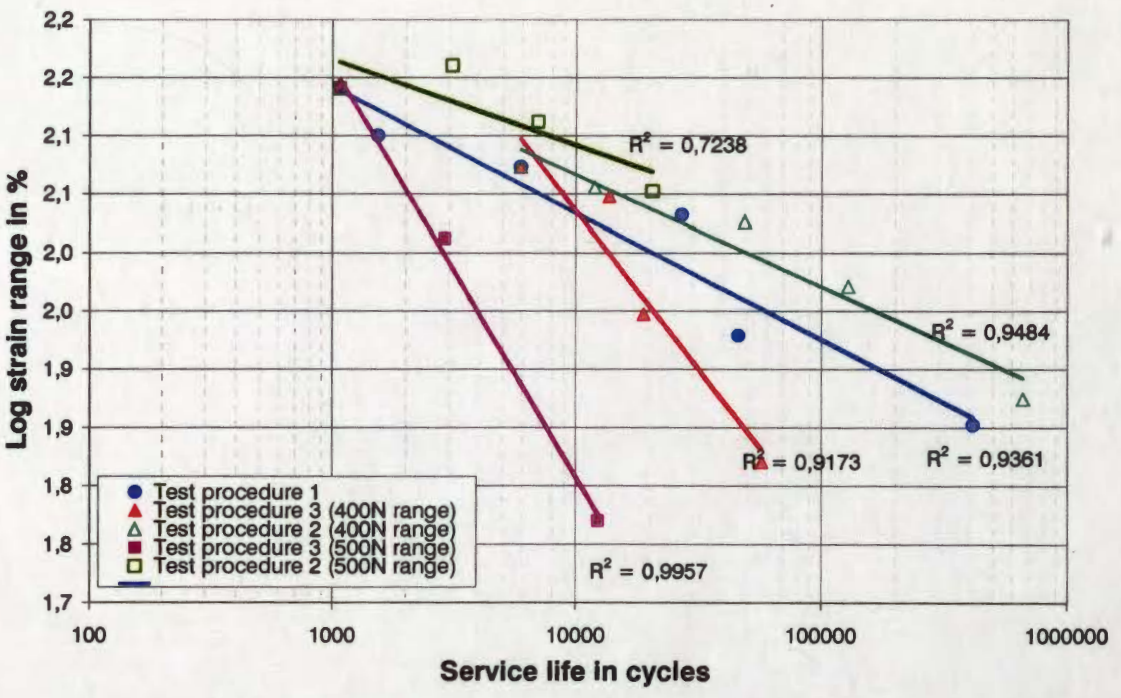

Figure 38 **Fatigue test results for filled EPDM, showing dynamic strain dependence.**

A correlation between the stored energy and the fatigue life of carbon black filled EPDM is given in Figure 39. This diagram shows that the stored energy can not be used as a general predictor for the fatigue behaviour of filled elastomers, but it can be seen that this predictor is useful for loadings with minimum stresses of zero or compression. The dynamic strain energy criterion is not applicable if loadings with minimum stresses in tension are present.

Two data points from test procedure 1 are omitted in all energy diagrams, because complete hysteresis loops were not recorded.

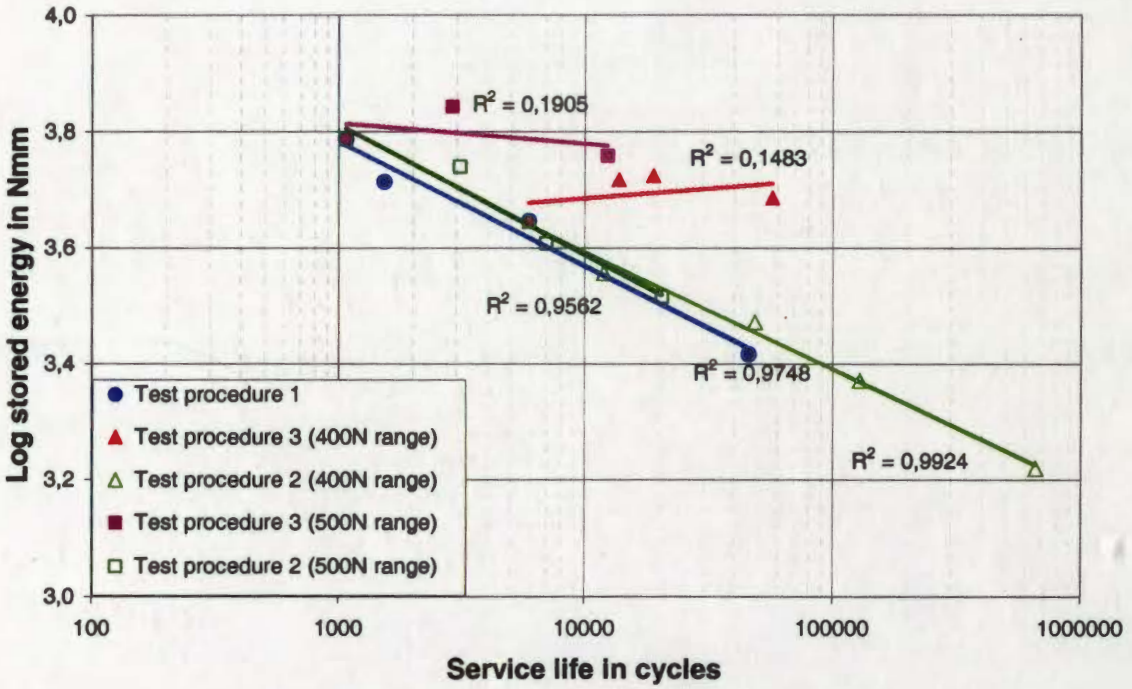

Figure 39 **Fatigue test results for filled EPDM, showing stored energy dependence.**

The total energy dependency is shown in Figure 40. Like the stored energy this criterion is not applicable if minimum loads are in tension but the deviation is slightly lower when compared with the stored energy plots.

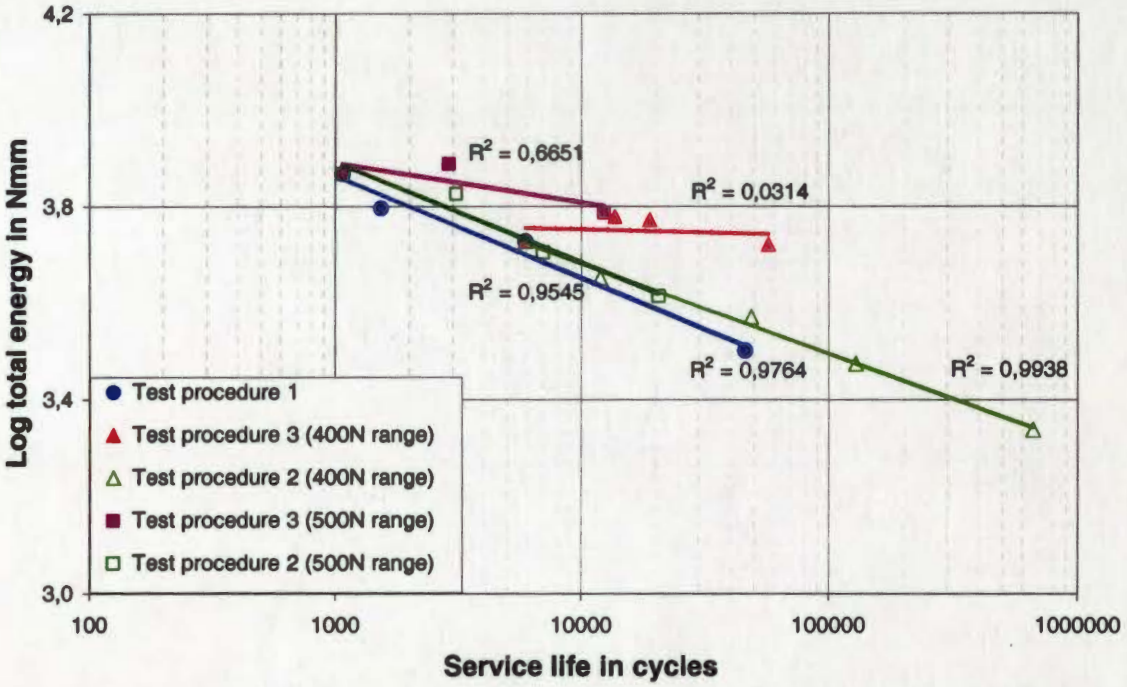

Figure 40 **Fatigue test results for filled EPDM, showing total energy dependence.**

None of the usual criteria for the prediction of fatigue life work if non-zero minimum loads are applied for a carbon black filled EPDM, particularly if the minimum loads are in tension.

3.2 Fatigue in Unfilled EPDM

The fatigue results for unfilled EPDM are shown in Figure 41. The test procedures were as for the filled rubbers (Figure 25) although the load ranges were smaller to reflect the lower stiffness in the unfilled material.

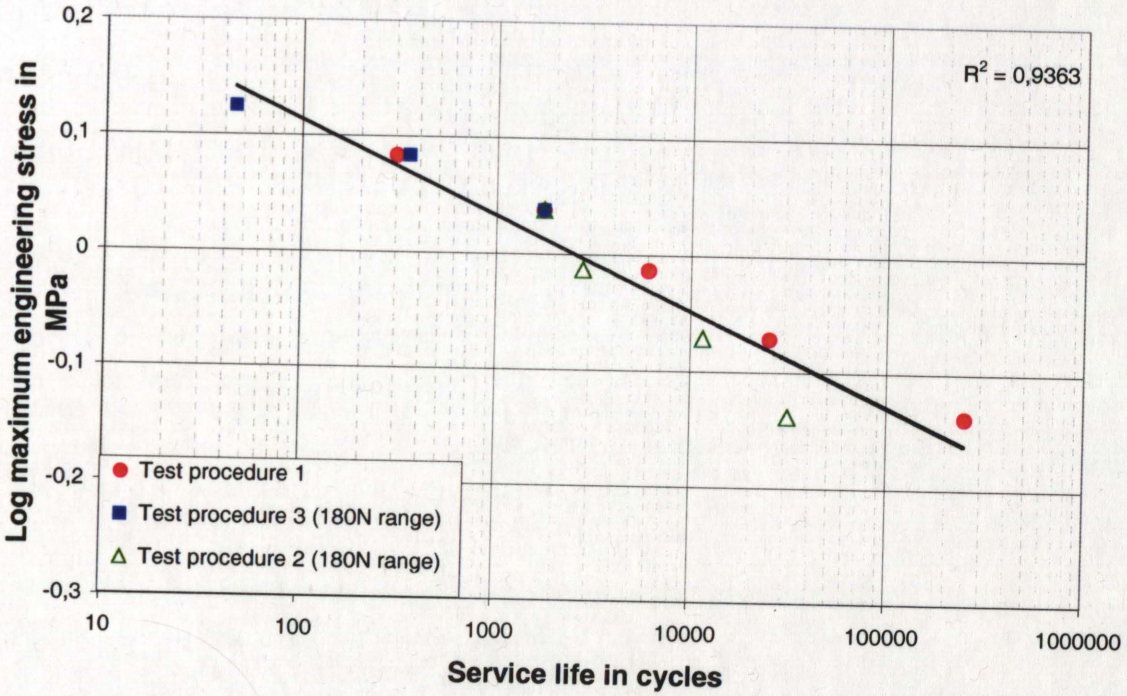

Figure 41 **Fatigue test results for unfilled EPDM, showing maximum stress dependence (Wöhler curve).**

The reduction in fatigue life with increase in stress range in tests using the first procedure is comparable with the behaviour exhibited by the filled EPDM. However, the fatigue lives using the second and third procedures decrease if the minimum load is non-zero. The fatigue life correlates well with the maximum engineering stress. The maximum stress is shown to be a reliable predictor of fatigue life for unfilled EPDM subjected to uniaxial loading (Figure 41).

Maximum dynamic strain can also be used to predict the fatigue life of unfilled EPDM (Figure 42).

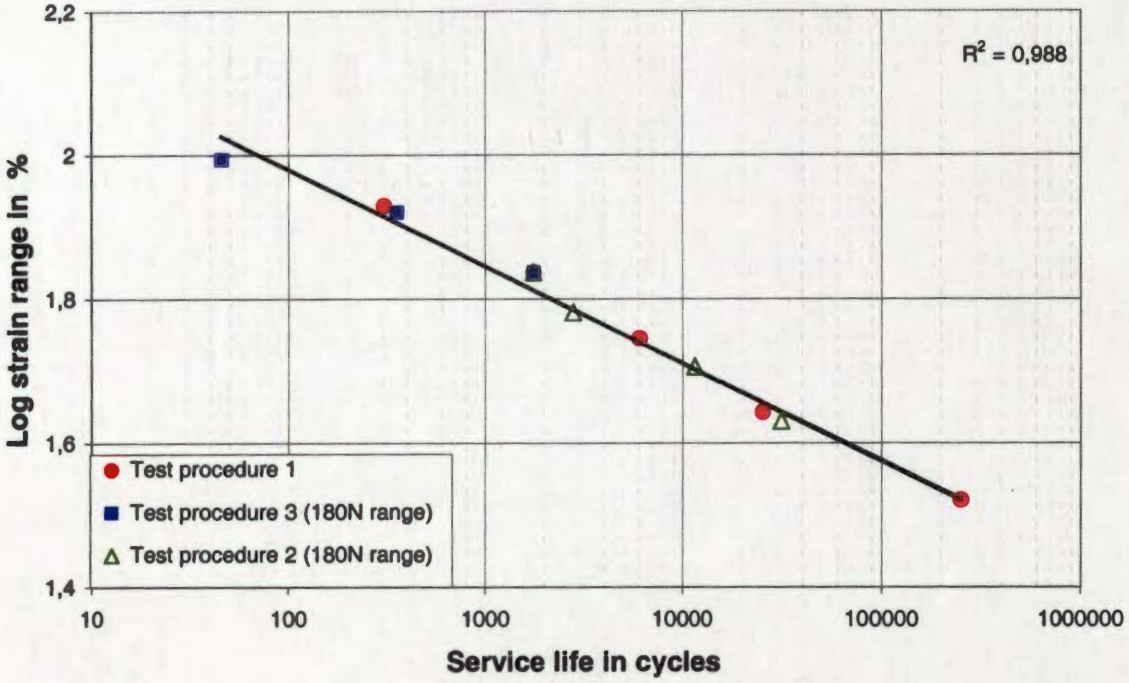

Figure 42 **Fatigue test results for unfilled EPDM, showing dynamic strain dependence.**

The dynamic strain dependency appears to be more precise than the maximum stress dependency shown in Figure 41.

Alternatively the stored energy can be used for the prediction of the fatigue life of unfilled EPDM-material as shown in Figure 43. Because of the very low levels of dissipated energy for the unfilled EPDM, the total energy dependency is nearly equal to that of the plot of the stored energy.

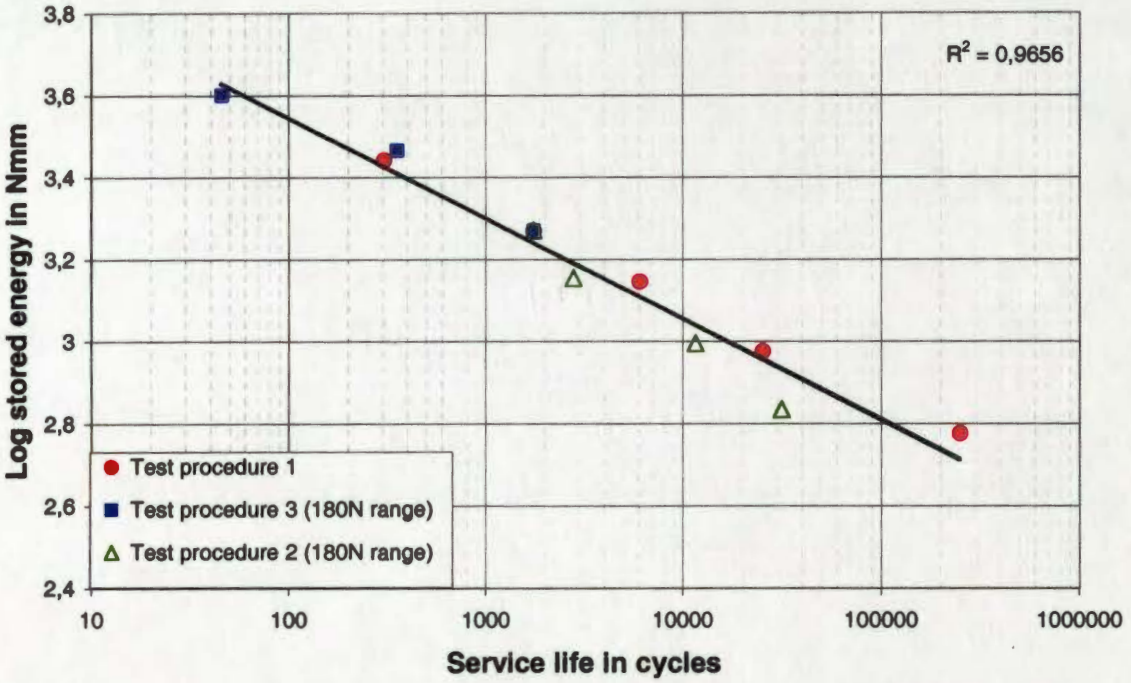

Figure 43 **Fatigue test results for unfilled EPDM, showing stored energy dependence.**

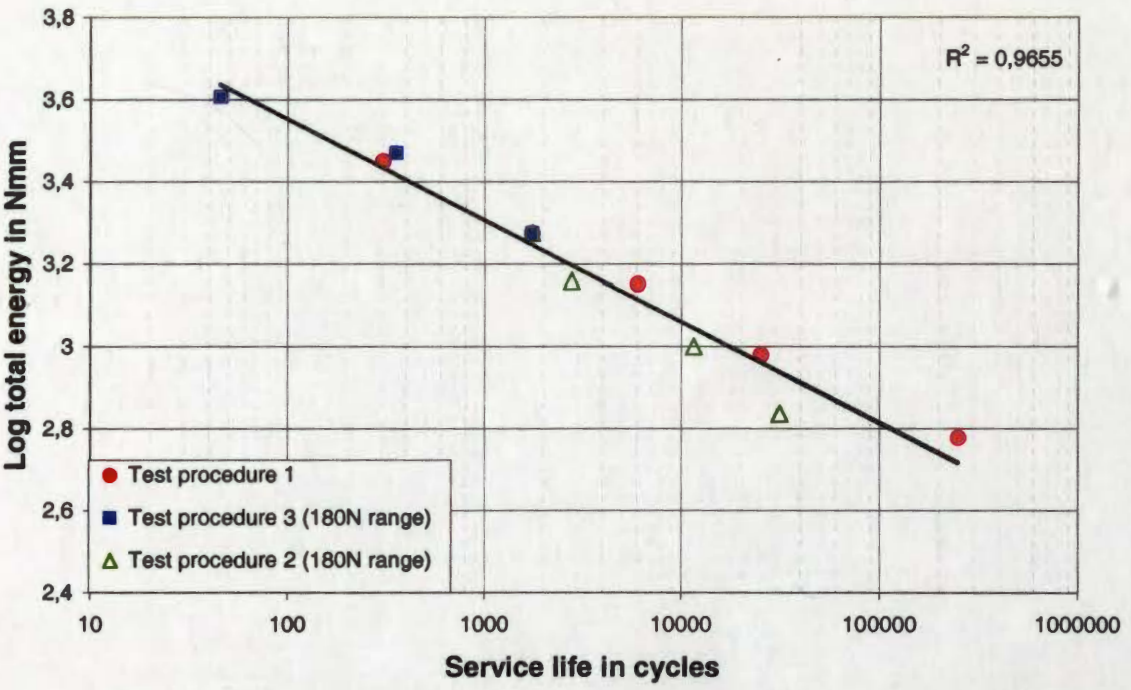

Figure 44 **Fatigue test results for unfilled EPDM, showing total energy dependence.**

The diagrams (Figure 41 - Figure 44) indicate that all four methods for the predictions of fatigue life can be applied to unfilled EPDM.

3.3 Fatigue in Carbon Black Filled SBR

All three test procedures described in Section 2.2 Methods of Fatigue Tests and Figure 25 were also applied to the E-SBR materials. The results from the fatigue tests on the carbon black filled SBR-rubber are shown in Figure 45 as a Wöhler-curve. Again the fatigue life is reduced with increasing maximum stress when a minimum stress of zero is applied (●). An increase in tensile minimum stress (▲, ■), or decrease to give a compressive minimum stress (△, □), causes an increase in fatigue life.

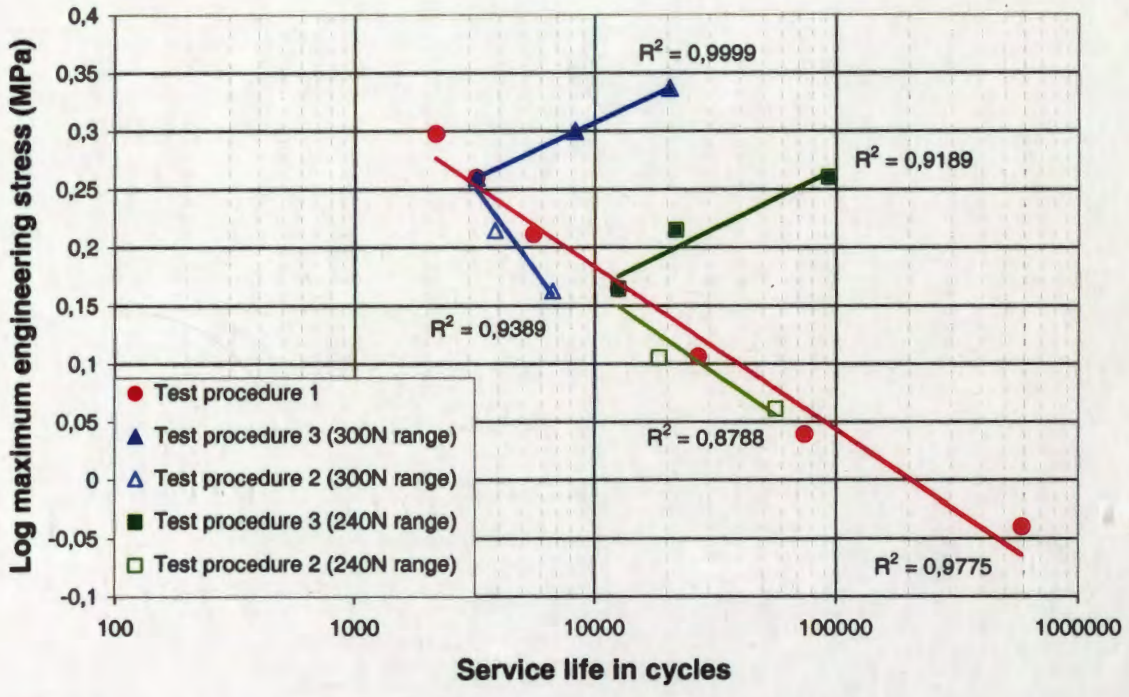

Figure 45 **Fatigue test results for carbon black filled SBR, showing maximum stress dependence (Wöhler curve).**

Higher load ranges result in lower fatigue life, but the increases in fatigue life with non-zero minimum stress is similar to the effect found with the carbon black filled EPDM in Figure 37 for test procedures 2 and 3.

Figure 46 indicates, that in contrast to carbon black filled EPDM (Figure 38), the maximum dynamic strain can be used as a criterion for determining fatigue life in carbon black filled SBR for all test conditions. In the case of the carbon black filled SBR the dynamic strain can be used as a fatigue life predictor for cycles when $\sigma_{min} = 0$ and for load applications where $\sigma_{min} \neq$ zero. In particular, the strain criterion can be used if the minimum load are not in tension.

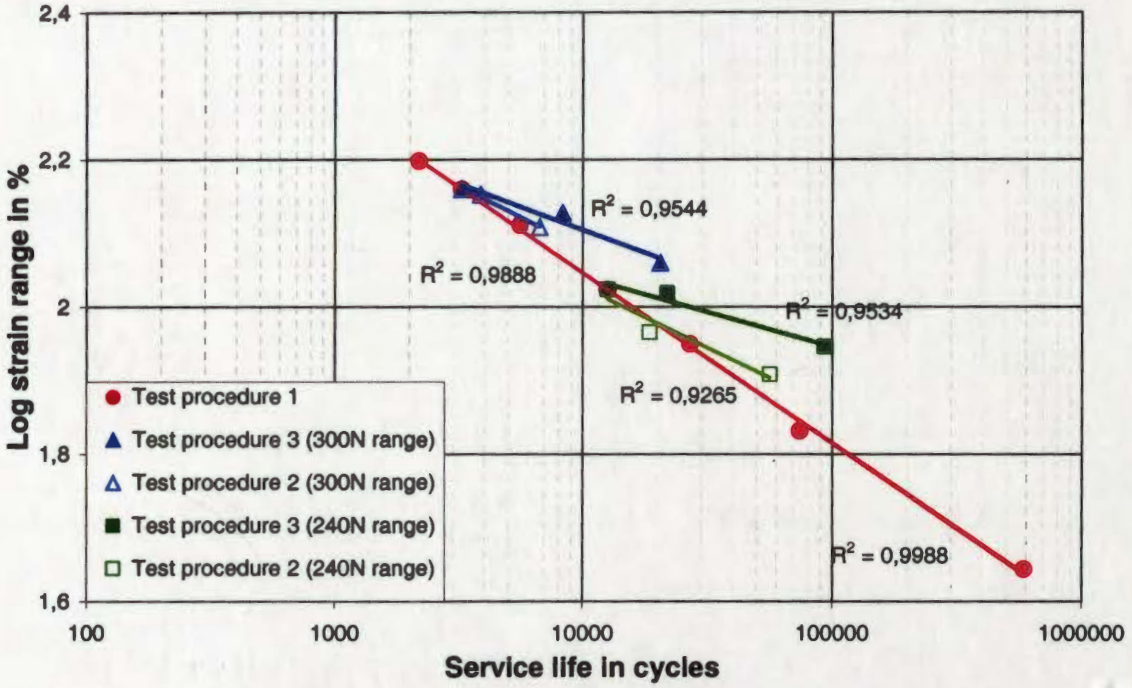

Figure 46 **Fatigue test results for carbon black filled SBR, showing dynamic strain dependence.**

The plot of the stored energy against fatigue life (Figure 47) is quite similar to that for the maximum stress dependence shown in Figure 45. At minimum stresses in tension the stored energy does not match the line with zero minimum stresses (•), while the minimum loads in compression give an almost acceptable match.

The total energy dependency is shown in Figure 48. Minimum stresses in tension show the same behaviour as above. But the compression data fit very well in the diagram of the total energy at zero minimum stresses.

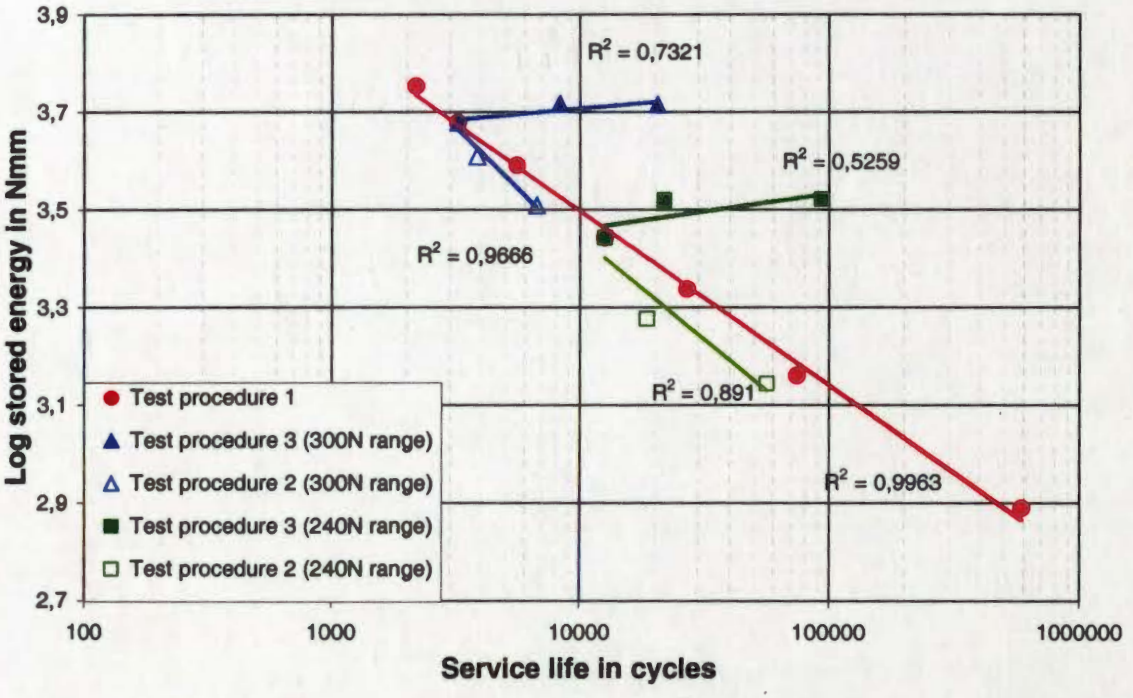

Figure 47 **Fatigue test results for carbon black filled SBR, showing stored energy dependence.**

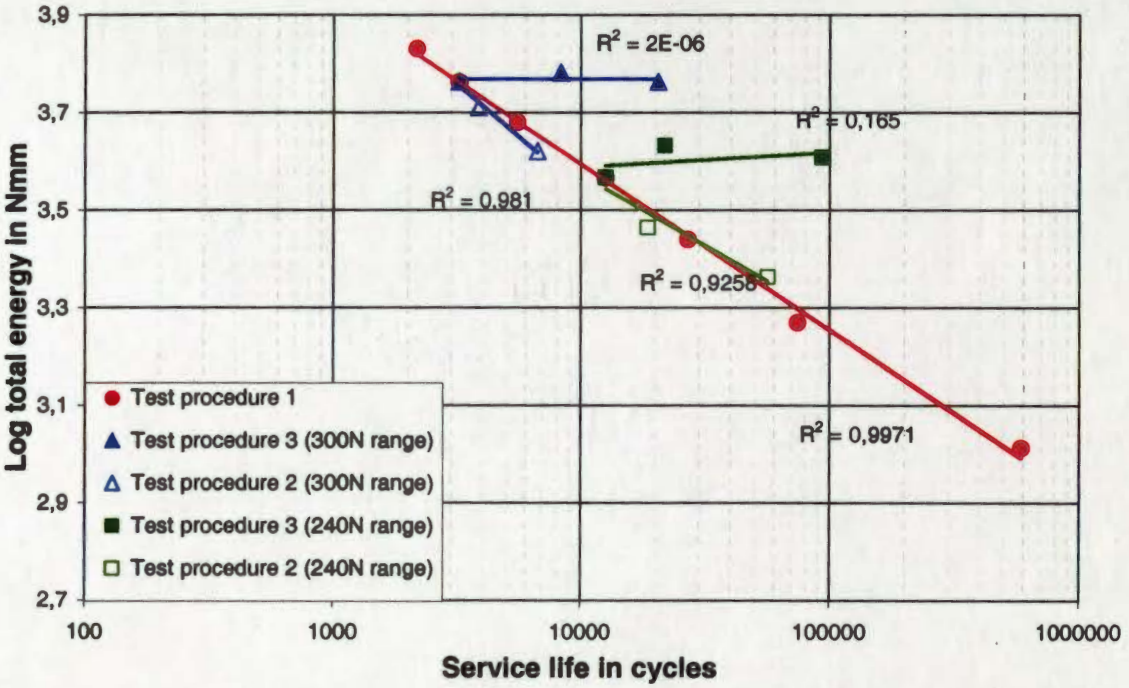

Figure 48 **Fatigue test results for carbon black filled SBR, showing total energy dependence.**

As for the carbon black filled EPDM (3.1 Fatigue in Carbon Black Filled EPDM, page 52), none of the normally accepted criteria for the prediction of fatigue life is applicable for carbon black filled SBR if non-zero minimum loads are applied especially if the minimum loads are in tension.

3.4 Fatigue in Unfilled SBR

The fatigue test results of the unfilled SBR are plotted as a Wöhler-curve in Figure 49. The data points of all three test procedures are on a single line with an overall correlation factor of $R^2 = 0,99$.

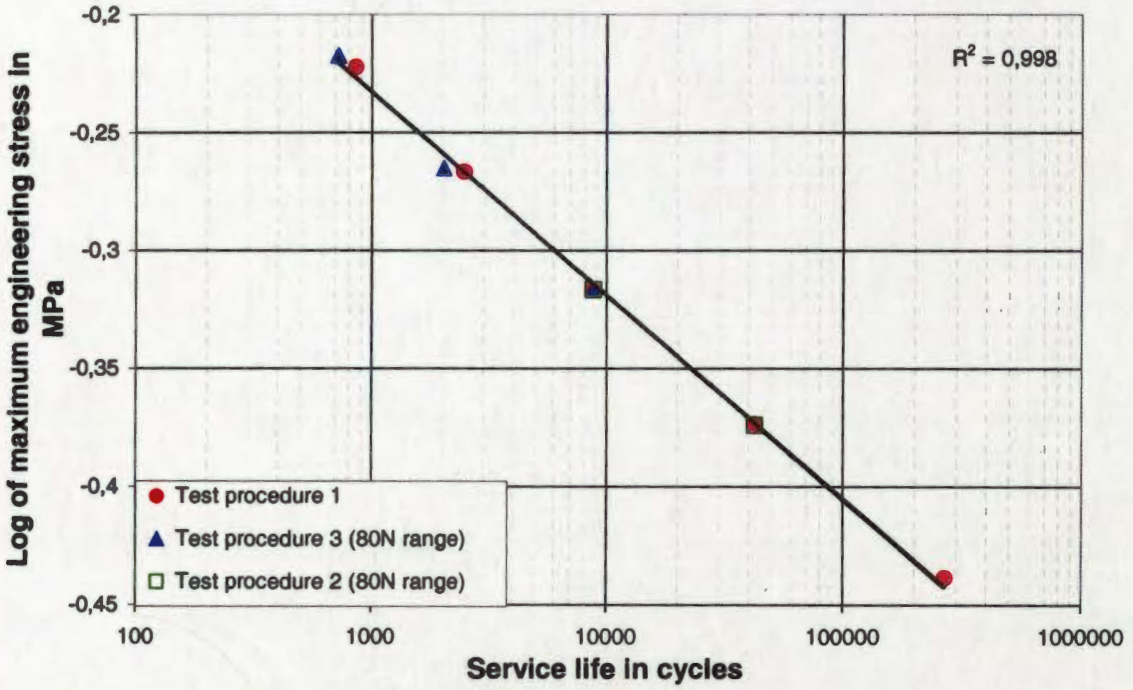

Figure 49 **Fatigue test results for unfilled SBR, showing maximum stress dependence (Wöhler curve).**

The plot of dynamic strain vs. service life is shown in Figure 50, again all data points of the three test procedures are approximately on a single line. This means that for the unfilled SBR the maximum dynamic strain criterion can be used.

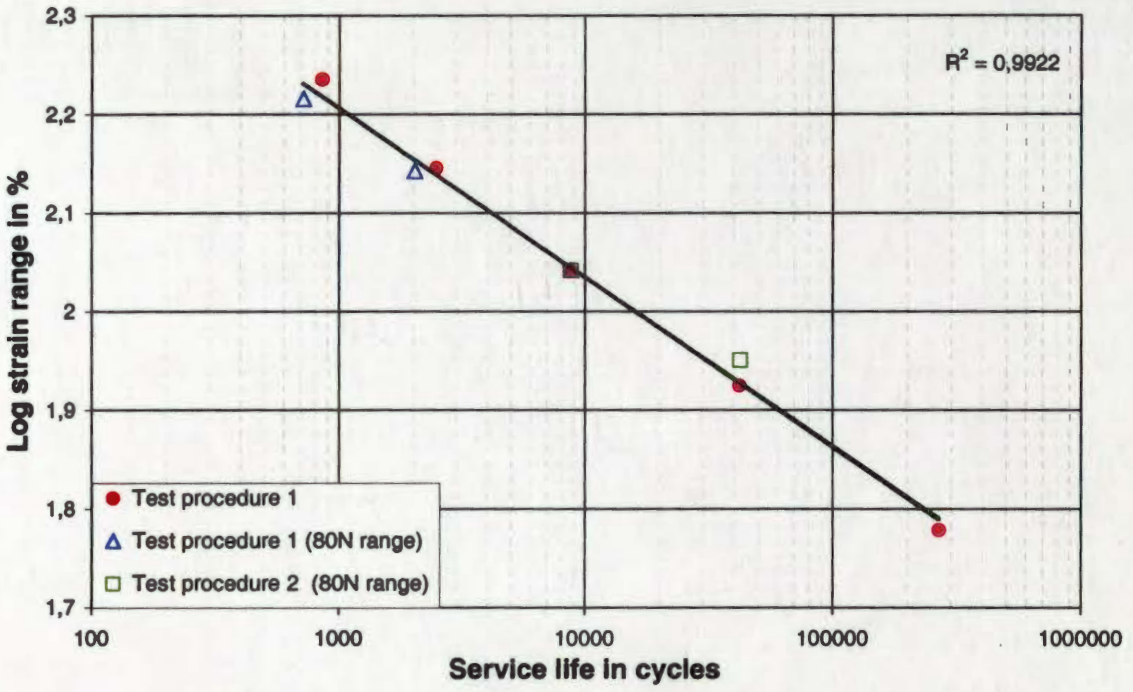

Figure 50 **Fatigue test results unfilled SBR, showing dynamic strain dependence.**

The fatigue results showing dependency on stored energy are plotted in Figure 51. This criterion fits equally well when compared with maximum stress having a correlation coefficient of $R^2 = 0,99$.

The dissipated energy of the unfilled SBR is much higher compared to the unfilled EPDM, but nevertheless the total energy dependence results in a plot virtually identical to the stored energy. Correspondingly the total energy is also a very good predictor for the fatigue life of unfilled SBR.

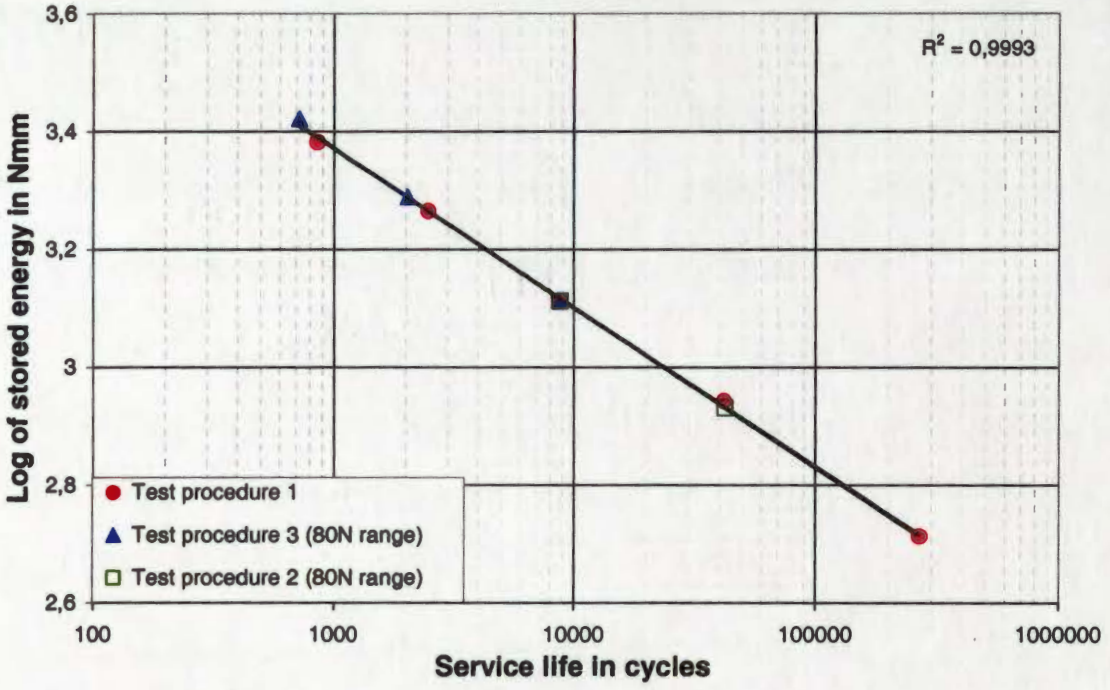

Figure 51 **Fatigue test results for unfilled SBR, showing stored energy dependence**

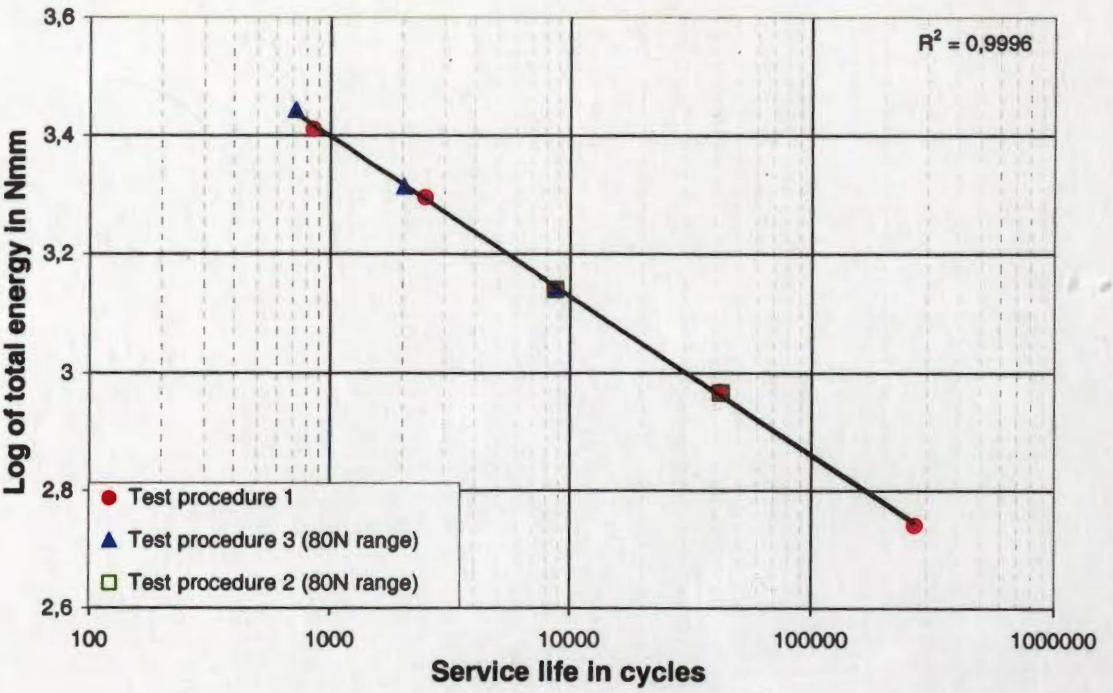

Figure 52 **Fatigue test results for unfilled SBR, showing total energy dependence**

As for to the unfilled EPDM (3.2 Fatigue in Unfilled EPDM, page 58) it is possible to use all four criteria for the prediction of the fatigue life for unfilled SBR.

3.5 Determining a Predictor for the Calculation of Fatigue Life

The fatigue data from these tests were correlated with several previously measured and evaluated data in order to find a predictor of the fatigue life for the elastomers tested particularly the carbon black filled ones.

For tests where σ_{min} was in compression or equal to zero the total or stored energy can be used to predict fatigue life irrespective of whether the material is filled or unfilled. If, however, σ_{min} is tensile both are inadequate to describe the failure properties of filled systems.

A more accurate prediction under all testing conditions and modes for the carbon black filled EPDM and SBR is achieved only by a variation of the commonly used energy criteria. These are the dynamic stored energy and the dynamic total energy evaluated as described in Figure 53.

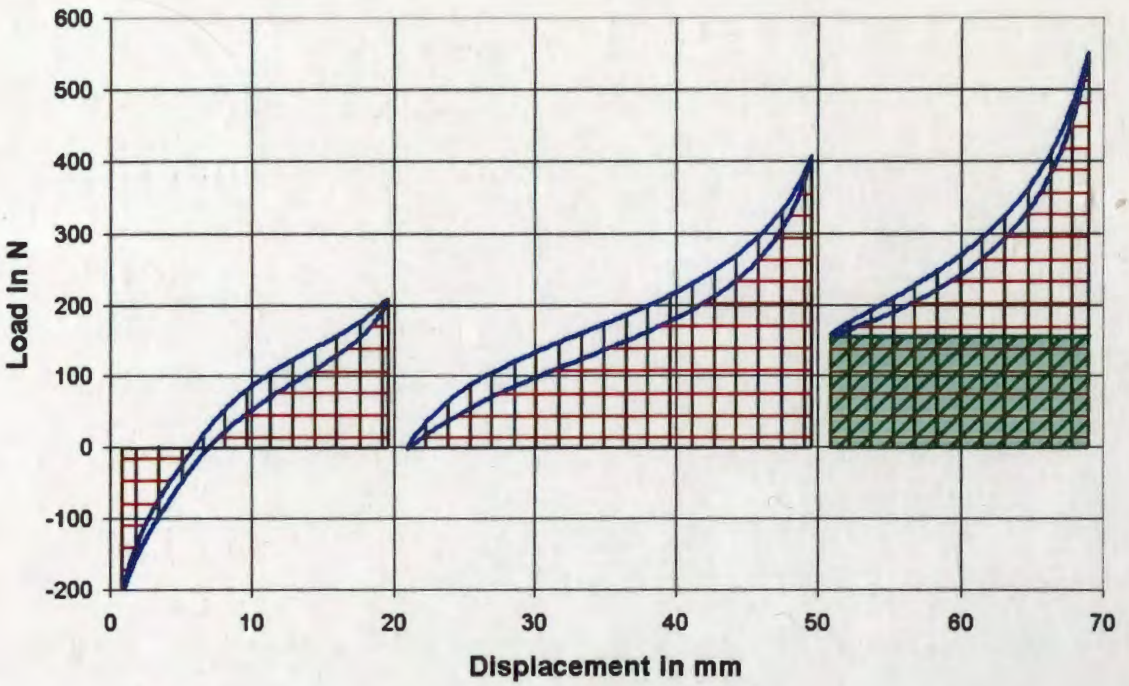

Figure 53 **Diagrammatic representation of the predictors dynamic stored energy and dynamic total energy for the different test procedures.**

These new predictors are as those described earlier in Section 2.2 Methods of Fatigue Tests, page 38 but having the value of the statically stored energy subtracted. The value of the statically stored energy is represented by the shaded portion in Figure 53 and only exists when minimum loads in tension are applied. For minimum loads in compression or equal to zero, the dynamic stored and total energy are equal to the overall stored and total energy respectively.

The plot of the dynamic stored energy against the fatigue life of the carbon black filled EPDM is shown in Figure 54. In contrast to the normal stored energy shown in Figure 39 the correlation with the number of cycles to failure is improved if minimum loads in tension are applied.

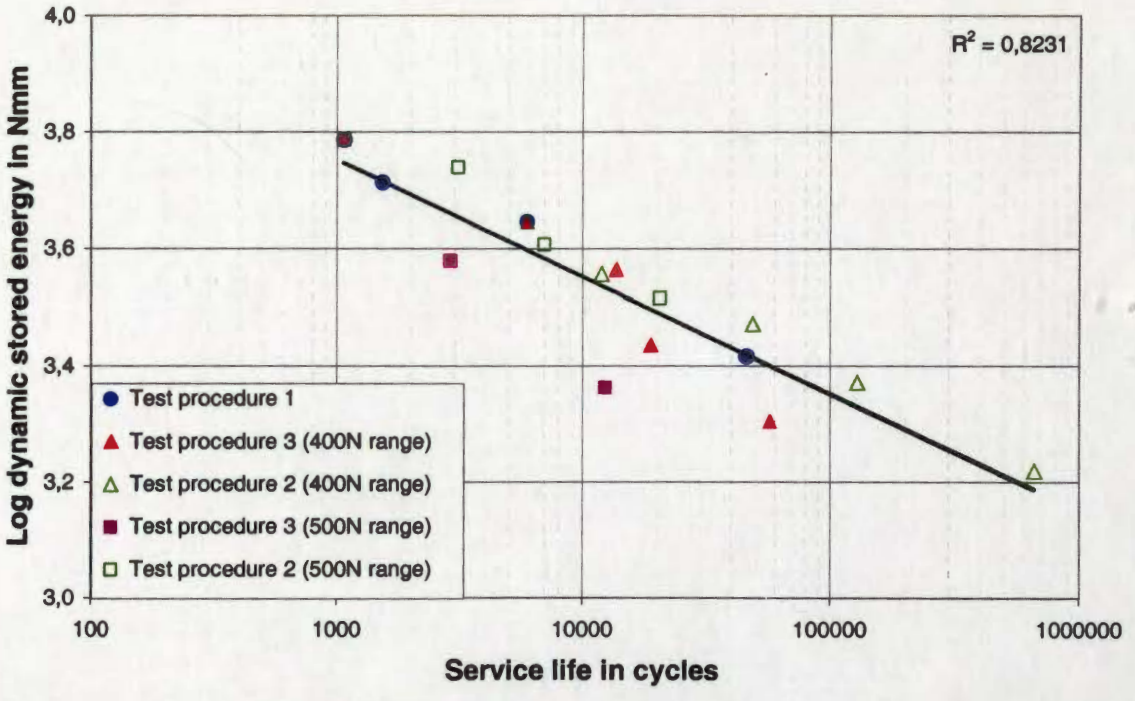

Figure 54 **Correlation of the predictor dynamic stored energy vs. fatigue life for a carbon black filled EPDM.**

The results for the dynamic total energy of the carbon black filled EPDM are shown in Figure 55. It can be seen that the correlation coefficient is lower (R^2 = 0,77). Tests with a higher minimum load in tension fit fairly well, while the data points in compression are exceptionally well represented as for zero minimum load. Nevertheless both new predictors give a higher correlation for fatigue life under all three test procedures than the usual ones described previously (Section 3.1 Fatigue in Carbon Black Filled EPDM, page 52).

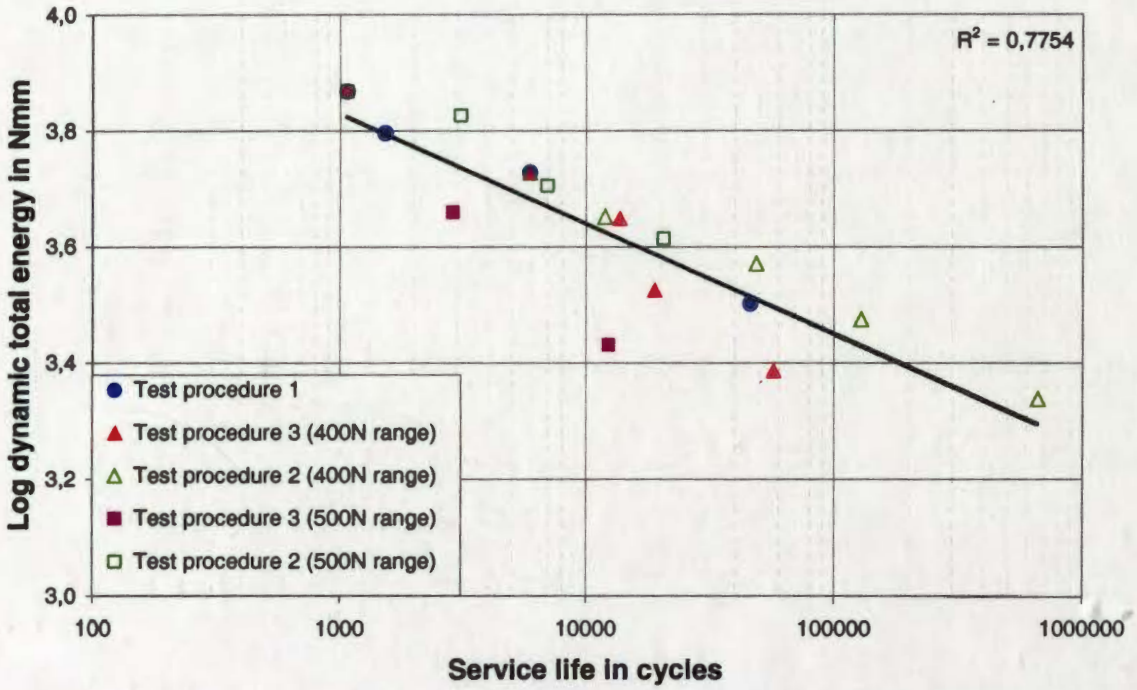

Figure 55 **Correlation of the predictor dynamic total energy vs. fatigue life for a carbon black filled EPDM.**

The plot of the dynamic stored energy vs. Service Life for the unfilled EPDM is shown in Figure 56. The unfilled EPDM is adequately characterised (R^2 = 0,94) even if the correlation coefficient is slightly smaller than in Section 3.2, Fatigue in Unfilled EPDM (page 58). Corresponding to the earlier description the correlation for the dynamic total energy (Figure 57) is nearly equal to that for the

dynamic stored energy and can also be used as a predictor for the fatigue life of unfilled EPDM.

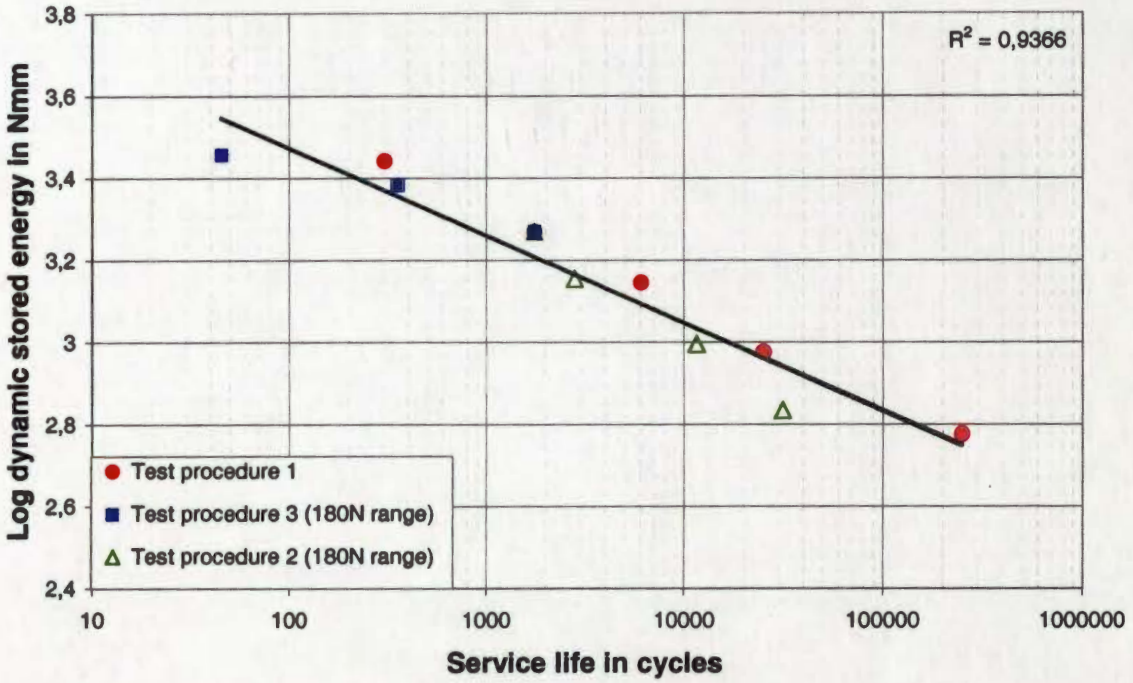

Figure 56 **Correlation of the predictor dynamic stored energy vs. fatigue life for an unfilled EPDM.**

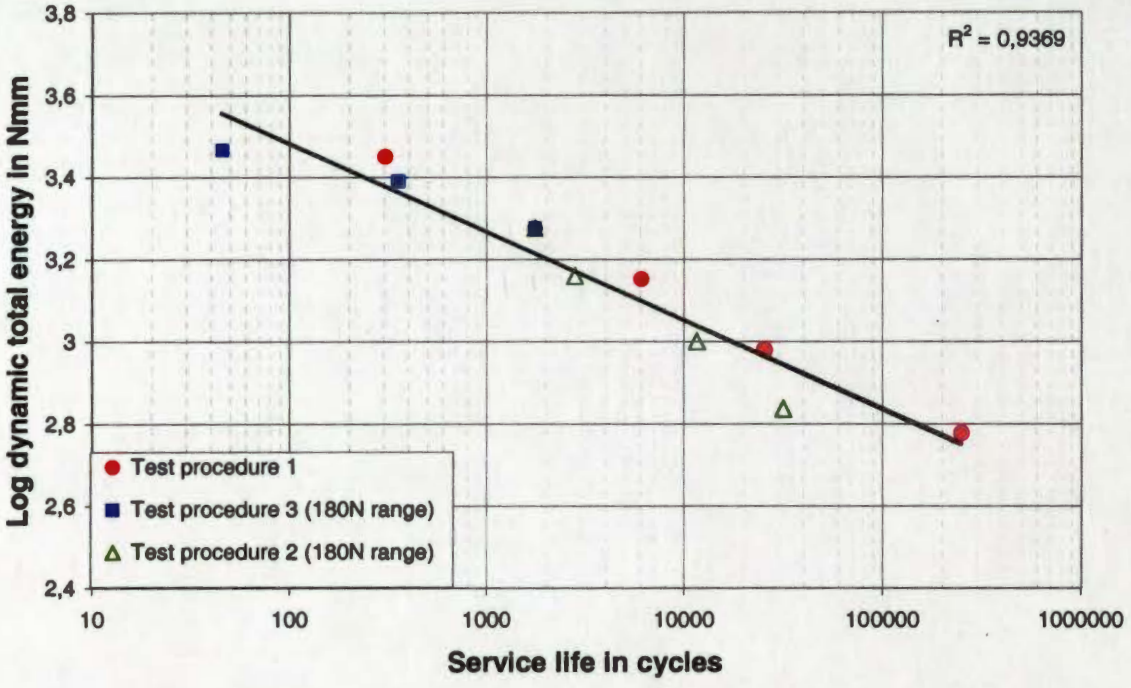

Figure 57 **Correlation of the predictor dynamic total energy vs. fatigue life for an unfilled EPDM.**

The dynamic stored energy dependence of the carbon black filled SBR material is shown in Figure 58. It can be see that the fatigue life properties are well matched for all 3 test procedures, even for the extreme values of minimum stress.

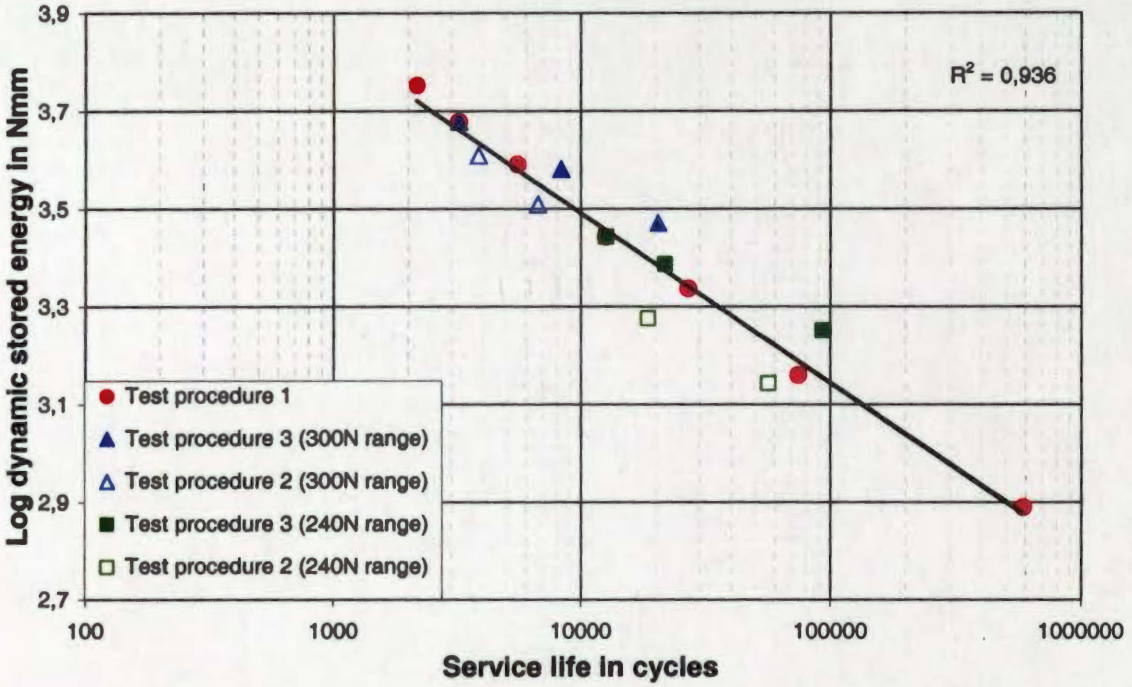

Figure 58 **Correlation of the predictor dynamic stored energy vs. fatigue life for a carbon black filled SBR.**

A similar, but improved result is shown in the dynamic total energy dependence of the carbon black filled SBR in Figure 59. This diagram gives a very high correlation coefficient of $R^2 = 0,96$ despite the very high differences in loadings applied in the three test procedures. Both dynamic energy criteria can be used for the prediction of the fatigue life of carbon black filled SBR.

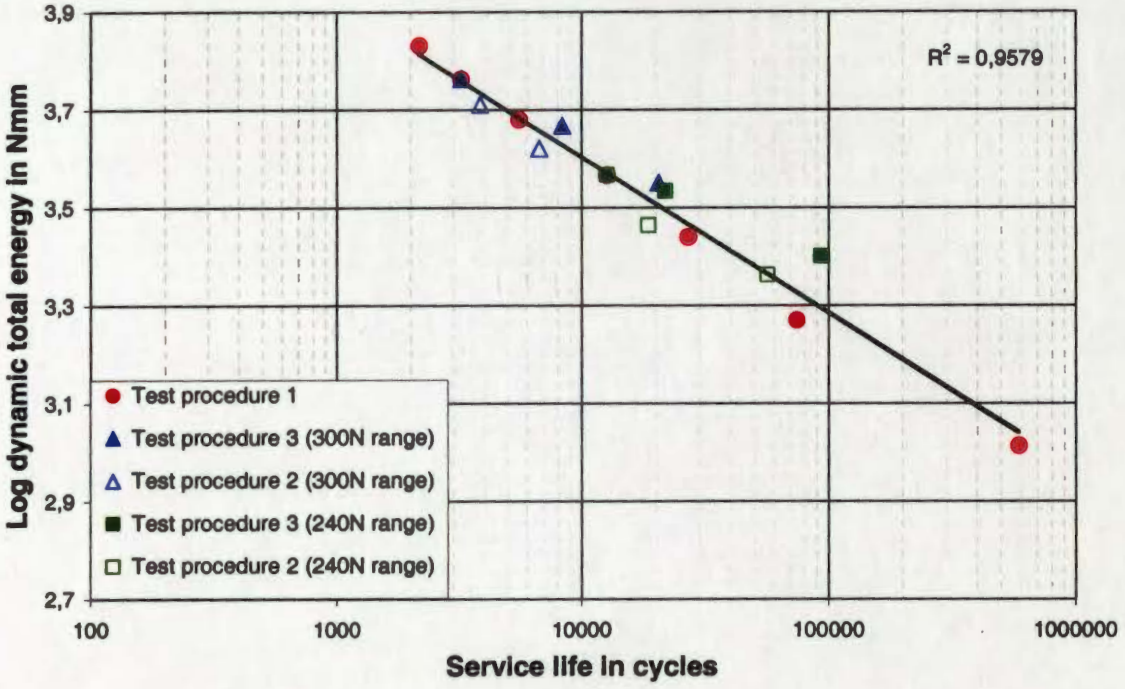

Figure 59 **Correlation of the predictor dynamic total energy vs. fatigue life for a carbon black filled SBR.**

The dynamic stored energy dependence for the unfilled SBR material is shown in Figure 60. The overall correlation coefficient of $R^2 = 0,96$ indicate that the dynamic stored energy can be used for the prediction of the fatigue properties of unfilled SBR.

The dynamic total energy dependency for the unfilled SBR is shown in Figure 61. Like the unfilled EPDM, the correlation for dynamic total energy is quite similar to that for the dynamic stored energy.

Accordingly the results for the unfilled EPDM material give a slightly better correlation for the stored energy or total energy for predicting the fatigue properties of the unfilled SBR. Nevertheless both dynamic energy criteria can be used for the unfilled SBR material.

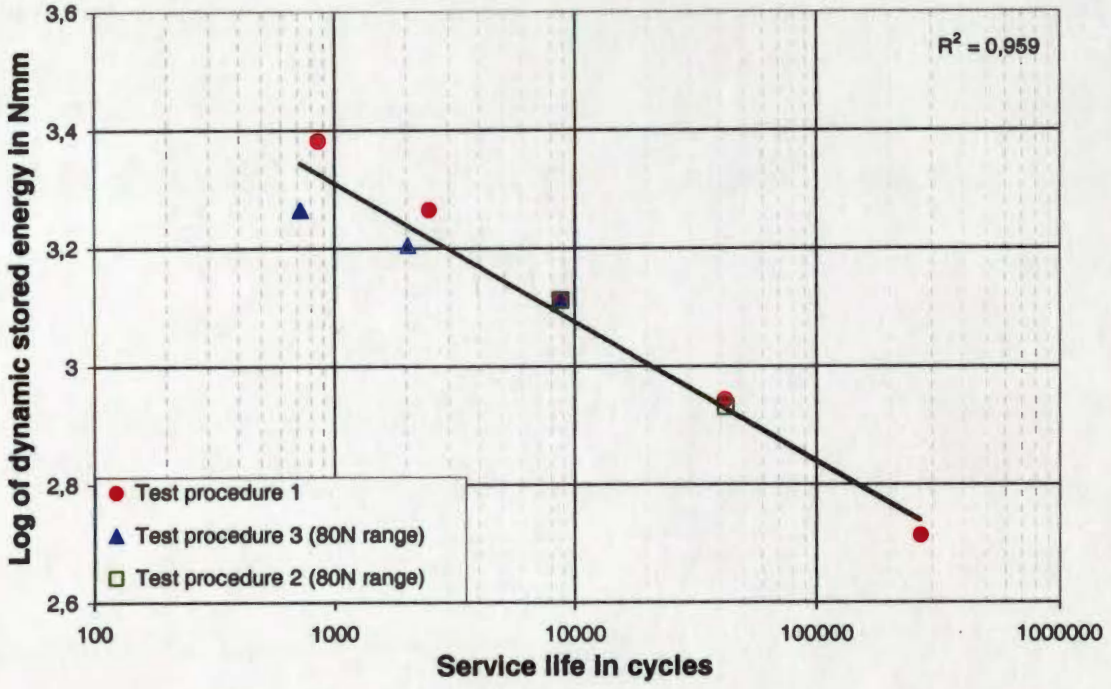

Figure 60 **Correlation of the predictor dynamic stored energy vs. fatigue life for an unfilled SBR.**

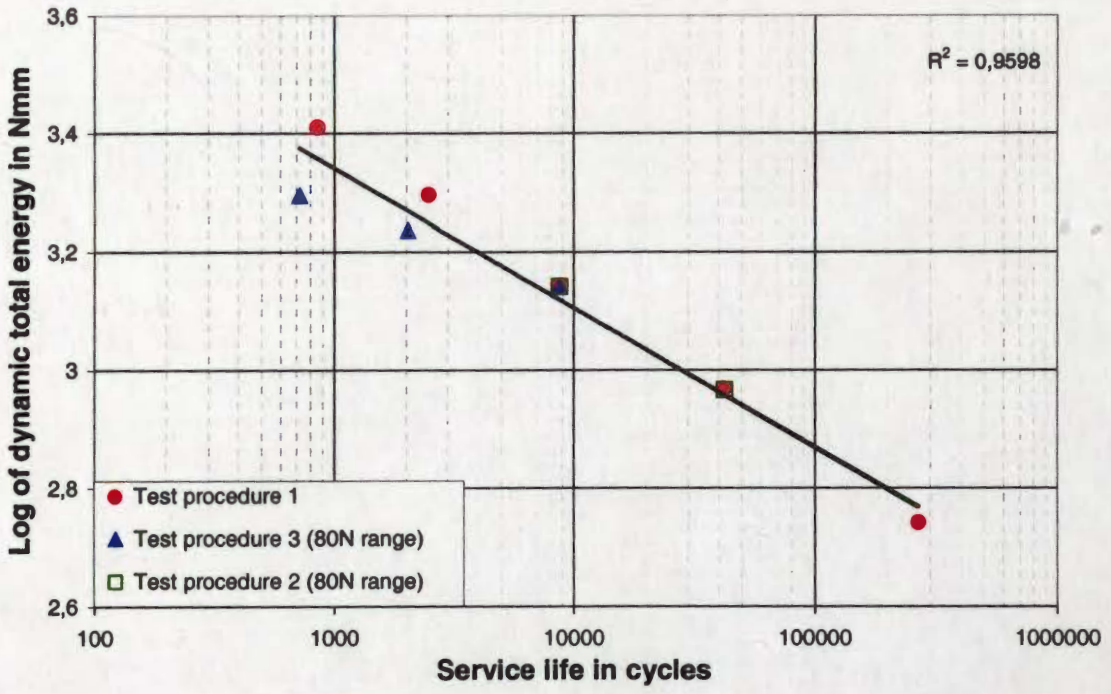

Figure 61 **Correlation of the predictor dynamic total energy vs. fatigue life for an unfilled SBR.**

3.6 Changes in Physical Properties during the Test of Filled EPDM

The data from all tests show that carbon black filled EPDM undergoes changes in physical properties during the load controlled cycles. Dynamic load cycles induce an increasing permanent set as each test progresses as shown in Figure 62. Furthermore, the displacement range permanently increases during the testing time while the breadth of the hysteresis loops diminishes, which indicates a reduction of the loss angle. Directly before complete failure, during a catastrophic crack propagation phase, a high decrease in stiffness is observed, simultaneous with a high increase of the dissipated energy or loss angle.

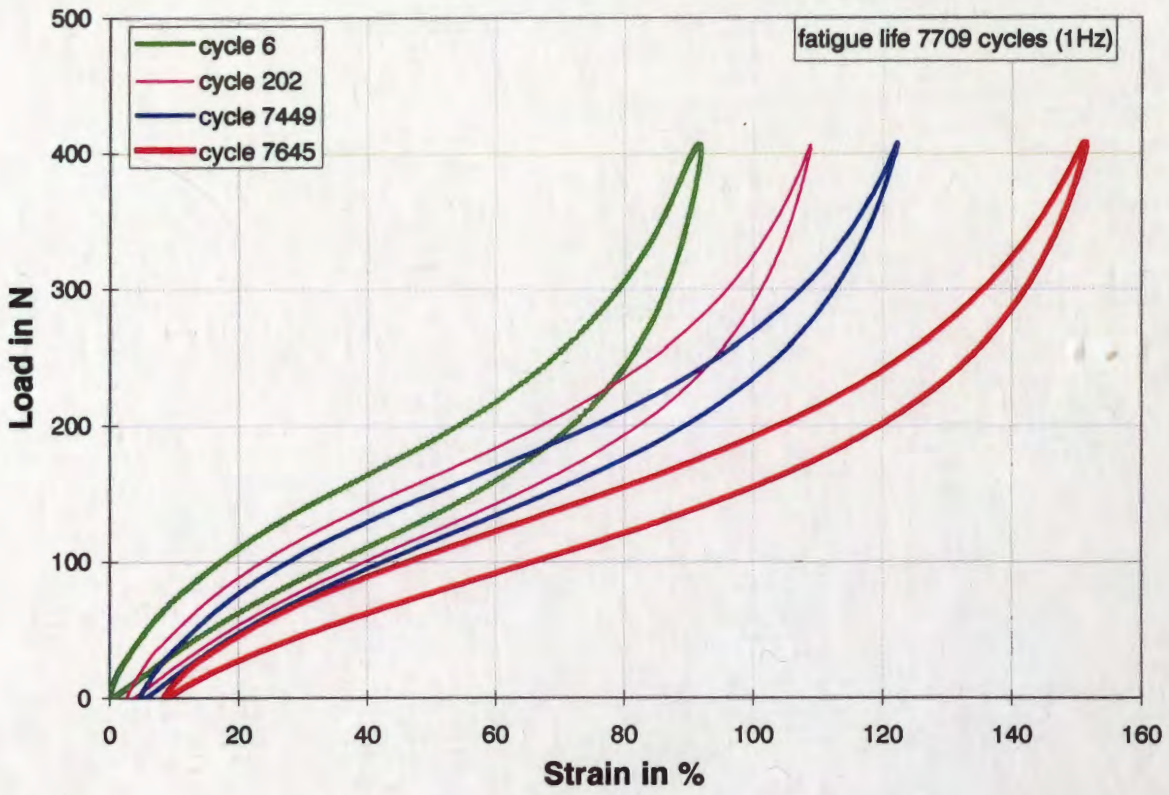

Figure 62 **Hysteresis loops of a filled EPDM specimen during fatigue testing.**

The modulus of filled rubbers is known to decrease significantly during the first few cycles of a physical test as a result of the stress softening (Mullins effect, Section 1.3). However these fatigue tests show that the stiffness and the loss angle (δ) or loss factor (tan δ) of the material decrease throughout the whole test until fracture (Figure 63 and Figure 64). Therefore the relative dissipated energy decreases after pre cycling. The dissipated energy per cycle reaches a plateau after a few hundred cycles as shown in Figure 65 as a consequence of the strain behaviour and the change in tan δ. It is only immediately before fracture, as the crack propagates, that the dissipated energy per cycle and tan delta increase. The same phenomenon can be seen under less severe test conditions when test specimens fail after a few hundred thousand cycles.

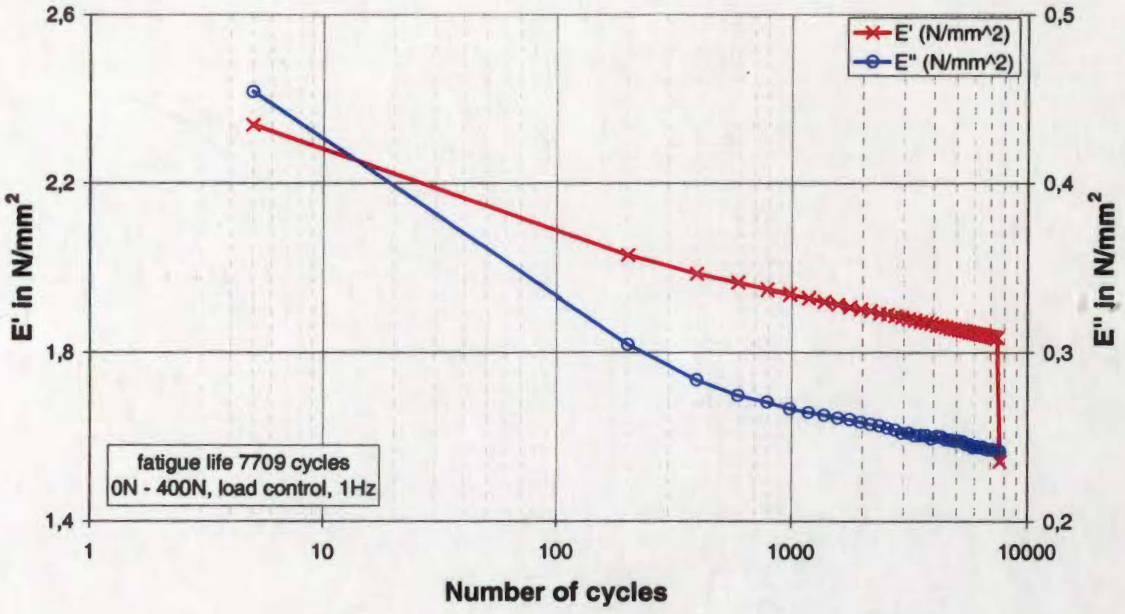

Figure 63 **Modulus curves of a filled EPDM during fatigue testing.**

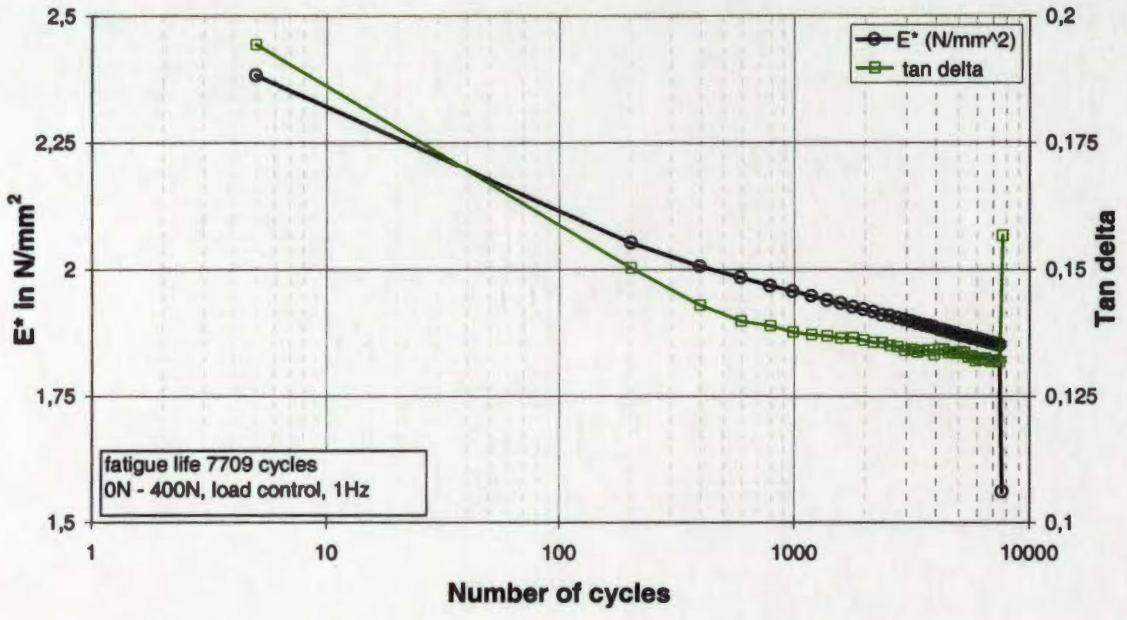

Figure 64 **Complex modulus curve and tan delta curve of a filled EPDM during fatigue testing.**

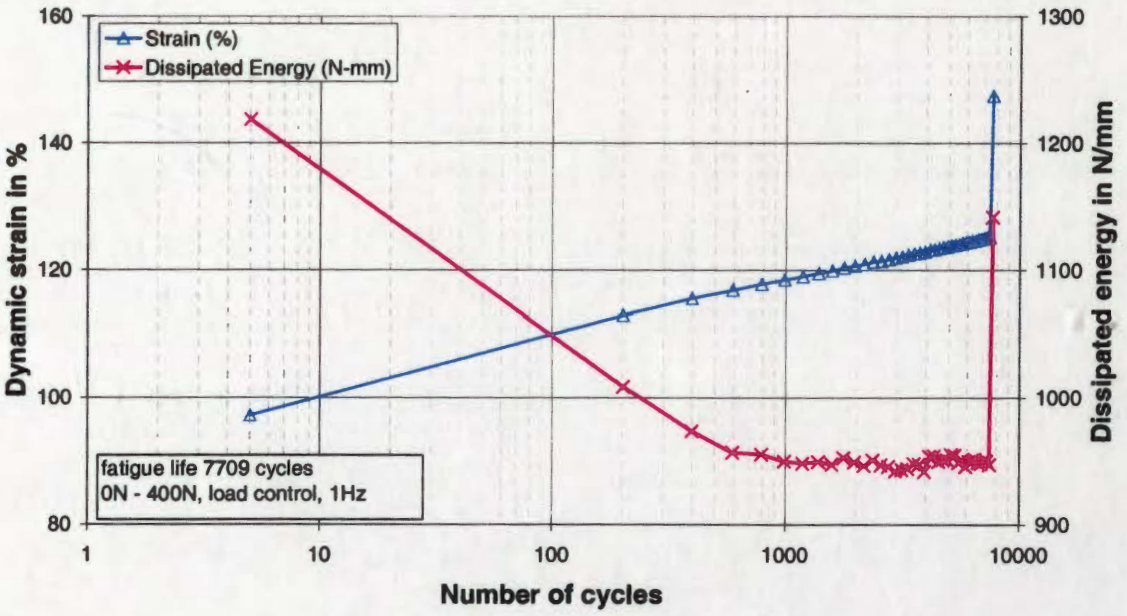

Figure 65 **Strain and dissipated energy per cycle of a filled EPDM during fatigue testing.**

Figure 66 shows the complex modulus curves for different test specimens tested under diverse testing conditions and procedures. It can be seen that

there is no direct correlation between the fatigue life and the absolute value of the complex modulus.

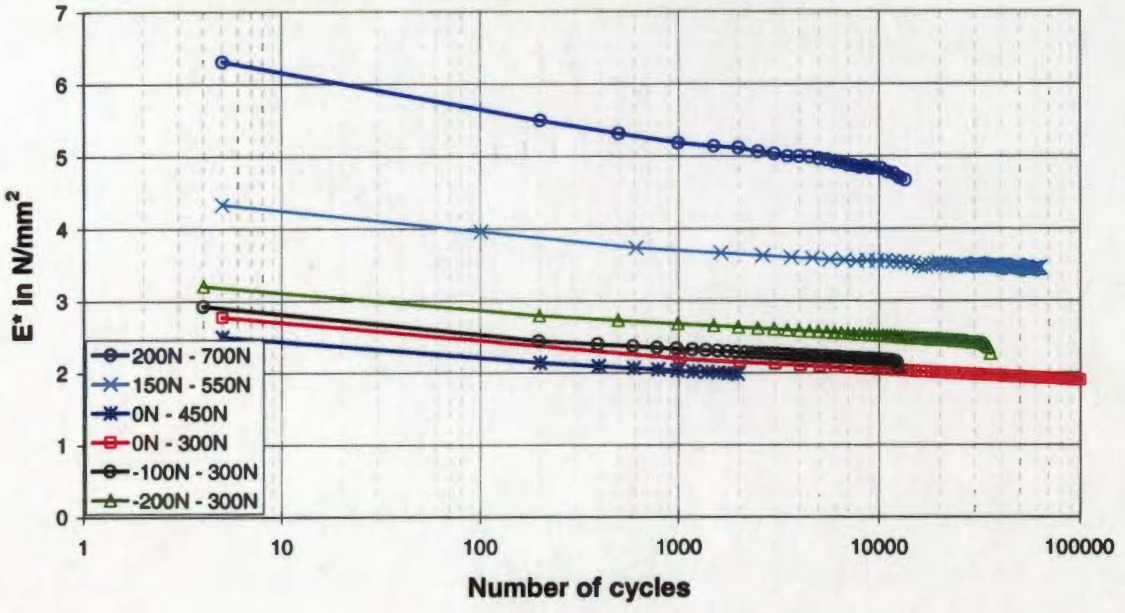

Figure 66 **Complex modulus curves of carbon black filled EPDM under different testing conditions during fatigue testing.**

If, however, the dynamic complex modulus during the fatigue tests is compared to the initial value, the end of service life is reached when the complex modulus E* has attained approximately 76 % of the one observed within the first cycles (Figure 67). This relative reduction in modulus E* is not dependent on the load case (amplitude, minimum load, compression or tension). The standard deviation for all different amplitudes and preloads is merely 5 %, and this value occurs irrespective of the test conditions and for different test specimens.

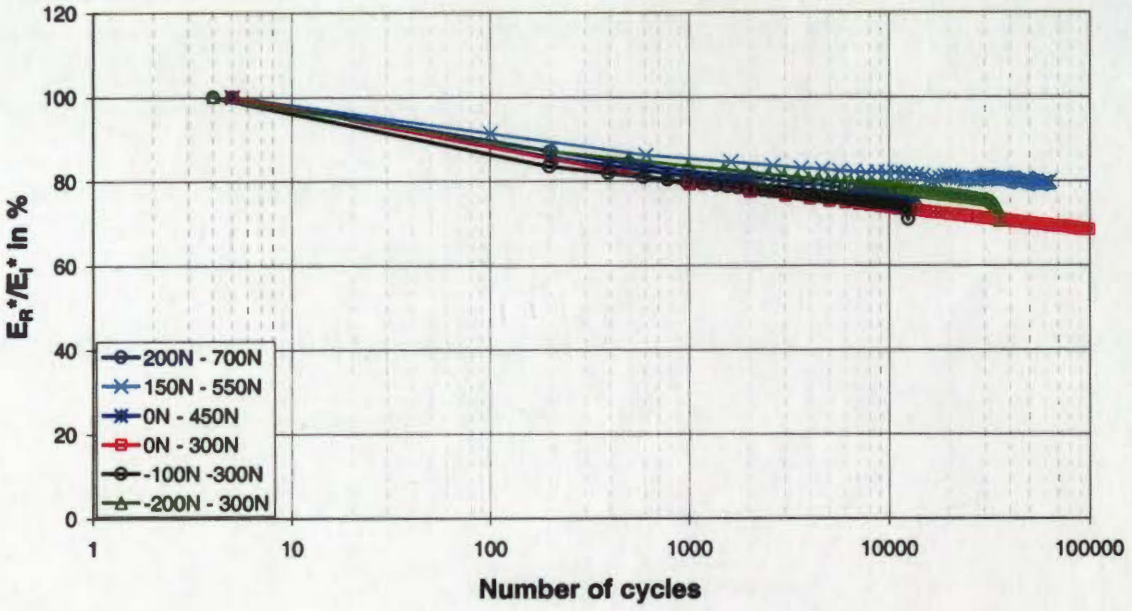

Figure 67 **Curves of the residual complex modulus divided by the initial complex modulus of carbon black filled EPDM during fatigue testing.**

3.7 Changes in Physical Properties during the Test of Filled SBR

The data from all fatigue tests on carbon black filled SBR exhibit the same phenomenon of changes in physical properties as those described for the carbon black filled EPDM in the proceeding Section 3.6. Figure 68 shows the complex modulus curves for a range of different test conditions. It can be seen that there is again no direct correlation between the modulus and the time to failure as with the filled EPDM material.

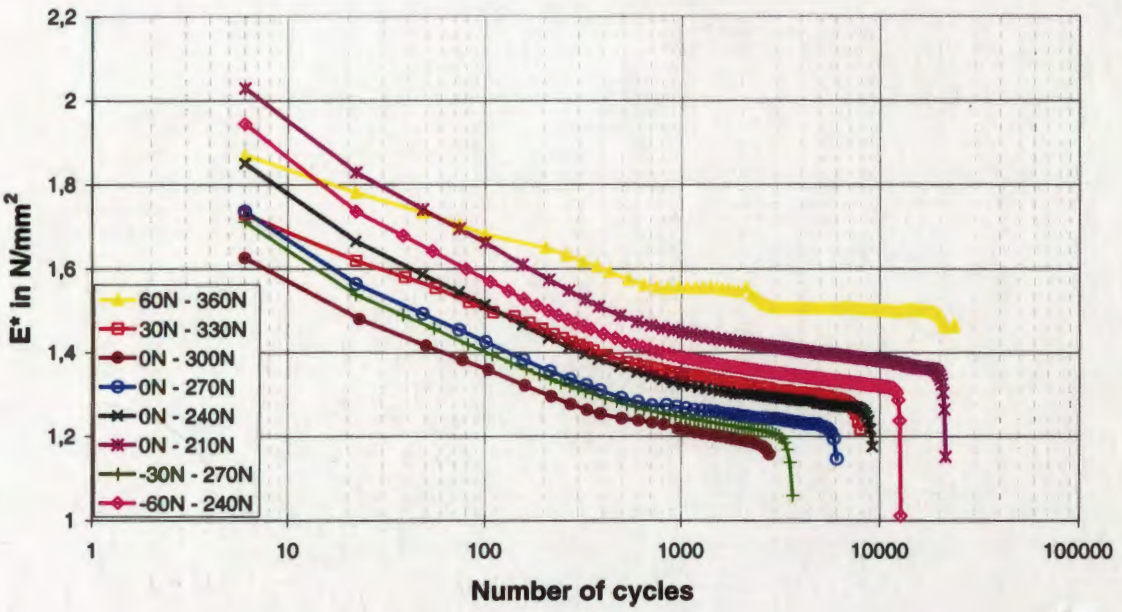

Figure 68 **Complex modulus curves of carbon black filled SBR under different testing conditions during fatigue testing.**

A comparison of the relative complex modulus curves for the filled SBR, where the residual modulus is divided by initial modulus, is shown in Figure 69. It is obvious that the filled SBR material is at the end of its service life when the complex modulus reaches approximately 71% of the initial modulus. For evaluation of this final value the last data point was used before the crack propagates. The last data points of Figure 69, showing a rapid decline in the

curve, were recorded during crack propagation, just before failure of the test specimen. These data were not used in the evaluation, because the test specimen was no longer intact at this moment and beyond.

The value of residual stiffness or stiffness loss appears to be independent of loading amplitude and applied minimum load.

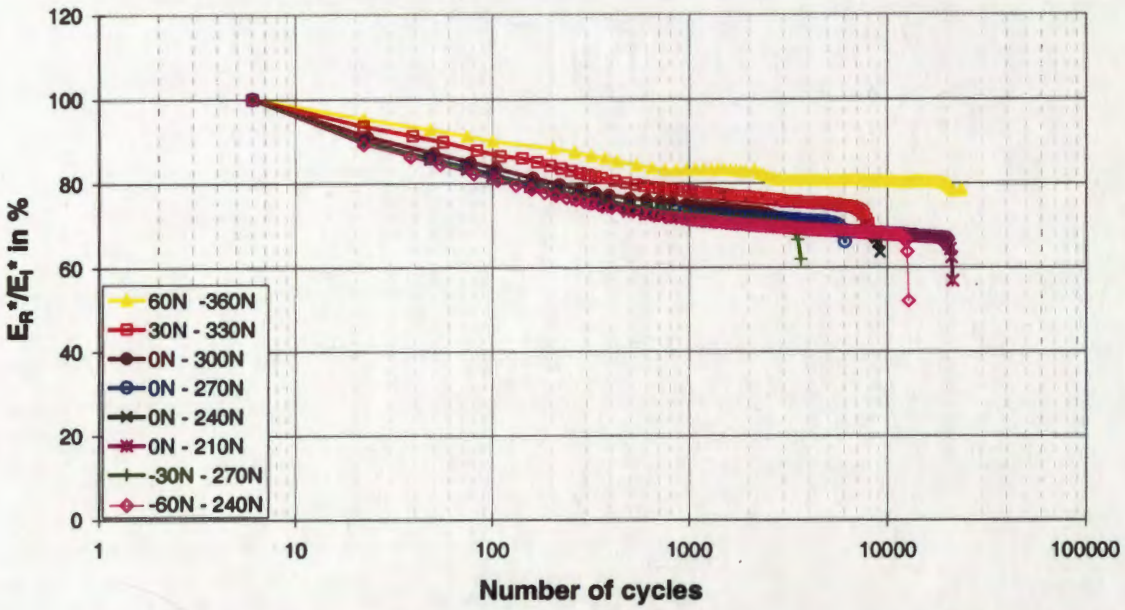

Figure 69 **Curves of the residual complex modulus divided by the initial complex modulus of carbon black filled EPDM during fatigue testing.**

These results may give a measure of stiffness loss at which a component manufactured from the material will fail. This finding potentially offers an important predictor for the maintenance and replacement of elastomeric components just prior to failure. It seems that there is a material specific 'loss of stiffness' when a component fails which is independent of the mode of loading. However, the dependency of frequency and temperature was not examined in this research.

4 Results of Dynamic Crack Propagation Tests

4.1 Dynamic Crack Propagation in Carbon Black Filled EPDM

The crack propagation properties of carbon black filled EPDM under displacement control with pulses of 50ms and a repetition rate of 10 Hz are shown in Figure 70. The numbers in all crack propagation captions indicate the applied minimum load.

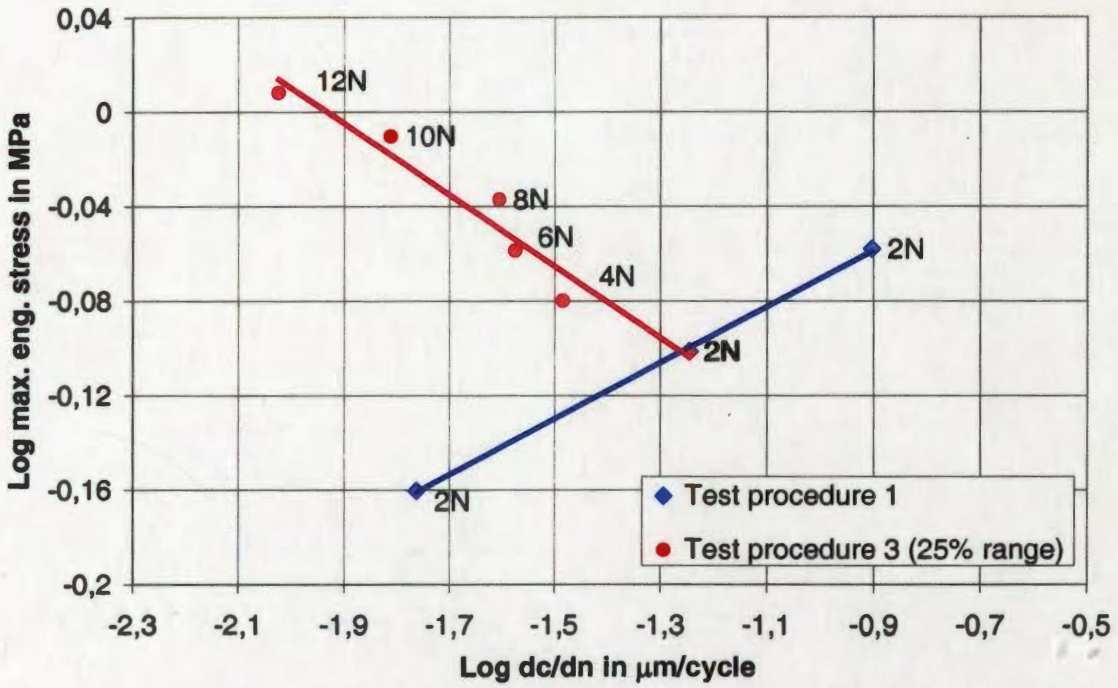

Figure 70 **Crack propagation rate results for carbon black filled EPDM, showing maximum stress dependence.**

All diamonds in this diagram represent mean values of the results of discrete integral strain amplitudes (20%, 25%, 30%) with a constant minimum load of 2N. The line, based on the diamonds, shows the established Wöhler behaviour if one calculates the cycles until 5 mm of crack length is reached or alternative until rupture assuming the crack growth rates were constant. With increasing

strain amplitude and hence maximum stresses the crack growth rate increases and the number of cycles till rupture decreases.

A minimum load variation with a constant strain amplitude of 25% is represented by the circles in Figure 70. The results show that with an increase of the minimum load at a constant displacement amplitude the crack growth rate is reduced by a factor of 8 within this parameter range. This resembles the finding that service life is increased by increased minimum load in fatigue tests.

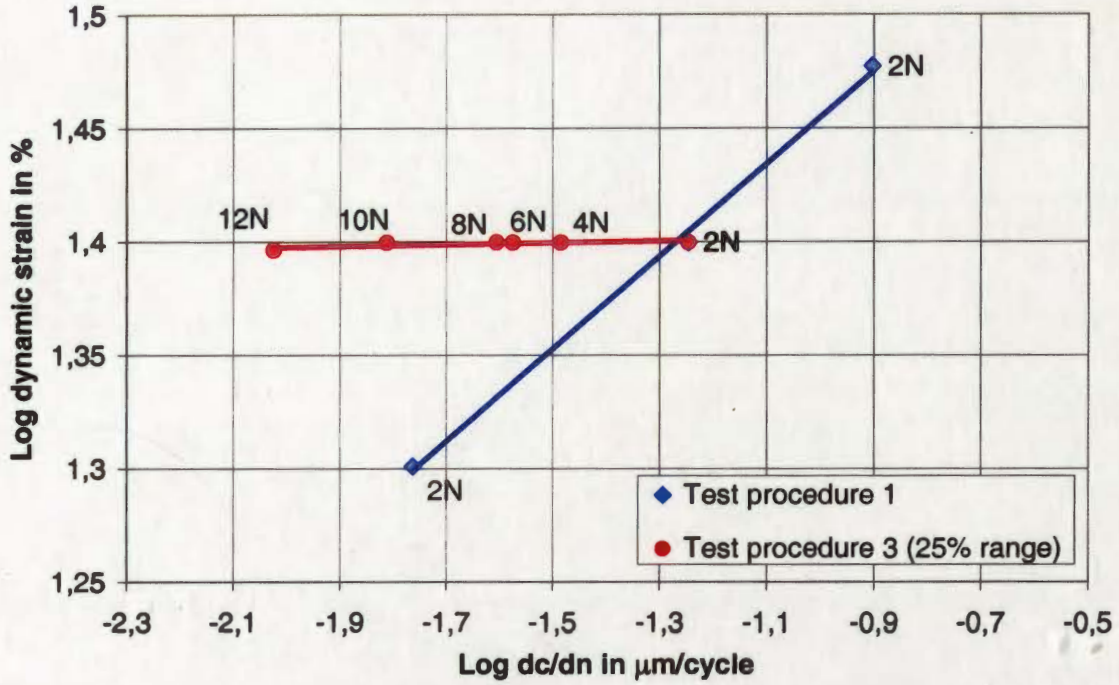

Figure 71 **Crack propagation rate results for carbon black filled EPDM, showing dynamic strain dependence.**

The dynamic strain dependency of this test series is shown in Figure 71. The diamonds show the strain amplitude variation at a constant minimum load of 2N. The results of the strain amplitude variation give a straight line in the log/log plot, with increasing amplitude the crack growth rate increases.

The minimum load variation at a constant amplitude of 25% is shown as circles (horizontal line) in the diagram. This plot shows that the crack growth rate is decreased with increasing minimum load. Note the permanent set is not recorded by the Tear Analyzer and therefore the dependence on maximum strain is not available.

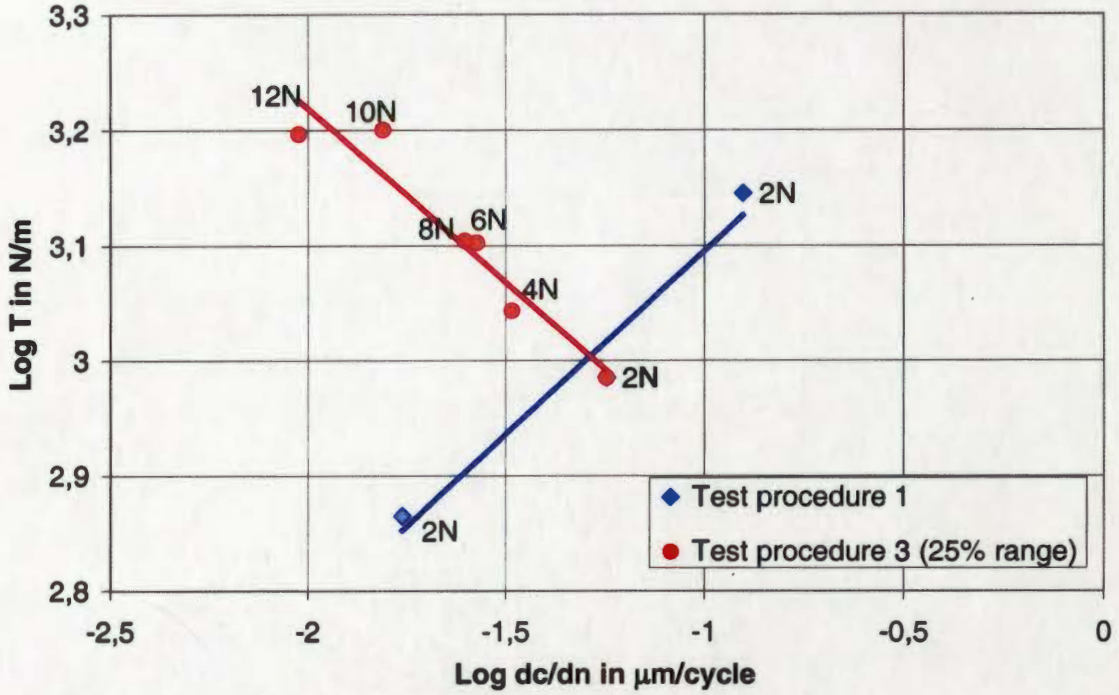

Figure 72 **Crack propagation rate results for carbon black filled EPDM, showing tearing energy 'T' dependence.**

Figure 72 shows a plot of the calculated tearing energy mean values of the stable crack propagation region. The results of test procedure 1 show the well known increase of the crack growth rate with increasing strain amplitude and tearing energy. Test procedure 3 contrasts with this result having increasing minimum load at constant strain amplitude leading to a decrease in the crack growth rate with increasing tearing energy.

4.2 Dynamic Crack Propagation in Unfilled EPDM

The crack propagation properties of unfilled EPDM under the same conditions are shown in Figure 73. Each diamond in this diagram represents the mean values of the results of a discrete strain amplitude (6%, 10%, 14%, 20%) for a constant minimum load of 1N. The plotted curve shows the Wöhler behaviour exhibited by the filled EPDM.

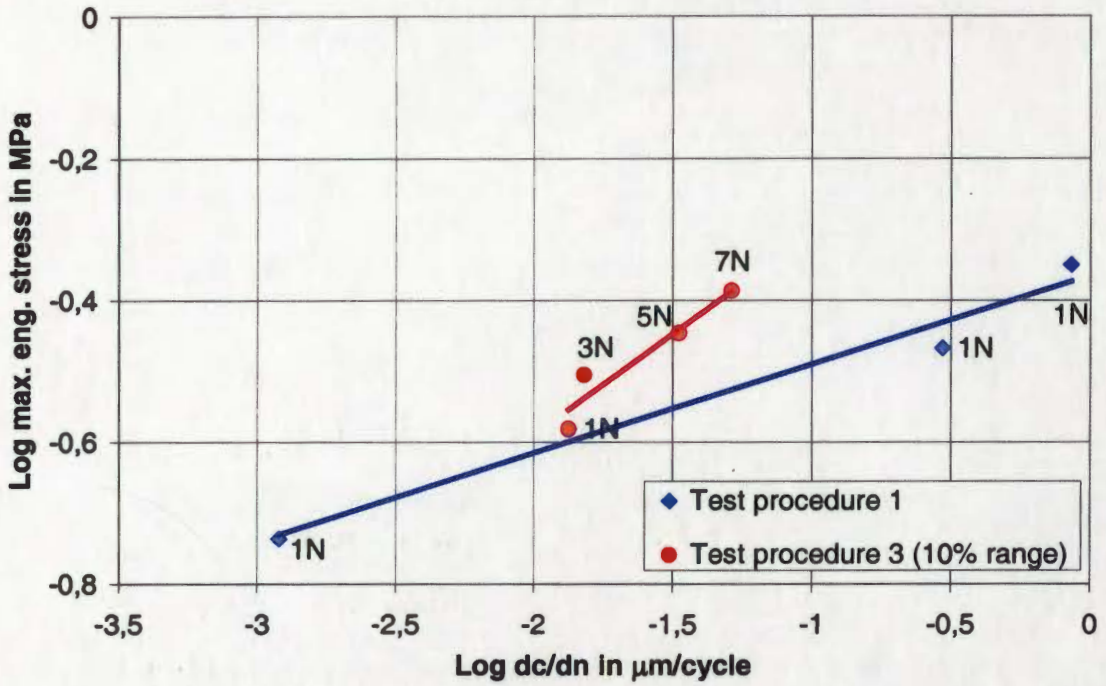

Figure 73 **Crack propagation rate results for unfilled EPDM, showing maximum stress dependence.**

A minimum load variation with a constant strain amplitude of 10% is represented by the circles in Figure 73. An increase of the minimum load at constant strain amplitude and hence increased maximum stress, increases the crack growth rate in contrast to the filled EPDM tests.

The dynamic strain dependency of this test series is shown in Figure 74. The diamonds show the strain amplitude variation at a constant minimum load of

1N. The results of the strain amplitude variation produce a straight line in the double logarithmic diagram. The crack growth rate increases with increasing amplitude.

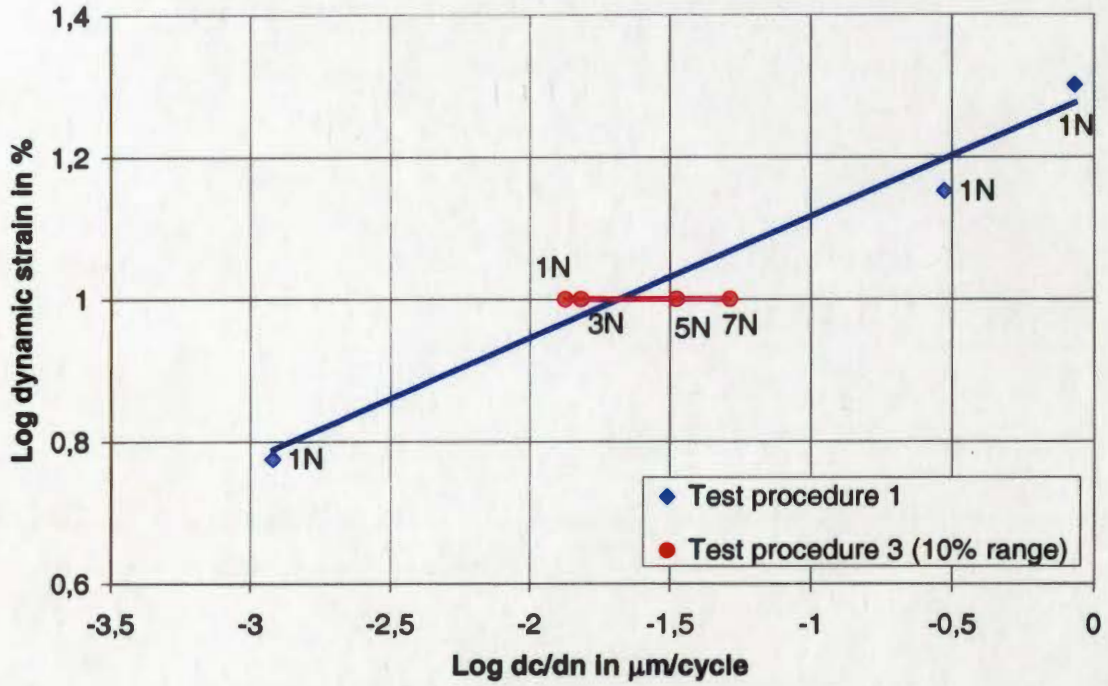

Figure 74 **Crack propagation rate results for unfilled EPDM, showing dynamic strain dependence.**

The minimum load variation at a constant amplitude of 10% strain is shown as circles (horizontal line) in the diagram, the crack growth rate is increased with increasing minimum load.

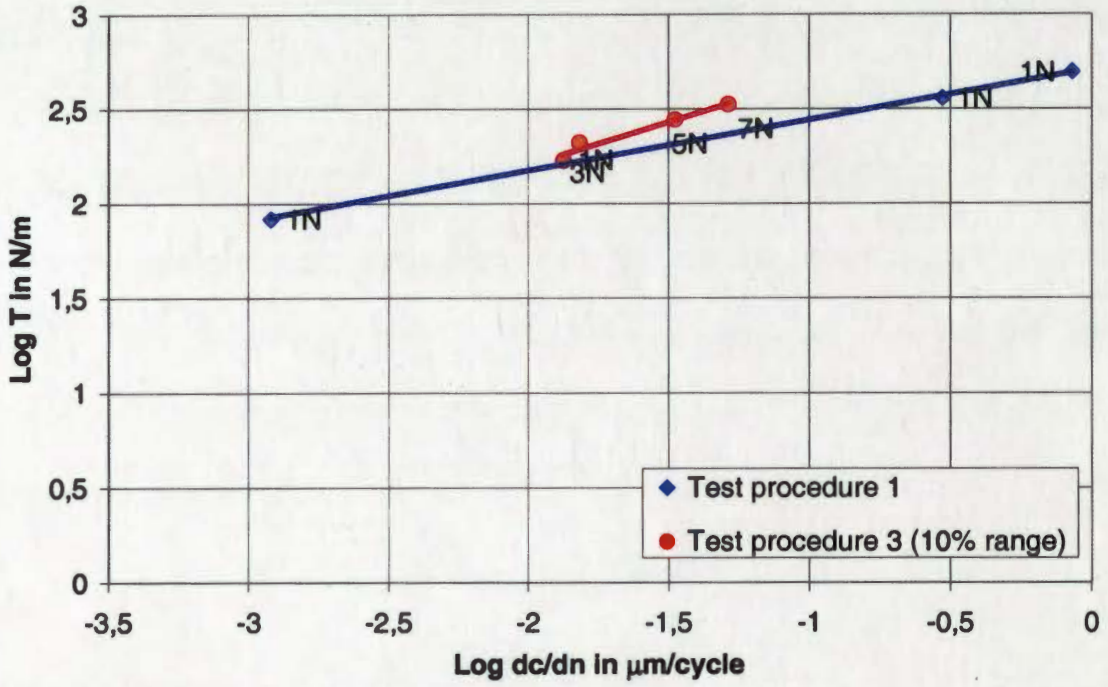

Figure 75 **Crack propagation rate results for unfilled EPDM, showing tearing energy 'T' dependence.**

Figure 75 shows a plot of the mean values of the calculated tearing energy vs. crack growth rate. The crack growth rate increases with increasing strain amplitude and tearing energy (test procedure 1). Test procedure 3 shows increasing minimum loads at constant strain amplitude and the crack growth rate increases simultaneously with increases in tearing energy. The tearing energy values of test procedure 3 are some what higher at similar crack growth rates compared with test procedure 1.

4.3 Dynamic Crack Propagation in Carbon Black Filled SBR

The crack propagation properties of carbon black filled SBR are shown in Figure 76. Each diamond in this diagram represents the mean value of the results of a discrete strain amplitude (20%, 30%, 40%) of a constant minimum load of 2N. This curve shows the well known Wöhler behaviour for the crack propagation properties, with increasing strain amplitude and hence increasing maximum stresses the crack growth rate increases.

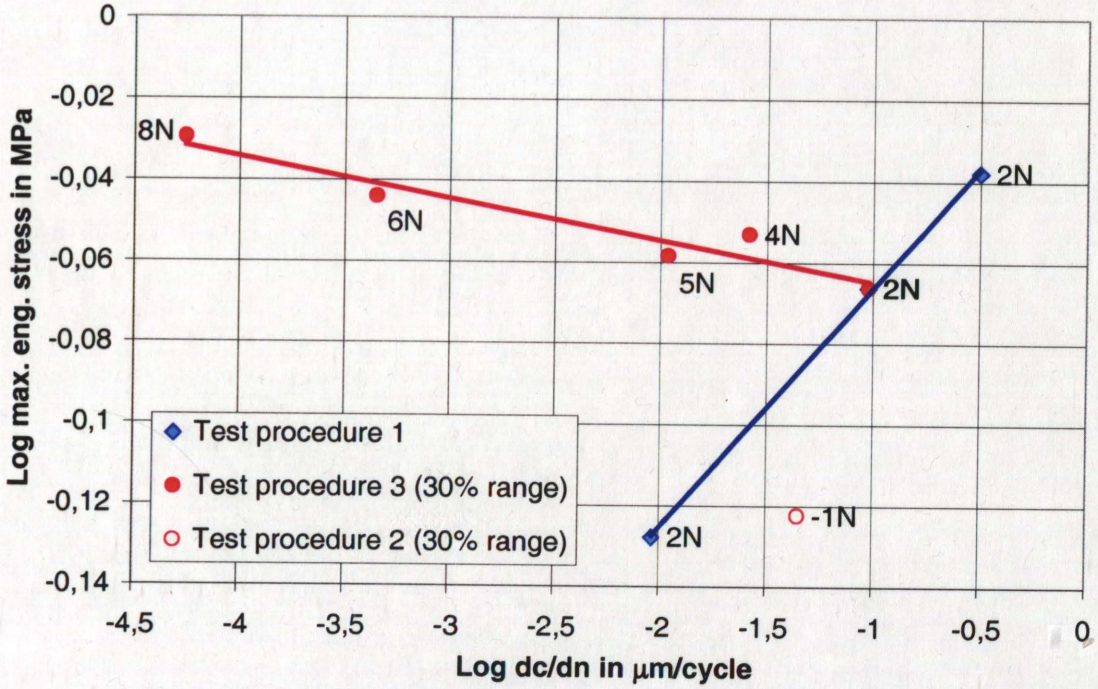

Figure 76 **Crack propagation rate results for carbon black filled SBR, showing maximum stress dependence.**

Test procedure 3 where minimum load is varied at a constant strain amplitude of 30% is represented by the circles in Figure 76. An increase of the minimum load reduces the crack growth rate by a factor of 213 within the parameter range used. The carbon black filled SBR was also tested at a minimum load of –1N with a consequent small tendency to buckle (test procedure 2) at 30%

strain amplitude shown in Figure 76 as an unfilled circle. It can be seen that with the greatly decreased maximum stress the crack propagation is slightly reduced.

The dynamic strain dependency of this test series is shown in Figure 77. The diamonds depict the strain amplitude variation at a constant minimum load of 2N. The results of the strain amplitude variation give a straight line in the double logarithmic plot, with increasing crack growth rate at increased amplitudes.

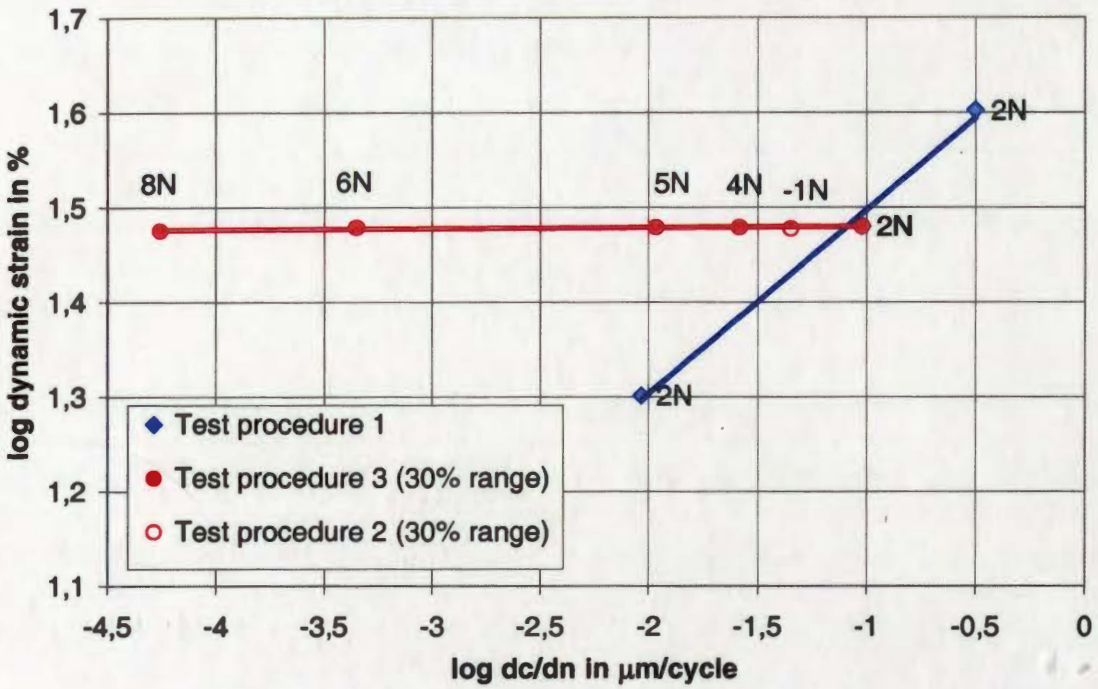

Figure 77 **Crack propagation rate results for carbon black filled SBR, showing dynamic strain dependence.**

The minimum load variation at a constant amplitude of 30% shown as circles (horizontal line) in the diagram causes a significant reduction of the crack growth rate with increasing minimum load. The result of the negative minimum load of –1N is indicated by the unfilled circle in Figure 77.

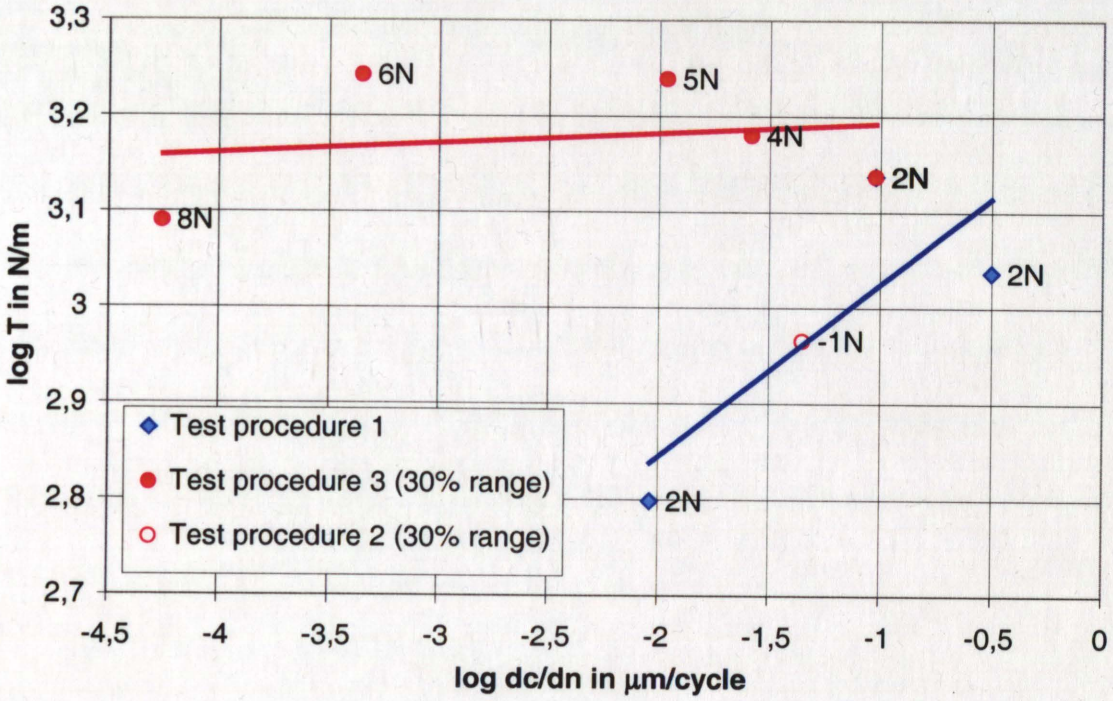

Figure 78 **Crack propagation rate results for carbon black filled SBR, showing tearing energy 'T' dependence.**

The tearing energy dependence is depicted in Figure 78. The results of test procedure 1 describe that with increasing strain amplitude the tearing energy increases and correspondingly the crack growth rate increases. Test procedure 3 contrasts with this result in that with increasing positive minimum load at constant strain amplitude the tearing energy is stable albeit with a very high scatter, but the crack growth rate decreases significantly. The result of test procedure 2 has a negative minimum load represented by an unfilled circle in Figure 78. The tearing energy and the crack propagation rate are reduced compared with the same strain amplitude of test procedure 1. This value corresponds well with the results of the strain amplitude variation of test procedure 1, but again the filled SBR has a high scatter in results.

4.4 Dynamic Crack Propagation in Unfilled SBR

The crack propagation properties under displacement control with pulses of 50ms and a repetition rate of 10 Hz for the unfilled SBR are shown in Figure 79. Each diamond in the diagram represent the mean value of the results of a discrete strain amplitude (20%, 25%, 30%) with a constant minimum load of 1N. The curve shows the well known Wöhler behaviour for crack propagation properties. With increasing strain amplitude and hence higher maximum stresses the crack growth rate increases.

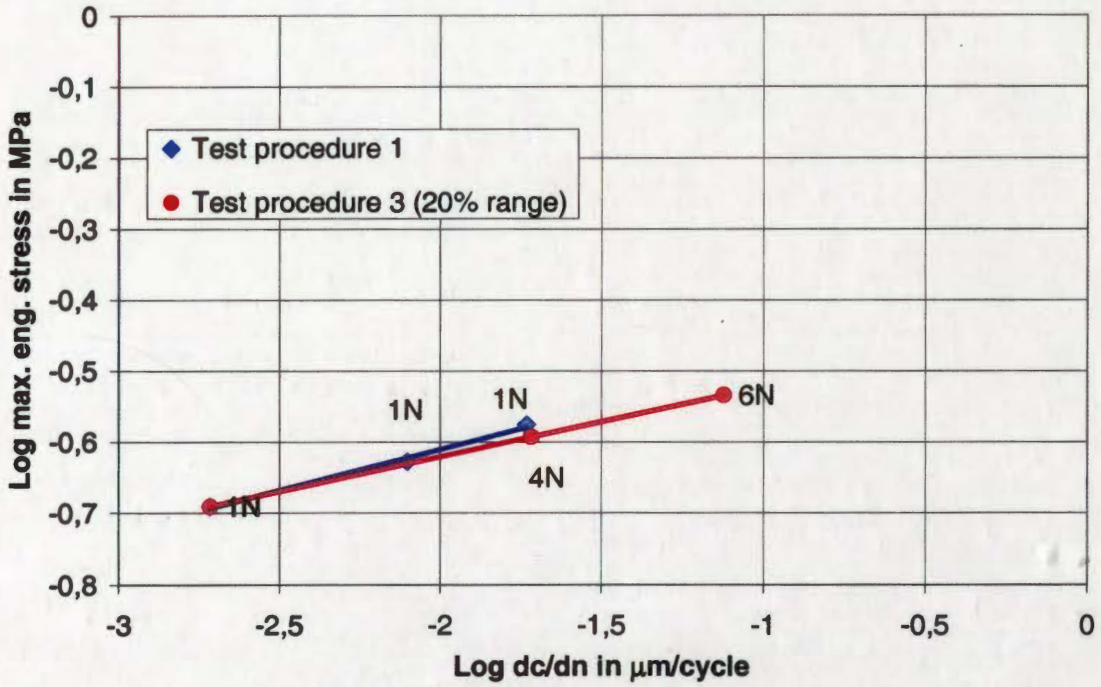

Figure 79 **Crack propagation rate results for unfilled SBR, showing maximum stress dependence.**

A minimum load variation with a constant strain amplitude of 20% is represented by the circles in Figure 79. The results show that an increase of the minimum load at a constant load amplitude and hence increased maximum stress, increased the crack growth rate. Both procedures, strain amplitude

variation and minimum load variation virtually show a single curve for maximum stress dependency.

The dynamic strain dependency of this test series is shown in Figure 80. The diamonds show the strain amplitude variation at a constant minimum load of 1N. The results of the strain amplitude variation give a straight line in the double logarithmic diagram. The crack growth rate increased when the amplitude was increased.

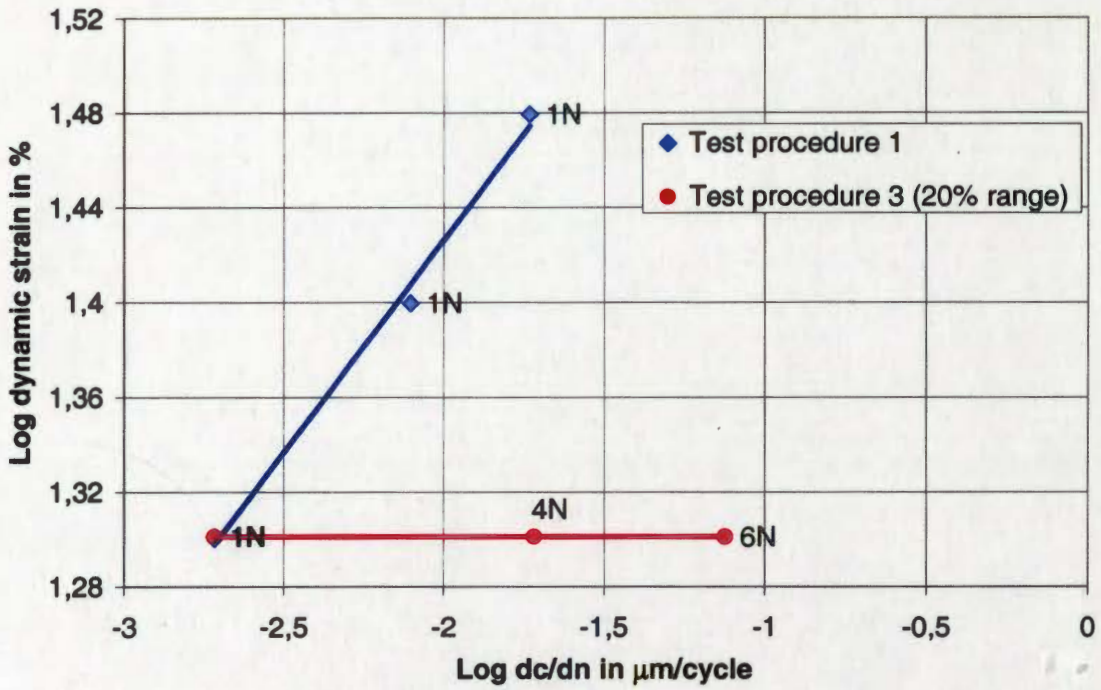

Figure 80 **Crack propagation rate results for unfilled SBR, showing dynamic strain dependence.**

The minimum load variation results in a horizontal line showing that increased minimum loads lead to an increase in crack growth rate.

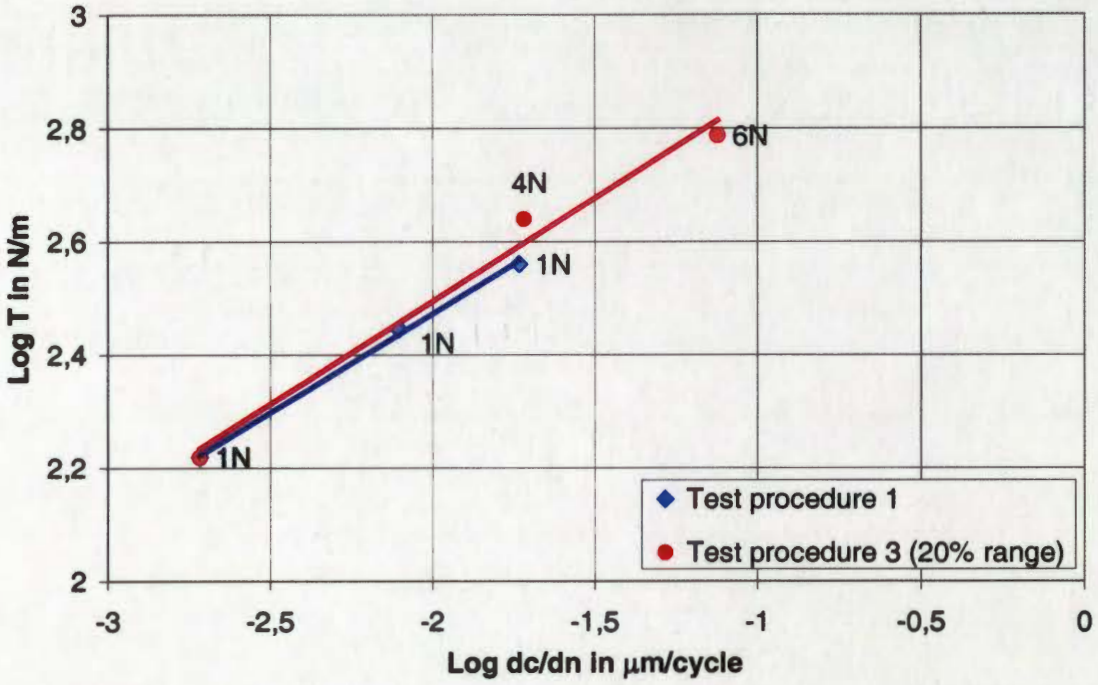

Figure 81 **Crack propagation rate results for unfilled SBR, showing tearing energy 'T' dependence.**

The dependence on the tearing energy 'T' of Figure 81 shows a normal behaviour and a single curve under both minimum load variation and under strain amplitude variation.

4.5 Comparison of Fatigue Life Test Results and Dynamic Crack Propagation Test Results

The maximum stress dependency on the fatigue life of the carbon black filled EPDM and the carbon black filled SBR can be seen in Figure 82. A comparison of the fatigue life properties of both materials show that the filled EPDM is superior to the filled SBR material under dynamic loading when the compared on a basis of maximum stresses.

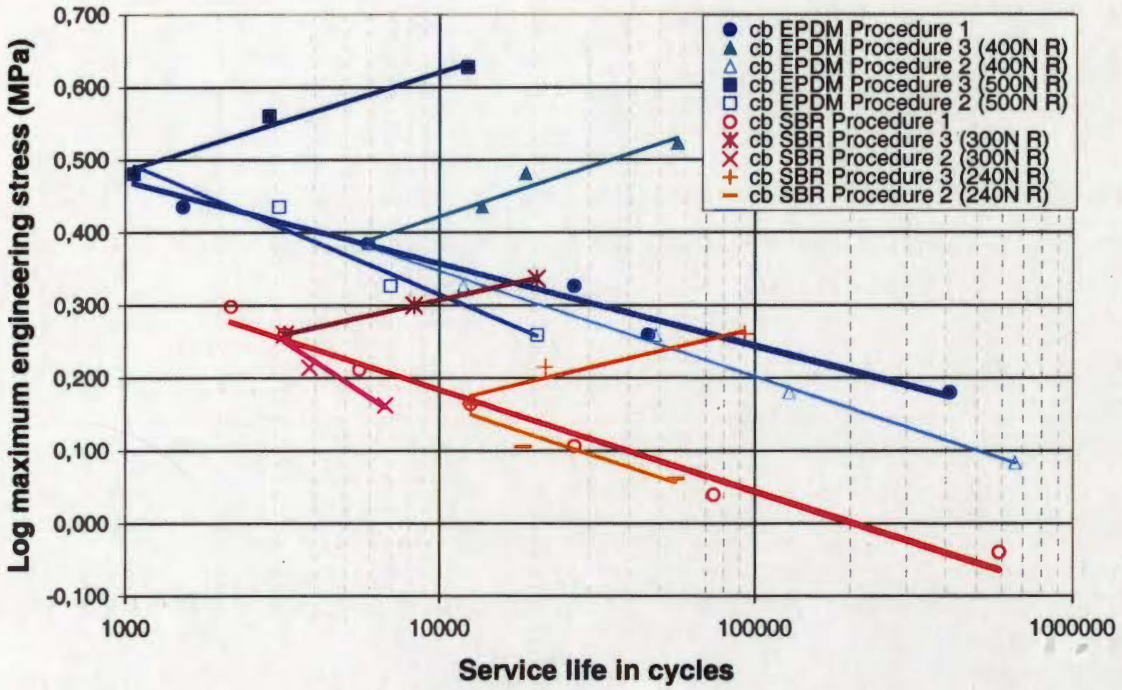

Figure 82 **Comparison of the fatigue properties of carbon black filled EPDM and carbon black filled SBR, showing maximum stress dependence.**

Figure 83 shows the dynamic strain dependency of the filled EPDM and SBR materials. This diagram suggests an overlapping of material properties of both materials under test procedure 1. The carbon black filled SBR material exhibits a lower fatigue life than the EPDM at higher strains.

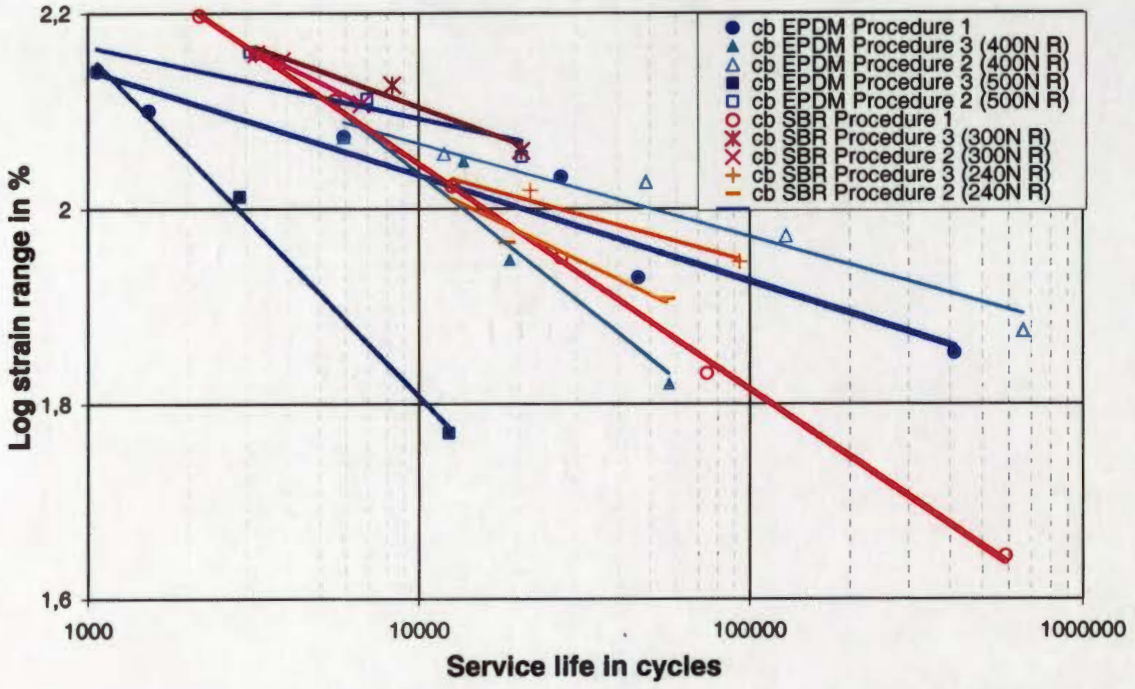

Figure 83 **Comparison of the fatigue properties of carbon black filled EPDM and carbon black filled SBR, showing dynamic strain dependence.**

A comparison of the maximum stress dependency on the dynamic crack propagation of the carbon black filled EPDM and the carbon black filled SBR can be seen in Figure 84. The SBR material exhibits slower crack propagation rates than the EPDM material at small amplitudes. The filled EPDM shows a slower crack growth rate for higher stresses leading to failure after a few thousand cycles. Increases in the minimum load of the carbon black filled EPDM induces very high stresses at relatively low crack growth rates. Increases in minimum loads applied to the filled SBR leads to pronounced decreases in crack growth rates.

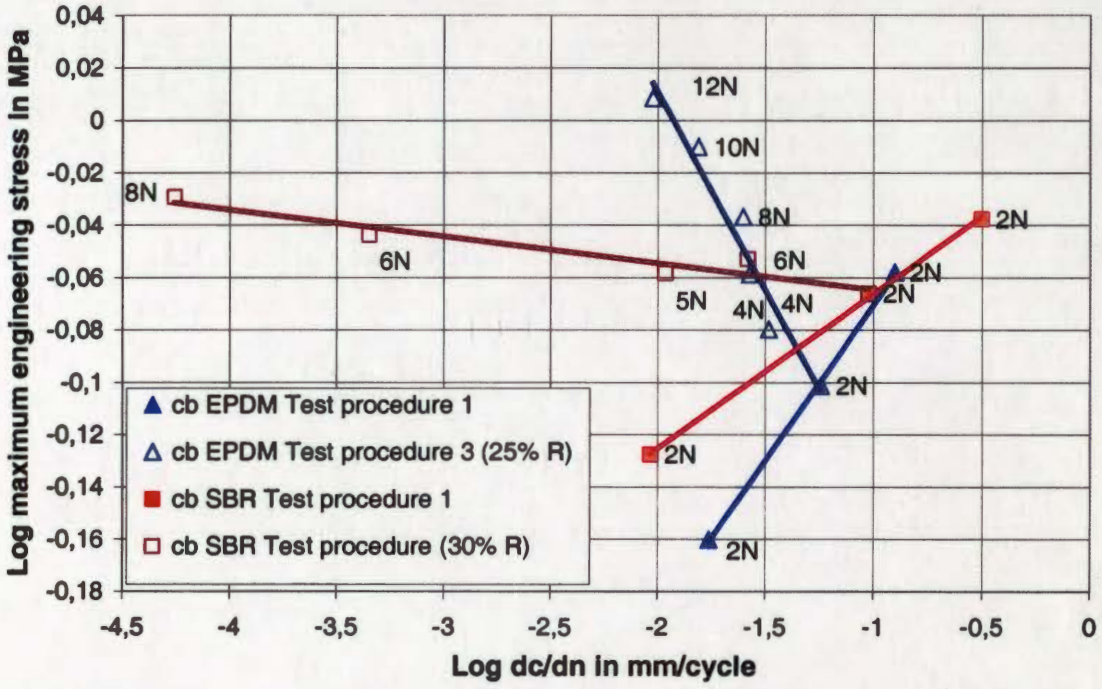

Figure 84 **Comparison of the dynamic crack propagation properties of carbon black filled EPDM and carbon black filled SBR, showing maximum stress dependence.**

The dynamic strain dependency on the dynamic crack propagation properties of the carbon black filled EPDM and SBR materials are shown in Figure 85. The filled SBR material exhibits a slower crack growth rate compared with the carbon black filled EPDM. This diagram shows very clearly how an increase in the minimum load causes a significant reduction in the crack propagation rate at constant strain amplitude. Additionally, it can be seen that the crack propagation rate of the SBR material is always less than for the EPDM material, compared under similar test conditions.

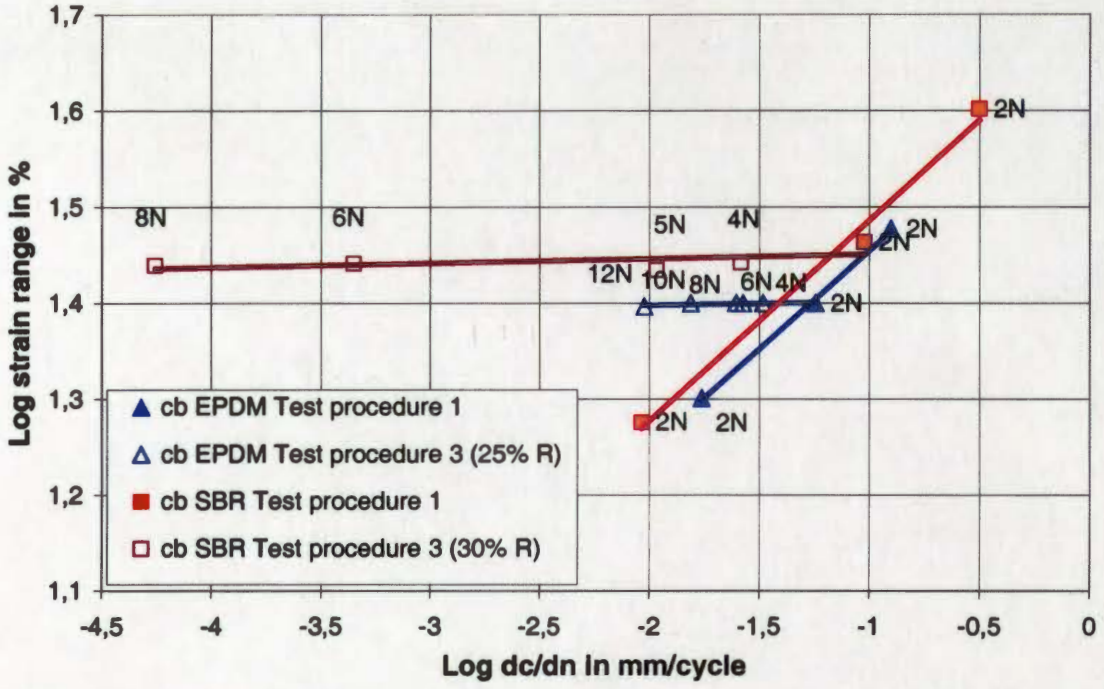

Figure 85 **Comparison of the dynamic crack propagation properties of carbon black filled EPDM and carbon black filled SBR, showing maximum dynamic strain dependence.**

A plot of the carbon black filled EPDM and SBR materials with respects to tearing energy is shown in Figure 86. The results of test procedure 1 of both materials are similar, especially if the high scatter of the carbon black filled SBR material is considered. Test procedure 3 highlights a difference between both filled materials. With increasing minimum load the tearing energy is increased for the EPDM material while the tearing energy for the SBR material remains approximately constant. But for both carbon black filled materials a reduction of the crack growth rate is observed with increasing minimum load.

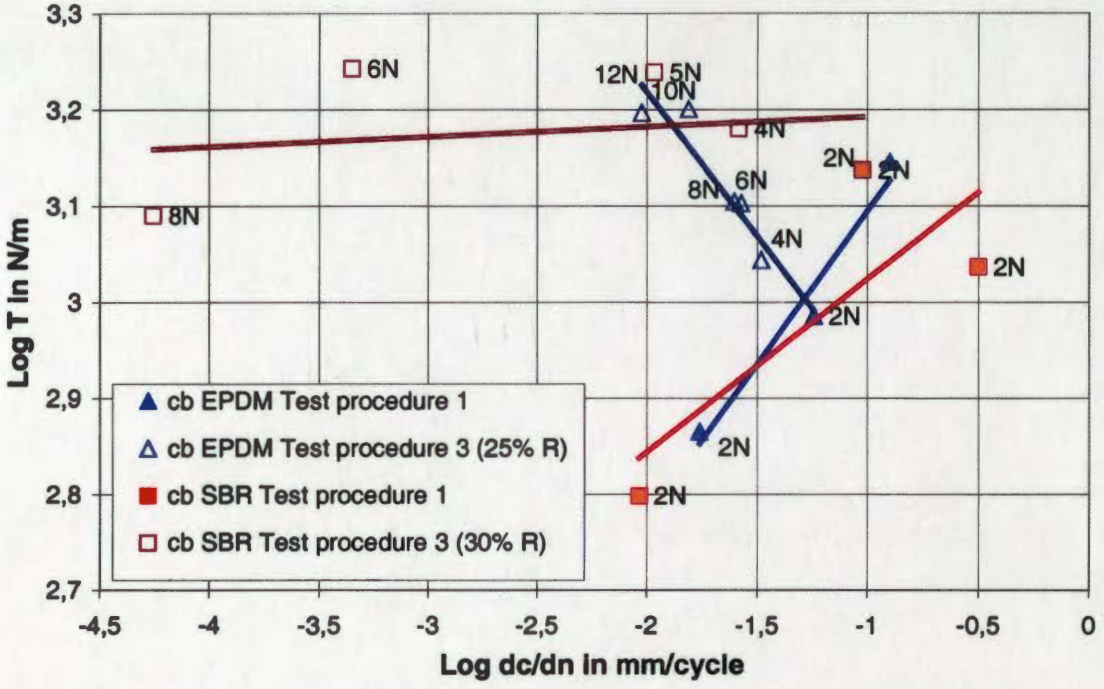

Figure 86 **Comparison of the dynamic crack propagation properties of carbon black filled EPDM and carbon black filled SBR, showing tearing energy 'T' dependence.**

A second Tear Analyzer test series was carried out to facilitate a direct comparison between the fatigue life and crack propagation properties of the carbon black filled materials. This test series was carried out under sinusoidal excitation at 1 Hz frequency. Only test procedure 1 was used with a minimum load of 2N. In this series, carbon black filled EPDM and SBR materials were tested simultaneously under the same dynamic strain amplitude. Figure 87 shows the maximum stress dependency of the sinusoidal crack propagation tests. It can be see that the crack growth rate of the carbon black filled SBR material is much lower when compared with the filled EPDM material.

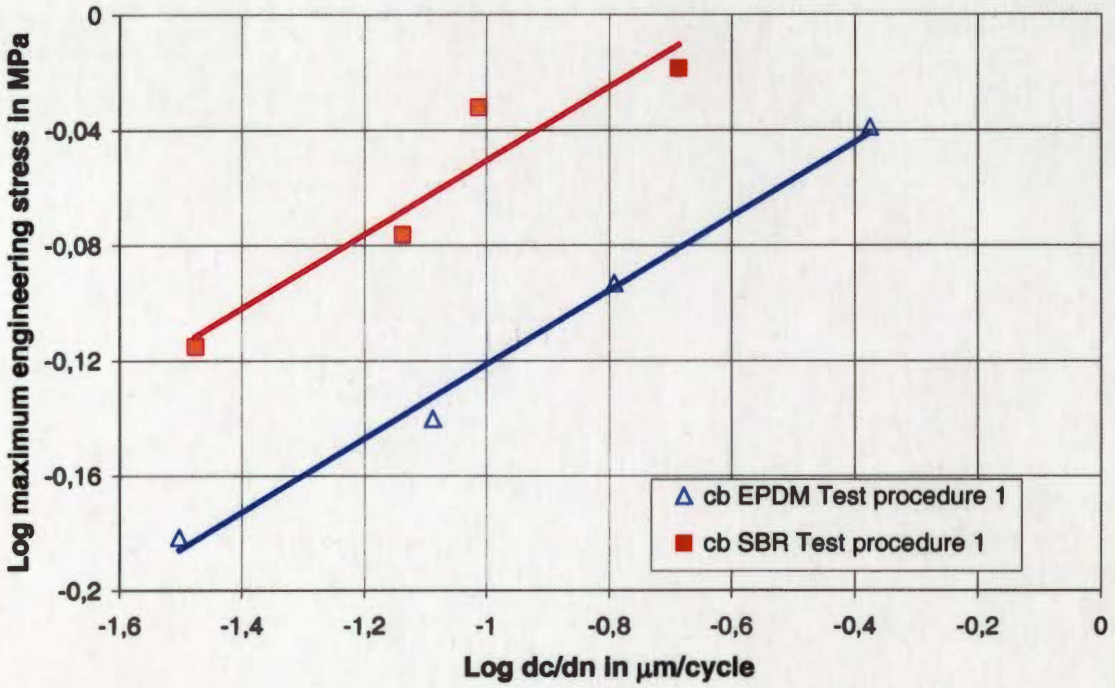

Figure 87 **Comparison of the dynamic crack propagation properties of carbon black filled EPDM and carbon black filled SBR under sinusoidal excitation of 1 Hz, showing maximum stress dependence.**

The dynamic strain dependency of both filled materials is plotted in Figure 88. The carbon black filled EPDM material appears to exhibit superior properties only at low strains. At higher dynamic strains the SBR shows a lower crack growth rate.

Figure 88 **Comparison of the dynamic crack propagation properties of carbon black filled EPDM and carbon black filled SBR under sinusoidal excitation of 1 Hz, showing maximum dynamic strain dependence.**

A comparison of the tearing energies calculated on the basis of the sinusoidal crack propagation tests is plotted for the filled EPDM and SBR materials in Figure 89. Both materials have similar crack growth rates at medium tearing energies. The EPDM material exhibits a lower crack growth rates at high tearing energies while the SBR has slower crack propagation at low tearing energies.

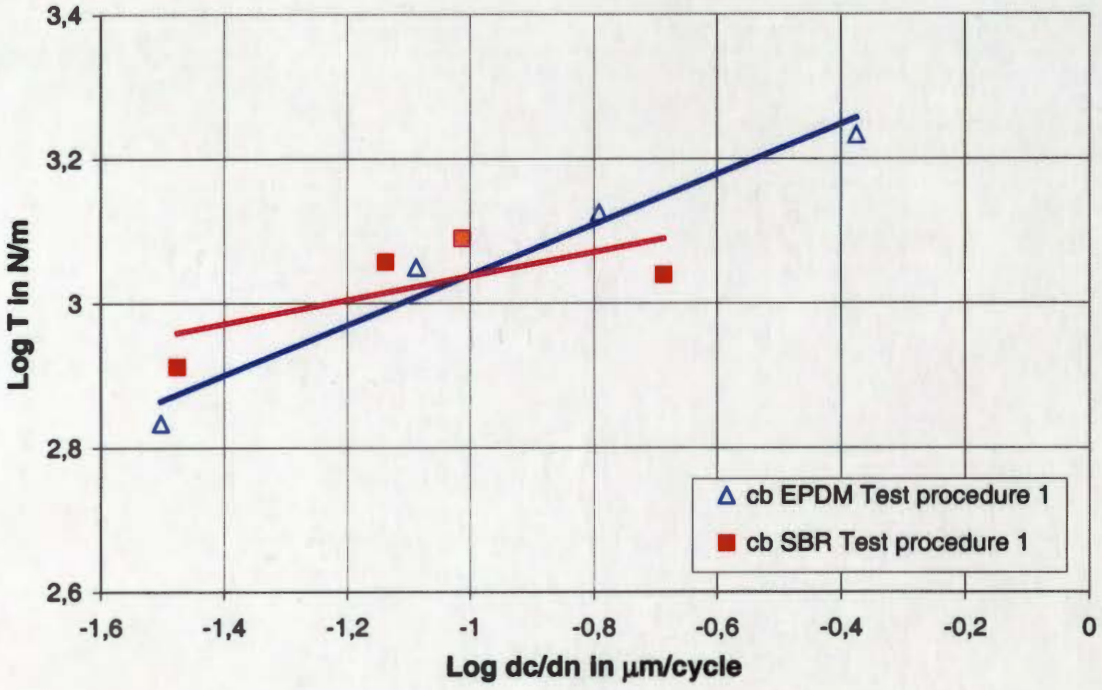

Figure 89 **Comparison of the dynamic crack propagation properties of carbon black filled EPDM and carbon black filled SBR under sinusoidal excitation of 1 Hz, showing tearing energy 'T' dependence.**

An unusual plot of maximum stress versus fatigue life data (Wöhler curve) for a crack propagation test is shown in Figure 90. The mean number of cycles to failure (complete rupture) of the test specimens tested under one condition are depicted In this diagram. It is evident from this plot that the carbon black filled SBR failed much later than the carbon black filled EPDM at all strain amplitudes in the tests.

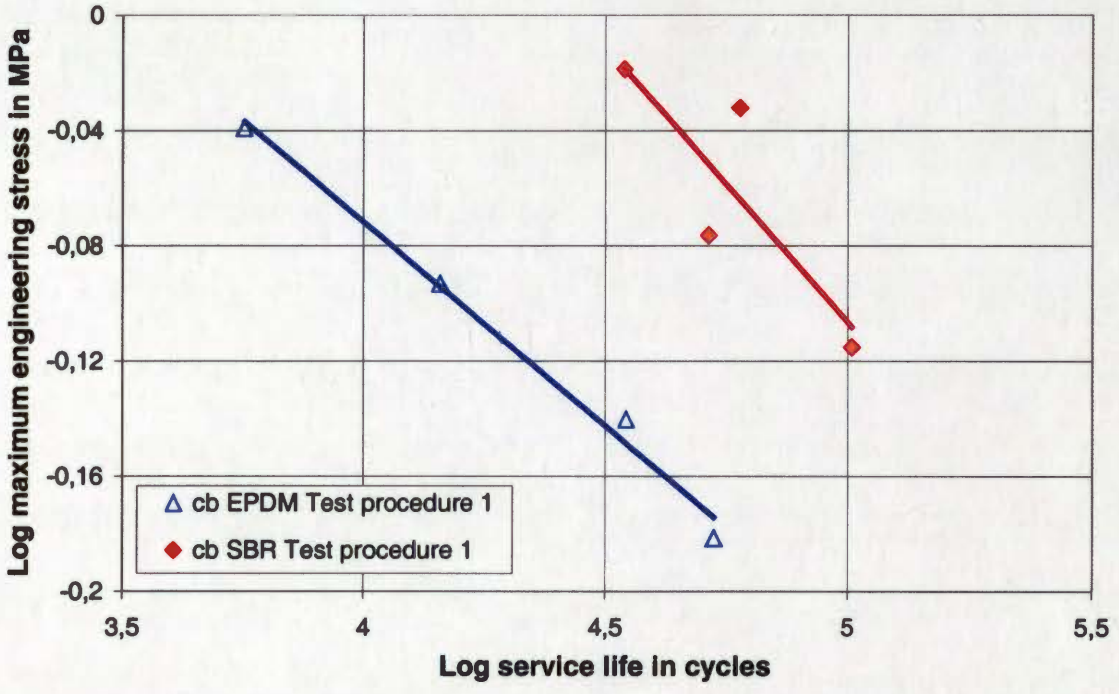

Figure 90 **Comparison of the service life of dynamic crack propagation tests of carbon black filled EPDM and carbon black filled SBR under sinusoidal excitation of 1 Hz, showing maximum stress dependence.**

5 Discussions

The results obtained from the fatigue tests on the non strain crystallising materials EPDM and SBR are at variance in two respects with the behaviour of such elastomers based on previous thinking. Gent [**45**] suggests, by comparison with strain crystallising rubbers, no comparable strengthening effect on raising the minimum strain levels in non-crystallising elastomers even when reinforcing fillers were added. The same result was found by Fielding [**46**]for carbon black filled non strain crystallising SBR. His experiments show that with increasing minimum strain at constant dynamic strain the fatigue life was reduced. These results were confirmed by calculations of Lindley [**47**] and compared with results for unfilled SBR. Fielding [**46**], Lindley [**47**] and Lake & Lindley [**9**] explained the absence of a minimum load effect for non strain crystallising rubbers having a time dependent (static) crack growth which does not exist in strain crystallising elastomers like natural rubber. This static crack growth phenomenon results in crack growth when just a minimum static strain is applied and an increase of the static loading increases the crack growth even in absence of a dynamic loading.

Another approach toward explaining the increased fatigue or crack growth resistance with increased minimum strain of strain crystallising rubbers is provided by considering the increase in hysteresis. Lake [**48**] showed first that higher hysteresis causes lower crack growth. Then Lake (and later Lindley [**47**]) explained that high strain hysteresis due to the occurrence of strain induced crystallisation confers great resistance to crack growth and fatigue. In

contrast the hysteresis of non strain crystallising rubbers results from viscoelastic behaviour and is generally of a lower order.

In a strain crystallising rubber, growth steps during repeated loading become very small if the material is not fully relaxed between each cycle **[45, 48, 49]**. A crystalline region develops at the crack tip and this crystallinity remains intact for repeated load applications and consequently crack growth is inhibited. Fatigue life becomes prolonged in this situation. However, the EPDM and SBR material used in this test programme not subject to this phenomenon and increased fatigue resistance at higher levels of tensile and compressive mean stress must have an alternative explanation. Possible reasons for increased fatigue life for higher mean stresses are considered below.

a) Compressive and tensile loading of elastomers each reduce the effective severity of natural flaws. Natural flaws are unavoidable with an effective initial size of about 25 μm **[8]** and are considered equivalent to a sharp edge cut of approximately 40 ± 20 μm depth **[45]**. If a compressive pre-load closes a stress raiser and a tensile pre-load 'smoothes out' a stress concentration, it is arguable that stress cycles become less injurious **[50]**.

b) Discounting the effect of hysteresis, the strain energy or tearing energy available in each cycle to propagate a crack can be less when σ_{min} or ε_{min} is not zero. This situation is shown in Figure 91. Increases in the ratio of T_{min} to T_{max} or ε_{min} to ε_{max} reduce the energy available to propagate the crack. This explanation is consistent with all tearing (energy) approaches described earlier.

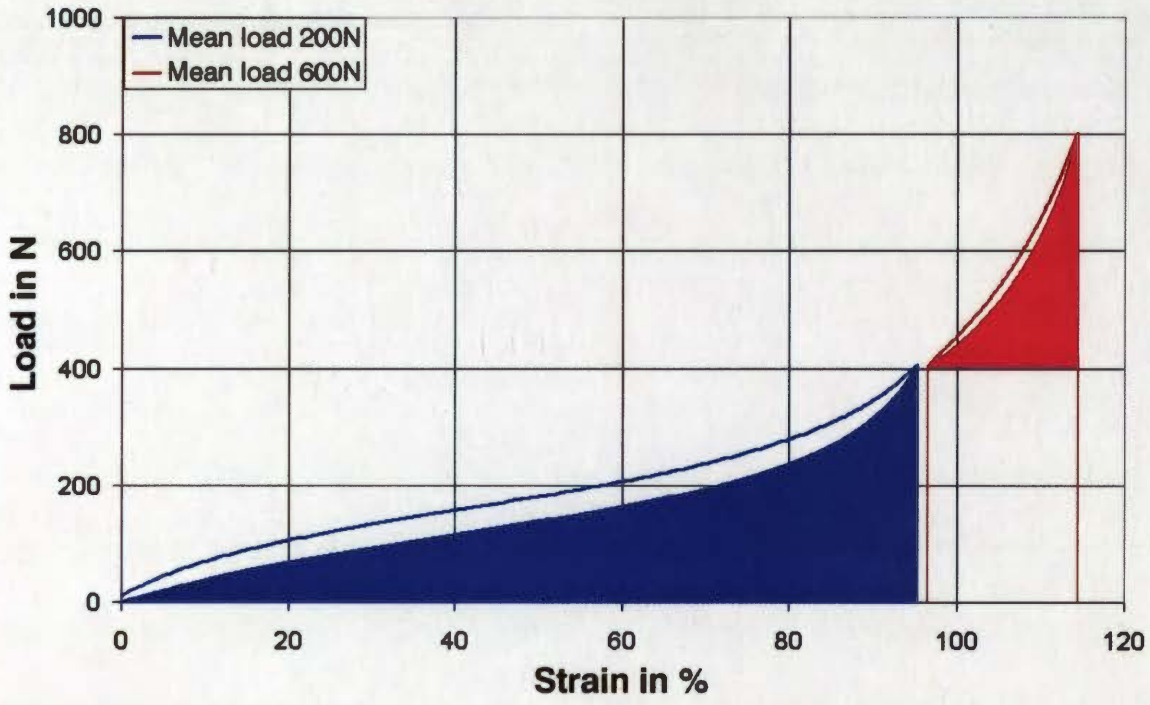

Figure 91 **Diagrammatic representation of dynamic stored energy for two load ranges.**

c) Lee and Donovan [**51**] found out that carbon black increases the size of the crystallised zone at a stressed crack tip which are known to stop propagating cracks.

d) Lake et. Al. [**52**] have shown that certain non-crystallising rubbers experienced the formation of anisotropic structures at crack tips resulting from filler particle alignment or aggregates. In tests on samples that were not completely relaxed between cycles, this produced similar increases in fatigue strength to those observed in tests on crystallising rubbers.

An additional result is that the dynamic crack propagation shows the same behaviour for non strain crystallising elastomers as found in fatigue to failure

tests. The crack growth rate in case of carbon black filled elastomers was reduced by applying a minimum load at a constant strain amplitude. In contrast to this finding the crack growth rate for the unfilled EPDM or SBR materials were increased with an increase of the minimum load at constant strain amplitude.

The literature [35] suggests that the use of a crack growth approach instead of actual long-term fatigue testing is appropriate for general use. The fatigue testing on dumbbell specimens in this research has shown that visible crack propagation occurs within less than the final 5% of the service life of all dumbbell specimens and in tests on unfilled materials, crack propagation was observed in a few cycles only. Gent [8] calculates for a tensile strip test specimen that the crack growth can only be observed by the naked eye when 90% of the fatigue life has elapsed. The difference between 90% (Gent [8]) and 95% (this research) can probably be explained by the different materials and testing methods used. Gent tested unfilled natural rubber which strain crystallises and so reduces the crack growth rate before rupture. Additionally Gent's tests were performed under displacement control that reduces the final crack growth compared with load controlled tests. Another difference in Gent's fatigue testing was the use of die-stamped dumbbell test specimens instead of the rotationally symmetric moulded ones used within this test programme. The failure in Gent's tests occurred mainly on the die-stamped edges and occasionally from surface flaws.

A calculation of the fatigue life for the carbon black filled EPDM- and SBR-materials was done using the equation given by Gent [8] in combination with the crack growth data of this research. It was necessary to use an initial crack (flaw) size for the SBR within the calculation that was at least 3 times larger when compared with the EPDM. Otherwise the calculation would predict a higher fatigue life for SBR than EPDM and exactly the opposite ranking is borne out by the experimental results observed on dumbbell specimens. This approach is, however, problematic because a microscopic examination of both materials with a resolution of approximately 1μm gave no evidence for initial flaws for the SBR being a few times bigger than for the EPDM.

The research on dumbbell specimens suggests that the start of the crack growth process (crack initiation) plays a certain role and seems to be insufficiently represented by crack propagation testing only. The start of visible crack growth is accompanied by a sudden decrease in modulus simultaneous with an increase in loss factor or dissipated energy. From this point on the cracks become easily visible caused by the high dynamic strains (100% - 200%) applied for the testing of the filled materials. Using the crack propagation approach solely might be erroneous because it is essential to predict how long a rubber product functions in its desired form as this time constitutes more than 95% of the whole service life. The disadvantage of the fatigue test compared with the measurement of crack growth is the far greater testing time and consequently much higher cost.

The standard fatigue crack propagation testing described in the literature used displacement (strain) controlled tests. This is only applicable if service conditions under forced displacement are to be simulated. But most of the service conditions of elastomeric products are under load control and testing under displacement control would be imprecise. Clauß [**40**] has also compared load and displacement controlled fatigue tests. One result was that the stiffer (lower carbon black dispersion) material failed much earlier under displacement controlled testing compared with the softer (good carbon black dispersion) material, but under load control both materials showed nearly the same fatigue resistance.

The results of the fatigue testing indicate that elastomeric materials fail after a material specific loss in complex modulus E* (or component stiffness). This predictor seems to be characteristic for each material because it is independent of the applied loading. It does not depend on the load amplitude or the applied minimum load and so is a very important indicator for the maintenance of machines with elastomeric parts. This predictor allows to measure the state of the rubber components easily and online and to replace them just before they fail. The dependency of the residual stiffness predictor on frequency and temperature was not examined in this research and there is a well known high dependency on these conditions. Additionally the effect of pauses during the testing time and their previously documented effect on the recombination of the filler network was not included in this research.

For simulations of the fatigue life of elastomers with FEA it is common to use stress or strain as criteria as suggested in the literature [**10, 11, 12**]. This is applicable for unfilled rubbers or for filled rubbers only if zero minimum loads appear in all parts of the component and consequently in all elements. This obviously would be a special case for a dynamically loaded component. The dynamic strain energy density can be used as a criterion in cases of minimum loads larger or equal to zero [**53, 54, 55, 56**]. If also negative (compressive) minimum loads are applied it is possible to use either the dynamic stored energy or the dynamic total energy criterion that has been developed within this thesis. These predictors have limited precision as seen in the case of carbon black filled EPDM but it appears to be the best compromise for all test procedures and both polymers. Other predictors that worked well for one material failed utterly for the other material.

Also, research at the Dublin Institute of Technology (DIT) [**57**]is underway to determine if the values of complex modulus at failure in uniaxial cyclic loading are replicated for multiaxial fatigue tests. These tests will use bubble inflation to cycle the same compounds of EPDM and SBR samples to failure.

The comparison of fatigue life and dynamic crack propagation results of this research show the importance of laboratory testing conditions to mirror the service conditions as closely as possible, because the carbon black filled materials used in practise show a moderate to very high dependency on the minimum load for its fatigue life. Additionally it can be seen that the fatigue life of EPDM material under sinusoidal excitation of 1Hz, subject to load control is

higher than that for with the SBR material. However, a comparison of the dynamic crack propagation with a sinusoidal excitation of 1Hz under displacement control results gives a completely opposite result. The filled SBR material is far superior to the filled EPDM materials, which means it has a much lower dynamic crack growth rate. If the cycles to failure of the crack propagation test are considered instead of the crack growth rate the better performance of the carbon black filled SBR material increases compared with the carbon black filled EPDM material. The dynamic crack propagation test with 50ms pulses and a repetition rate of 10Hz gives the same ranking as the sinusoidal crack propagation test under 1Hz. The carbon black filled SBR material has a slower crack propagation rate than the filled EPDM. This pulsed testing condition simulates the in service loading of a passenger car tyre and the results give the expected ranking with the SBR displaying superior properties,

The comparison of the tested materials for fatigue to failure and dynamic crack propagation test show that the change from one testing method to the other can give rise to a complete change in ranking. Consequently it is very important to know the exact service conditions to achieve a good laboratory simulation. Additionally it must be known what causes the failure of a rubber component in service. Is it the initiation of a crack or is it the crack growth or rather the development of the crack? If this information is not available it is not possible to conduct a proper simulation of a rubber material in the laboratory.

6 Conclusions

This research has shown that fatigue resistance of active carbon black filled non strain crystallising EPDM and SBR rubber materials increases when compressive or tensile preloads (minimum loads) are applied under load controlled testing. The increase of fatigue life results from the active filler and its filler-filler and filler-polymer interaction since this phenomenon does not occur in the unfilled EPDM or SBR. This research has shown that a cyclic condition where the minimum stress is zero is the most severe for an active filled elastomer. This demonstrates that like other solids, compression is less severe for elastomers than is tension.

The results of this research show that the established predictors, maximum stress [**10**] and maximum strain [**11**, **12**] can not be used for determining the fatigue life of carbon black filled elastomers if non-zero minimum loads are applied. This is potentially a critical problem because most rubber compounds contain carbon black and they are often used under preloads. The energy criteria [**30** ,**13**, **14**] also suggested allow a better prediction of the fatigue properties of the carbon black filled elastomers. But even these energy concepts are not precise enough for an accurate prediction of the fatigue properties of elastomers in all circumstances.

As a first approximation, two new fatigue life predictors the dynamic stored energy method and the dynamic total energy method were developed. The fatigue life of carbon black filled SBR and less so of carbon black filled EPDM, can be predicted by relating fatigue life to the dynamic stored energy. This is so for situations with pre-load and no pre-load. Additionally it is possible to

predict the fatigue life of both unfilled materials also very well with this method. These predictors are the much used stored energy and total energy methods applied in tests when the minimum stress is zero or compressive. Only for minimum loads in tension the static part (dynamic displacement range times minimum load) of the stored energy and total energy is subtracted to give a measure of dynamic stored energy and dynamic total energy.

The new prediction criteria can be incorporated into non-linear FEA and design optimisation software. They will allow more precise simulation of the fatigue life of carbon black filled elastomeric components, especially for non zero minimum loads which are those most commonly encountered in service.

During the fatigue test on carbon black filled EPDM and SBR, the stiffness of the material and the loss factor (tan δ) decrease throughout the entire test. A component manufactured from the EPDM material tested will fail in fatigue when the complex stiffness K* (corresponding to the complex modulus E*) attains a value of approximately 76% of the initial complex modulus. In the case of the SBR material the value is approximately 71% of the initial complex modulus. This value is independent of the applied load amplitude or variations in the minimum load. So the loss in the complex stiffness (modulus) could be used as an indicator close to the failure of a rubber component. This indicator allows an "online" measurement of the actual state of rubber components simply and online. This indicator can be used by maintenance engineers to exchange elastomeric parts just before they fail.

The conditions of a laboratory simulation of fatigue life should be as close as possible to service conditions. Particularly if a rubber product is used under load control, the testing should also be carried out under load control, otherwise the results can be misleading. The first reason for this is stress softening during the whole fatigue life which was demonstrated throughout the test programme. Another reason for this is illustrated when materials of different stiffnesses are compared under displacement control. The stiffer material will always be more rigorously tested than the softer material and it should fail much earlier, because a higher stiffness leads to higher stresses and strain energy densities. Additionally a change of the testing conditions, as for example in the tests from the sinusoidal load controlled test under 1Hz to the 50ms pulses with 10Hz repetition frequency under displacement control, lead to an inversion in the fatigue properties for the filled and unfilled materials at least in respect of the maximum stress dependency.

The dynamic crack propagation properties showed the same minimum load dependency as did the fatigue life tests for both non strain crystallising elastomers. In the case of carbon black filled elastomers the crack growth rate was reduced by applying a minimum load at a constant strain amplitude. For the unfilled EPDM or SBR materials the crack growth rate was increased with an increase in the minimum load at fixed strain amplitude.

The comparison of the fatigue to failure and the dynamic crack propagation tests under sinusoidal loading at 1Hz shows a ranking inversion for the carbon black filled EPDM and SBR. It has to be questioned if the testing of crack growth is representative of the fatigue life of rubber components. Crack growth

tests describe and compare less than about the final 5 % of the service life of a rubber product. It is certainly more important to derive material/product data from the intact component and determine how long it remains intact. So the crack initiation properties are of higher interest for manufacturers than the time it takes to totally fail the product. It must, therefore be assumed that fatigue to failure tests are relevant testing conditions for practical applications of the material, but they are much more time consuming than crack propagation tests.

7 Outlook

The results of this PhD-thesis should be validated in the different ways listed below.

(i) Tests should be carried out on other elastomeric materials to develop a unique fatigue criterion for lifetime predictions and incorporation into FEA-software.

(ii) The characterisation of a material parameter that describes fatigue behaviour under different test conditions of pre-stressing and pre-straining for all different types of elastomers should be determined. Furthermore the influence temperature, frequency and pulse parameters have on the residual stiffness predictor must be examined.

(iii) Additionally dynamic crack propagation should be examined and correlated with the fatigue results for different materials and testing conditions.

(iv) The dependency of the fatigue life and crack propagation properties of elastomeric materials with different glass transition temperatures and reinforcement on varying conditions should be examined.

(v) Multi-axial fatigue tests should be conducted to determine if the values obtained for complex modulus (E*) at failure are the same for both complex loading and uniaxial deformations.

The results of this research give designers the opportunity to understand the fatigue behaviour of elastomeric materials, to simulate their fatigue properties more precisely and to increase the service lives of elastomeric components.

8 Appendix

List of publications and conference contributions

1. T. Alshuth and F. Abraham, "Strategies to Predict Dynamic Properties of Elastomer Products", *DKT 2000*, Nürnberg, DKG, September (2000)

2. F. Abraham, T. Alshuth, S. Jerrams, Poster: "Dependence of Fatigue Life of Elastomers on Stress Amplitude and Prestress", *Kautschuk Herbst Kolloquium 2000*, Hannover, DIK, 6.-8. November (2000) 405

3. T. Alshuth, F. Abraham, M. Klüppel, J. Schramm, "Fatigue Life of Elastomers - Parameter Influence, Criteria and FE-Applications" *DKG*, Hannover, December (2000), no paper

4. T. Alshuth, F. Abraham, "Fatigue Properties of Elastomers – Parameter Dependence and Criteria", *Rubber Symposium of the Countries on the Danube*, Budapest, 26-28 April (2001)

5. F. Abraham, T. Alshuth, S. Jerrams, "The Dependence on Mean Stress and Stress Amplitude of the Fatigue Life of Elastomers", *IRC 2001*, Birmingham, IOM, 12-14 June (2001)

6. F. Abraham, T. Alshuth, S. Jerrams, "Parameter Dependence of the Fatigue Life of Elastomers ", Conference: *Service Life Prediction of Elastomer Components*, London, IOM, 15 October (2001)

7. T. Alshuth, F. Abraham, S. Jerrams, "Parameter Dependence of the Fatigue Properties of Elastomer Products ", *Meeting of the Rubber Division, American Chemical Society*, Cleveland, Ohio, 16-19 October (2001)

8. F. Abraham, T. Alshuth, S. Jerrams, "Parameter Dependence of the Fatigue Life of Elastomers", Book: *Service Life Prediction of Elastomer Components*, London, IOM, 15 October (2001), accepted for publication

9. S. J. Jerrams and F. Abraham, "Predicting fatigue in non strain-crystallising rubbers", *Rubber Compounders and Processors Forum,* Midlands Plastic and Rubbers Group, The Institute of Materials, Burton College, 17th October (2001)

10. F. Abraham, T. Alshuth, S. Jerrams, "Ermüdungsbeständigkeit von Elastomeren – Einfluss der Spannungsamplitude und der Unterspannung", *KGK Kautschuk Gummi Kunststoffe*, Nr. 12/2001, **54**. Jahrgang (2001) 643

11. F. Abraham, T. Alshuth and S. Jerrams, "The Dependence on Mean Stress and Stress Amplitude of the Fatigue Life of EPDM Elastomers", *Plastics, Rubber and Composites*, Vol. 30, No. **9** (2001) 421

12. F. Abraham, T. Alshuth "Lebensdauer von SBR- und EPDM-Elastomeren in Abhängigkeit der Vorkraft und der Kraftamplitude", *DKG Bezirksgruppe Rheinland-Westfalen*, Bad Neuenahr-Ahrweiler, DKG, 20-21 März (2002)

13. F. Abraham, T. Alshuth, S. Jerrams, "Parameterabhängigkeit und Kriterien der Ermüdung von Elastomeren", *Fortbildungsseminar: Bruchmechanik und Lebensdauer von Elastomeren*, Hannover, DIK, 25-26 März (2002)

14. T. Alshuth, F. Abraham, "Ermüdung von Elastomerwerkstoffen, Belastungsabhängigkeit und Kriterien", *IV. Hamburger Dichtungstechnisches Kolloquium – Dynamische Dichtungen*, TU Hamburg-Harburg, 23-24 Mai (2002)

15. F. Abraham, T. Alshuth, S. Jerrams, "The Dependence on Minimum Stress and Stress Amplitude of the Fatigue Life of Non Strain Crystallising Elastomers", EUROMECH Colloquium 438: *Constitutive Equations for Polymer Microcomposites: On the Border of Mechanics and Chemistry*, Vienna, 15-17 July (2002)

16. F. Abraham, T. Alshuth, S. Jerrams, "The Effect of Minimum Stress and Stress Amplitude on the Fatigue Life of Non Strain Crystallising Elastomers", *1. International Conference on Materials & Tribology 2002 (MT2002)*, Dublin, 12-13 September (2002)

17. A. Tabacović, S. Jerrams, B. Bowe, F. Abraham, "Surface Flaws in Elastomers and the use of Surface Treatments", *1. International Conference on Materials & Tribology 2002 (MT2002)*, Dublin, 12-13 September (2002)

18. T. Alshuth, F. Abraham, "Fatigue of Elastomers – Damage Criteria, Parameters for FEA-Calculation", *Internationale Fachtagung: Polymerwerkstoffe 2002*, Halle (Saale), 25-27 September (2002)

19. M. Bogun, F. Abraham, L. Muresan, R.H. Schuster, H.J. Radusch, "Continuous and Discontinuous Mixing under Aspects of the Material Quality", *Meeting of the Rubber Division, American Chemical Society*, Pittsburgh, Pennsylvania, 8-11 October (2002)

20. F. Abraham, T. Alshuth, "Ermüdungs- Rissfortschrittseigenschaften von verstärkten Elastomeren", *Kautschuk Herbst Kolloquium 2002*, Hannover, DIK, 30. Oktober - 1. November (2002) 405

21. F. Abraham, T. Alshuth, S. Jerrams, "Ermüdungsbeständigkeit von Elastomeren – Einfluss der Spannungsamplitude und der Unterspannung Teil 2", *KGK Kautschuk Gummi Kunststoffe*, Nr. 12/2002, **55**. Jahrgang (2002) 674

22. T. Alshuth, F. Abraham, S. Jerrams, "Parameter Dependence of the Fatigue Properties of Elastomer Products", *Rubber Chemistry and Technology*, (2002), No.4, Vol. **75** (2002), 635

9 References

1 N. André, G. Cailletaud and R. Piques, "Haigh diagram for fatigue crack initiation prediction of natural rubber components". *KGK Kautschuk Gummi Kunststoffe,* **52.** Jahrgang, Nr 2/99 (1999) 120

2 S.M. Cadwell, R.A. Merrill, C.M. Sloman and F.L. Yost, "Dynamic fatigue life in rubber". *Industrial and Engineering Chemistry, Analytical Edition.*, **12** (1940) 19

3 G.J. Lake and A.G. Thomas, Chapter 5, Strength, "*Engineering with Rubber – how to design rubber components*", A.N. Gent, Ed., Hanser Verlag, Berlin, Germany (1991) 95

4 A.R. Payne, *Rubber. Chem. Technol.*, **36** (1963) 432

5 A.R. Payne, *Rubber. Chem. Technol.*, **36** (1963) 444

6 A.I. Medalia, *Rubber. Chem. Technol.*, **46** (1973) 877

7 J.A.C. Harwood, L. Mullins, A.R. Payne, *Journal of Applied Polymer Science*, **9** (1965) 3011

8 A. N. Gent, P. B. Lindley and A. G. Thomas, "Cut Growth and Fatigue of Rubbers. I. The Relationship between cut growth and Fatigue", *Journal of Applied Polymer Science*, **8** (1964) 455

9 G.J. Lake and P.B. Lindley, "Cut Growth and Fatigue of Rubbers. II. Experiments on a Noncrystallizing Rubber" *Journal of Applied Polymer Science*, **8** (1964) 707

10 J.T. Baumann, "Replacing the Tearing Energy Parameter". *RD ACS Conference Chicago April 1999* (1999)

11 M. Caspers, T. Barth and R. Schenk, "Lebensdauervorhersage von Gummi-Metall-Bauteilen mit Hilfe der FEM", *KGK Kautschuk Gummi Kunststoffe,* **44**. Jahrgang, Nr 7/91 (1991) 659

12 A. Schöpfel, H. Idelberger, D. Schütz and D. Flade, "Betriebsfestigkeit von Elastomerbauteilen", *DVM-Tag 1996, Bauteil´96, Elastomerbauteile*, (1996) 103

13 R.S. Rivlin and A.G. Thomas, "Rupture of Rubber. I. Characteristic Energy for Tearing." *Journal of Polymer Science,* Vol. **10**., No. 3. (1953) 291

14 G.L. Lake and P.B. Lindley, "The Mechanical Fatigue Limit for Rubber", *Journal of Applied Polymer Science*, Vol. **9** (1965) 1233

15 G. Kolb, Elastomere, *Kontakt + Studium, Band 5*, W. Gohl u.a., Lexika Verlag, (1975) 21

16 L. R. G. Treloar, *The Physics of Rubber Elasticity*, Oxford, At the Clarenden Press, (1949) 2

17 G. Kraus, *Angew. Makromol. Chemie*, 60/61, (1977), 239

18 L. Mullins, *I.R.I Trans.,* **22** (1947) 235

19 L. P. Smith, "*The Language of Rubber",* Butterworth Heinemann, Oxford, (1993) 42

20 L. Mullins, *Rubber. Chem. Technol.,* **42** (1969) 339

21 W. L. Holt, *Ind. Eng. Chem.*, **23** (1931) 1471

22 E.M. Dannenberg, *Trans. Inst. Rubber Ind.*, **42** (1966) 26

23 A. V. Tobolsky and H. F. Mark (EDS), *Polymer Science and Materials*, Wiley, New York, Ch. 13. (1971)

24 Aleksandrov and Lazurkin, *J. tech. Phys. U.S.S.R.*, **9** (1939) 1249; *Rubber. Chem. Technol.*, **13** (1940) 886

25 U. Eisele, *KGK Kautschuk Gummi Kunststoffe*, **40.** Jahrgang, Nr 6/87 (1987) 539

26 J.H. Magill, "Crystallization and Morphology of Rubber", *Rubber. Chem. Technol.*, **68** (1995) 507

27 K.-H. Schwalbe, *Bruchmechanik metallischer Werkstoffe*, Carl Hanser Verlag (1980)

28 J.W. Bergmann, R. Heidenreich, H. Bügler, W. Oberparleiter, *IABG-Bericht B-TF-2355* (1988)

29 A.Wöhler, *Journal: Bauwesen*, **20** (1870) 73-106

30 A.A. Griffith, Phil. Trans. R. Soc. London, Ser. **A 221** (1920) 163

31 A. G. Thomas, *Journal of Polymer Science*, **18** (1955) 177

32 G.J. Lake, *Prog. Rubber Technol.*, **64** (1991) 89

33 H.W. Greensmith, *Journal of Applied Polymer Science* . **7** (1963) 993

34 P.B. Lindley, *J. Strain Anal.,* **7** (1972) 132^

35 R. Seldén "Fracture mechanics analysis of fatigue of rubber - a review" *Progress in Rubber and Plastics Technology,* Vol. **11**, No 1, The Institute of Materials/RAPRA (1995)

36 G.J. Lake, P.B. Lindley, *Rubber Journal,* 146, **10** (1964) 24

37 A. Schallamach, *Gummi, Asbest, Kunstst.,* **10,** (1973) 844

38 M.D. Ellul, Chapter 6, "Mechanical Fatigue", *Engineering with Rubber – how to design rubber components*, A.N. Gent, Ed., Hanser Verlag, Berlin, Germany (1991) 129

39 G.J. Lake, *Prog. Rubber Technol,* **45** (1983) 102

40 G. Clauß, "Das Hysteresis-Meßverfahren zur dynamischen Prüfung von Kunststoffen – ein Verfahren zur Lebensdauervorhersage auch für Elastomer-Bauteile", *Lebensdauer und Ermüdung von Elastomeren, DIK Fortbildungs-seminar,* Hannover 8. – 9. Juli (1999)

41 H.G.Elias, "Polymere – Von Monomeren und Makromolekülen zu Werkstoffen", *Hüthig*, Heidelberg (1996)

42 German Specification: DIN 53 513, "Bestimmung der visko-elastischen Eigenschaften von Elastomeren", Ausgabe Januar (1983) 197

43 U. Eisele, S. Kelbch und H.-W. Engels, "The Tear Analyzer – A New Tool for Quantitative Measurements of the Dynamic Crack Growth of Elastomers", *Kautsch. Gummi Kunstst.* **45** (1992) 1064

44 S.A. Kelbch, U. Eisele, H. Magg, A.J.M. Sumner, "Predictive Testing für die Rißbeständigkeit von Elastomerbauteilen", *Lebensdauer und Ermüdung von Elastomeren, DIK Fortbildungsseminar,* Hannover 8. – 9. Juli (1999)

45 A.N. Gent, "Strength of elastomers" *Chapter 10, Science and Technology of Rubber 2nd Ed.,* Ed. by Mark, Erman and Eirich, Academic Press Inc. (1994) 471

46 J.H. Fielding, "Flex life and crystallization of synthetic rubber. *Industrial and Engineering Chemistry,* **35** (1943) 1259

47 P.B. Lindley, "Non-Relaxing Crack Growth and Fatigue in a Non-Crystallizing Rubber", *Rubber. Chem. Technol.,* **47** (1974) 1253

48 G. J. Lake, "Mechanical Fatigue of Rubber" *Rubber. Chem. Technol.,* **45** (1972) 309

49 G. J. Lake and P. B. Lindley, *Rubber Journal,* **146** (10), 24 and (11),30 (1964)

50 S. Jerrams and A. Tabakovic, "The Influence of Mean Stress on the Fatigue Properties of Natural Rubber" *IRC 2001, Birmingham* (2001) 327

51 D.L. Lee and J.A. Donovan, "Microstructural Changes in the Crack Tip Region of Carbon Black Filled Natural Rubber", *Rubber. Chem. Technol.*, **60** (1987) 910

52 G. J. Lake, A. Samura, S. C. Teo and J. Vaja, *Polymer*, 32, (16), (1991) 2963

53 F. Abraham, T. Alshuth and S. Jerrams, "The Dependence on Mean Stress and Stress Amplitude of the Fatigue Life of Elastomers", *IRC 2001, Birmingham* (2001)

54 F. Abraham, T. Alshuth, S. Jerrams, "Ermüdungsbeständigkeit von Elastomeren", *KGK Kautschuk Gummi Kunststoffe,* **54.** Jahrgang, Nr. 12/2001 (2001) 643

55 T. Alshuth, F. Abraham and S. Jerrams, "Parameter Dependence and Prediction of Fatigue Properties of Elastomer Products", *RD ACS, 160th Fall Technical Meeting, Cleveland, Ohio, 16-19 October* (2001)

56 F. Abraham, T. Alshuth and S. Jerrams, "The Dependence on Mean Stress and Stress Amplitude of the Fatigue Life of EPDM Elastomers", Plastics, *Rubber and Composites*, No. 8, Vol. **30** (2001)

57 N. Murphy, C. Spratt, R. Johannknecht and S. Jerrams, "Investigation of large cyclical, equi-biaxial stresses and strains in thin elastomeric sheets by bubble inflation", *1. International Conference on Materials & Tribology 2002 (MT2002), Dublin, 12-13 September* (2002)